JRC Scientific and Technical Reports

Neutron Physics Unit
Scientific Report 2007

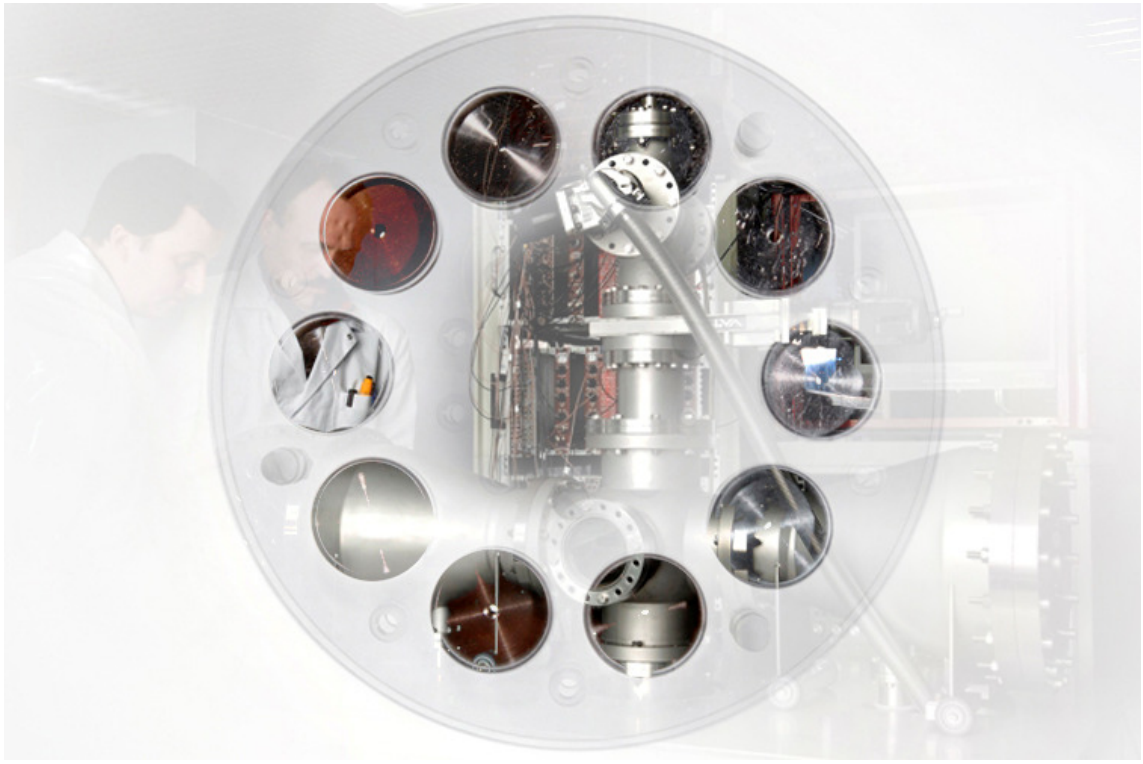

EUR 23440 EN - 2008

JRC
EUROPEAN COMMISSION

irmm
Institute for Reference Materials and Measurements

The mission of the IRMM is to promote a common and reliable European measurement system in support of EU policies.

European Commission
Joint Research Centre
Institute for Reference Materials and Measurements

Contact information
Address: Retieseweg 111, B-2440 Geel
E-mail: peter.rullhusen@ec.europa.eu
Tel.: +32 (0)14 571 411
Fax: +32 (0)14 571 862

http://irmm.jrc.ec.europa.eu/
http://www.jrc.ec.europa.eu/

JRC 46824

EUR 23440 EN
ISBN 978-92-79-09532-0
ISSN 1018-5593
DOI 10.2787/65683

Luxembourg: Office for Official Publications of the European Communities

Neutron Physics Unit

Scientific Report 2007

Preface

The year 2007 was a busy year for the Neutron Physics unit of IRMM, with considerable burden for our staff and the machines. In January, the EFNUDAT* project started with a kick-off meeting at the FZK in Karlsruhe. This EU project aims at coordinating nuclear data measurement activities at several laboratories in Europe, fostering the exchange of expertise, coordinating common research projects, and supporting transnational access to the participating facilities. Our own transnational access programme NUDAME continued being very successful and in January the third meeting of the programme advisory committee was held in Geel. Two major workshops were organised by our unit: G. Lövestam organised at IRMM on behalf of DG RELEX a workshop on the feasibility of source region identification of conflict diamonds using analytical techniques; and A. Plompen organised on behalf of the CANDIDE project the NEMEA-4 workshop in Prague. In addition, we faced the audits for three certificates (ISO 9001, ISO 14001 and OHSAS 18001) which we all achieved.

At GELINA, the recently implemented arrays with HPGe detectors (GAINS, not yet completed) and C_6D_6 detectors and the increased use of fast digitisers for signal processing contributed to a considerable increase in performance of the measurement set-ups. Measurements continued on fission products relevant for criticality safety, in cooperation with ORNL. A new project for measurements on ^{241}Am started in cooperation with CEA and ITU, with transmission measurements carried out at GELINA and (n, 2n) cross section measurements at the Van de Graaff. The project will continue with capture measurements at GELINA. Cross-section measurements at GELINA for neutron inelastic scattering were completed on ^{56}Fe. Cross sections of the ^{10}B(n, α) reaction previously measured at the Van de Graaff accelerator are being complemented with measurements at GELINA, aiming at determining the cross sections, branching ratios and angular distributions up to about 3 MeV. At a CANDU meeting with AECL at our sister institute IE in Petten a common project was proposed for measuring elastic neutron scattering on deuterium and preparatory work for this new project started at GELINA, with the help of a seconded national expert from Romania.

At the Van de Graaff accelerator, the measurements on neutron induced fission of ^{231}Pa were successfully completed and (n, 2n) cross sections were measured on ^{241}Am using the activation technique. The NEPTUNE beam chopper was utilised successfully in a NUDAME experiment for measuring the decay of a shape isomer in ^{235}U in neutron-induced fission of ^{234}U. The instrument is further being used in search of a shape isomer in ^{239}U. The measurements on prompt fission neutron spectra on ^{235}U are continuing with different detector geometries, in search of the angular dependence of the spectra a possibly also asymmetry effects. The direct measurements of the ^{16}O(n, α) reaction using a time projection chamber revealed some discrepancies with previous adjustments adopted in the ENDF/B-VII evaluated file and will be complemented with measurements using different neutron production targets for a better background assessment and improved energy resolution.

*http://www.efnudat.eu/

In 2007, seven seconded national experts, three visiting scientists, three post-docs and three PhD students have been working at our unit. In addition, a total of 48 external scientists have been using our facilities for experiments, 38 of them for experiments in the frame of our transnational access programme NUDAME. The increasing demand of beam time at our facilities by external users is challenging and encouraging for us. Exchange of experience and know-how with groups from other research organisations is stimulating and proved to be very helpful in developing new techniques for data acquisition and analysis.

P. Rullhusen
Unit Head
Neutron Physics Unit

Neutron data for innovative nuclear applications

Measurements of the neutron inelastic cross section on ^{56}Fe

A. Negret[1], *C. Borcea*[1,2], *A. J. M. Plompen*[1], *M. Stanoiu*[1,2]

[1] European Commission, JRC-IRMM, B-2440 Geel
[2] IFIN "Horia Hulubei", P.O. Box MG-6, RO-76900 Bucharest-Magurele

The importance of iron as a structure material for any nuclear system is obvious. Therefore the target accuracy studies for the 4th generation nuclear reactors and for accelerator driven systems result in very tight uncertainty limits for the main iron isotope, ^{56}Fe. It is considered that the uncertainty of neutron inelastic cross section of ^{56}Fe should be reduced from 7 - 25 % to a level of 2 % [1, 2].

A considerable effort was dedicated to the measurement of the cross sections for the ^{56}Fe(n, n'γ) reaction using the GAINS setup installed in the 200 m cabin of flight path 3 of GELINA [3]. Because of the importance of this cross section and of the discrepancies we found in the first results compared to the previous measurements from other laboratories, we made various careful and rather extensive checks in order to make sure that the results are consistent.

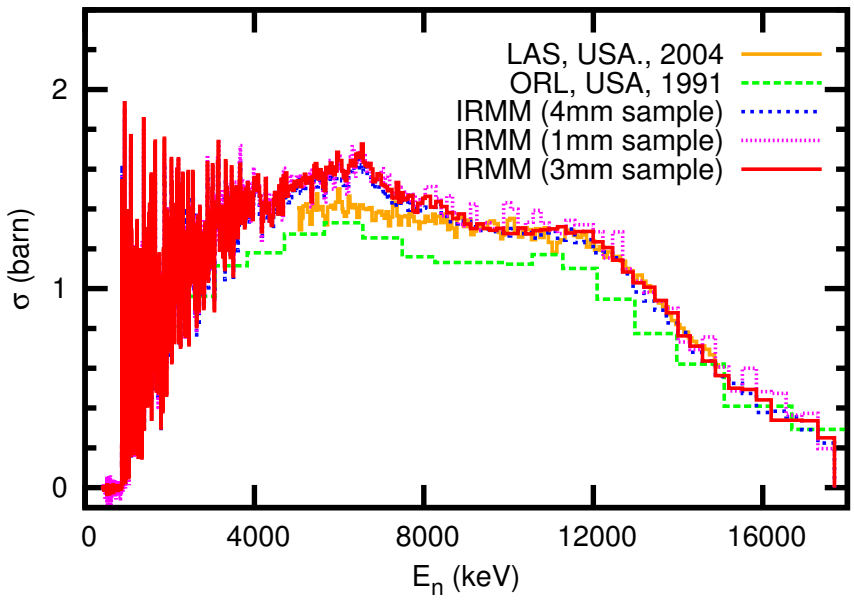

Fig. 1: Gamma production cross section of the strongest transition in ^{56}Fe (846.78 keV) - comparison of our measurement with previous results

GAINS is an array of 8 HPGe detectors read-out by a digitizer-based acquisition system. A fission chamber monitors the neutron beam. The efficiency of each detector is measured with a calibrated source. Using an MCNP simulation the efficiencies are then extrapolated to the

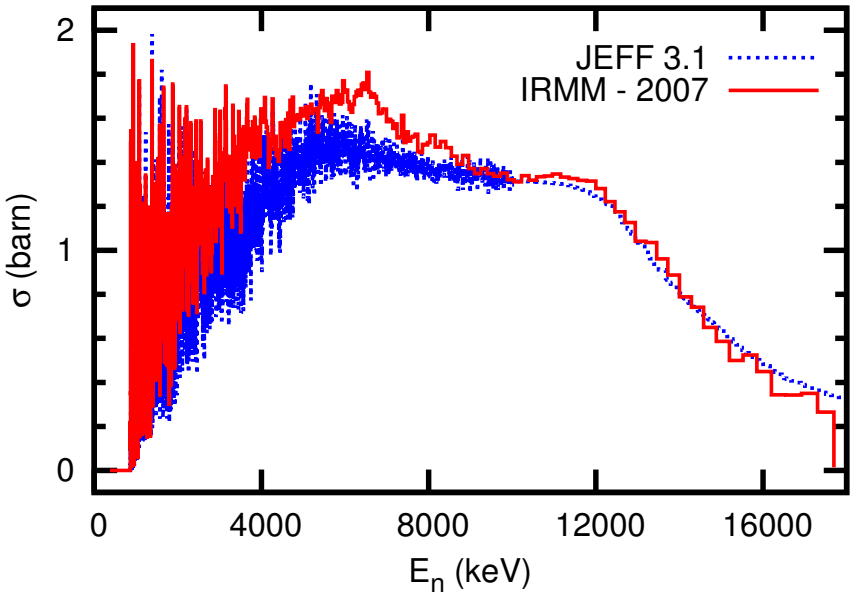

Fig. 2: Comparison of total neutron inelastic cross section of ^{56}Fe with the JEFF 3.1 evaluation

finite geometry of the measured sample. A second MCNP simulation is used to deduce multiple scattering corrections. Using these ingredients, the gamma production cross sections of various transitions are measured as a primary experimental result. Further, using an external level scheme one can deduce level production cross sections and the total inelastic cross section [4].

Measuring the gamma transitions from ^{56}Fe is not trivial. The most important γ-ray from ^{56}Fe (846.7 keV) overlaps with the strongest transition in ^{27}Al. As aluminium is present in the structure of the detection system, the possibility of having an uncontrolled background exists. Moreover, the background in this energy region has a component (specific triangular shape) from the γ-rays emitted after the (n, n') excitations of germanium from the detectors.

A few samples were irradiated during two measurement campaigns. Comparing the data from the iron samples with spectra obtained under identical conditions with a lead and a nickel sample assured us that the contamination of the main peak from the aluminium transitions is negligible. In order to make sure that all corrections made via MCNP simulations (i. e. the efficiency calibration and the multiple scattering corrections) do not introduce hidden errors, the data taking and the data analysis was independently performed for three natFe samples of 1, 3 and 4 mm.

Fig. 1 compares the gamma production cross section for the three samples with the results previously obtained at Los Alamos National Laboratory (LAS) and Oak Ridge National Laboratory (ORL). The three measurements performed at IRMM overlap very well but they diverge, especially at $E_n < 9$ MeV from the previous experimental results.
The total inelastic cross section obtained from our data is compared in Fig. 2 with the JEFF

3.1 evaluation which is based on the ORL data previously shown.

In conclusion, a new measurement of the neutron scattering on ^{56}Fe was performed. Extensive care and time was dedicated to data taking, various consistency checks and data analysis. The results show significant deviations from the previous experiments and, as a consequence, from the latest data evaluations.

[1] G. Aliberti, G. Palmiotti and M. Salvatores, *Global target accuracy study*, Proceedings of the NEMEA-4 workshop (2007)

[2] G. Aliberti, G. Palmiotti and M. Salvatores, *Target accuracy assessment for an ADS design*, Proceedings of the NEMEA-4 workshop (2007)

[3] A. Negret, C. Borcea, J. C. Drohe, L. C. Mihailescu, A. J. M. Plompen and R. Wynants, *A new setup for neutron inelastic cross section measurements*, Proceedings of the ND2007 conference (2007)

[4] L. C. Mihailescu, L. Oláh, C. Borcea and A. J. M. Plompen, *A new HPGe setup at Gelina for measurement of γ-ray production cross-sections from inelastic neutron scattering*, Nucl. Inst. Meth. A531 (2004)

Measurement of the ^{241}Am(n, 2n) reaction cross section with the activation technique

C. Sage[1], *A. J. M. Plompen*[1], *V. Semkova*[1,2], *R. Jaime Tornin*[1]

[1] European Commission, JRC-IRMM, B-2440 Geel
[2] Institute for Nuclear Research and Nuclear Energy, Bulgarian Academy of Sciences, BU-1784 Sofia

The (n, 2n) reaction plays a role in the detailed estimates of the isotope concentrations in function of burnup in fast reactors with large fraction of minor actinides. Few measurements of (n, 2n) reaction cross section for actinides have been carried out, primarily on account of the difficulty to obtain unambiguous result. Neutron-multiplicity measurements require a trigger that vetoes fission events, whereas for (n, 2nγ) measurements the associated γ-rays typically carry only a limited fraction of the total cross section of the (n, 2n) reaction. The latter comes from the deformed character of the nuclei involved, which results in an excitation spectrum dominated by rotational bands of which the lowest excited states decay by low energy transitions with large conversion coefficients. In addition, in many cases the activation technique can not be used in view of the long half live of the end product. The present experiment is of interest to nuclear model calculations since it will allow to study the complex competition with the fission, elastic and inelastic scattering processes for Am. In view of the relative uniqueness of this case, this will lead to valuable information regarding neighbouring nuclides [1].

The ^{241}Am(n, 2n)^{240}Am reaction cross section was measured by means of activation technique. The irradiations were carried out at the 7 MV Van de Graaff accelerator at IRMM, Geel. The ^{240}Am activity induced in the samples during irradiations were determined by γ-spectrometry using high-resolution HPGe detector. A detailed description of the measurement procedure has been given earlier [2].

Samples and irradiation procedure The samples were prepared by a method specially developed for present study by the ITU. This method is based on the production of porous alumina granules by powder metallurgy. The Am (originations from CEA) was then introduced into the porous particles by infiltration of the nitrate solution. Following drying to eliminate water, and calcination to convert to the oxide, the resulting powder was pressed into pellets of 12 mm diameter and 2 mm thickness. The samples weight in average 400 mg and the average Am content is 40 mg. The Al_2O_3-Am material was then encaplulated into aluminium containers (provided by IRMM). The sample geometry was examined by X-ray radiography and Am content determined by calorimetry. The mass of the ^{241}Am in the samples was determined by γ-spectrometry at IRMM as well and the results agree within 2 % uncertainties.
The irradiations were carried out at the 7 MV Van de Graaff accelerator at IRMM, Geel. Quasi mono-energetic neutrons with energies between 13.5 and 20.5 MeV were produced via the ^{3}H(d, n)^{4}He reaction (Q = 17.59 MeV) employing a solid-state Ti/T target (2 mg/cm^2 thick) on a silver backing (0.4 mm thick) at incident deuteron energies of 1, 2, 3 and 4 MeV. The samples, each sandwiched between monitor foils, were placed at 0^o relative to the incident deuteron beam at 2 cm distance from the target. The cross section at E_n = 13.3 MeV was

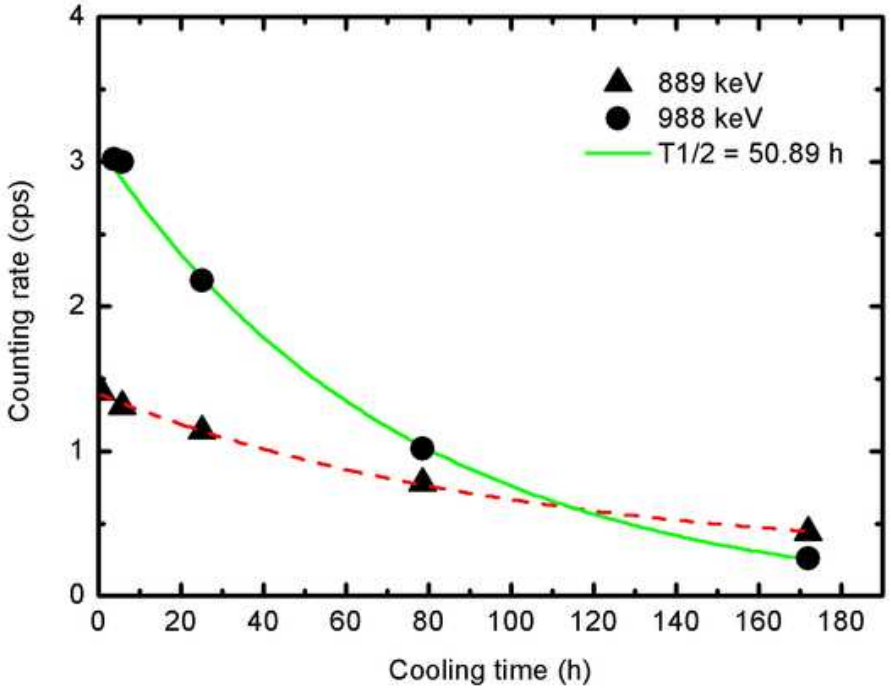

Fig. 1: Intensity as a function of the time after end of irradiation for both 899 keV and 988 keV γ-lines in comparison with results from the fitting

obtained using 1 MeV deuterons at 125^o neutron emission angle. The ^{2}H(d, n)^{3}He reaction (Q = 3.269 MeV) on a deuterium gas target was used for the production of neutrons with energies 8.2 MeV (E_d = 5.5 MeV) and 9.0 MeV (E_d = 6.3 MeV) at forward direction.
A long-counter operated in multichannel-scaling acquisition mode was used to record the time profile of the neutron flux during the irradiation in order to correct for fluctuation of the flux.

Neutron energy and flux determination The neutron energy and yield distributions as a function of deuteron energy and emission angle for the primary ^{3}H(d, n)^{4}He neutrons were determined by the program code EnergySet [3] that is based on the reaction cross sections tables of Ref. [4] and the stopping powers of Ref. [5]. The neutron fluence rate was determined by the ^{27}Al(n, α)^{24}Na IRDF-2002 standard cross section.
To account for the contribution of the low energy neutrons the neutron flux density distributions were determined by the spectral index method that involves the ^{115}In(n, n')^{115m}In, ^{58}Ni(n, p)^{58}Co, ^{27}Al(n, p)^{27}Mg, ^{27}Al(n, α)^{24}Na, ^{56}Fe(n, p)^{56}Mn and ^{93}Nb(n, 2n)^{92m}Nb dosimetry reactions with distinct energy thresholds combined with results from time-of-flight spectrum measurements.
For the ^{2}H(d, n)^{3}He the flux spectrum at the sample center was determined from the kinematics of the reaction, the differential cross section, the length of the gas cell, the distance sample-

to-gas-cell and the sample diameter.

Measurements of radioactivity The radioactivity of the samples was measured by γ-ray spectrometry. A HPGe detector with 100 % relative efficiency was used. The data acquisition was controlled by the Maestro system supplied by EG&E Ortec and the γ-ray spectra were analysed by Genie-2000 spectrometry software of Canberra.
The decay data for both ^{241}Am and ^{240}Am given in Tab. 1 were taken from Ref. [6]. Concerning the ^{241}Am only those γ-rays which were present in the spectrum with considerable intensity after the shielding was introduce are included in Tab. 1. The intensity of the interfering 887.3 keV γ-line is given as well. The γ-ray spectra of the samples themselves were measured

Tab. 1: Summmary of decay data for ^{241}Am and ^{240}Am

nucleus	half-life	E_γ (keV)	I_γ (%)
^{240}Am	50.8(3) h	987.76(6)	73(4)
		888.80(5)	25.1(13)
^{241}Am	432.6(6) y	59.5409(1)	35.9(4)
		208.01(3)	7.91(19)E-4
		322.52(3)	1.52(4)E-4
		332.35(3)	1.49(3)E-4
		335.37(3)	4.96(11)E-4
		368.65(3)	2.17(5)E-4
		376.65(3)	1.38(3)E-4
		662.40(2)	3.64(9)E-4
		722.01(3)	1.96(4)E-4
		887.3(3)	2.2(5)E-7

prior to the first irradiation. The sample activity of about 3 GBq primarily consists of the well known 60 keV γ-ray, but a large number of γ-rays with emission probabilities as high as 10^{-6} were present in the spectrum as well. It was found out that the 888.8 keV γ-line will be probably contaminated but the region around 987.8 keV was free from background activity. The measurement geometry was optimised in order to reduce the dead time caused by the very high counting rate. A shielding of 3 mm copper and 7 mm lead placed on the top of the detector cap was sufficient to absorb completely the 60 keV γ-line and reduced the dead time to less than 10 %. The detector was additionally shielded from the side with 10 mm copper cylinder to avoid detection of scattered γ-rays. The distance between the sample and the detector was 8 cm.
The detector efficiency for the 987.8 keV γ-rays was determined by Monte Carlo simulation of the measurement geometry using the MCNP code [7].

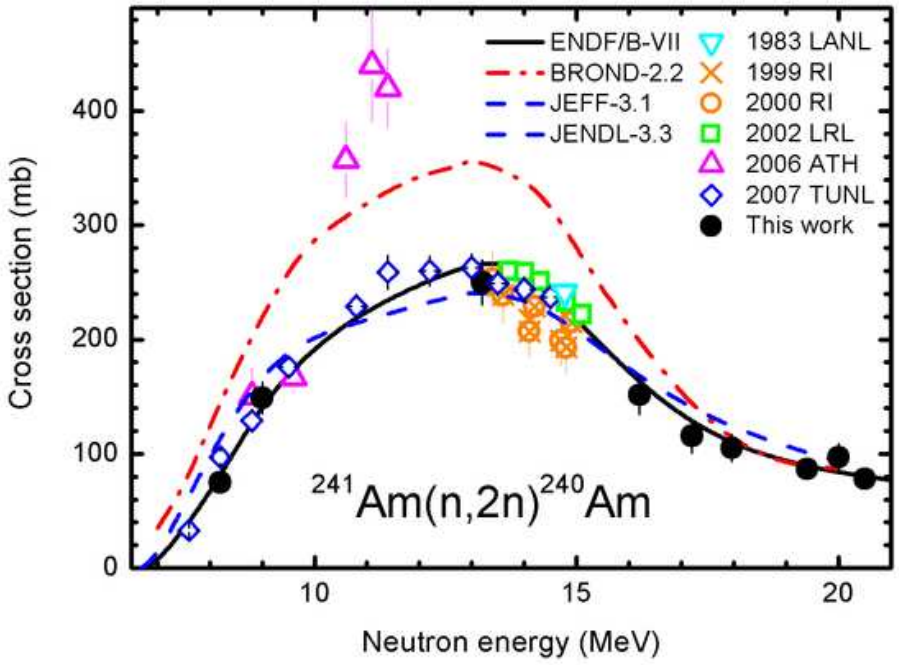

Fig. 2: Comparison of the experimental ^{241}Am(n, 2n)^{240}Am reaction cross sections with evaluated data

The intensity of the both 888.8 keV and 987.8 keV γ-ray lines were measured as a function of the cooling time after irradiation. As can be seen from the Fig. 1 the 988 keV decay corresponds to the 50.8 h half life of ^{240}Am.

Data analysis The cross sections were determined by the well known activation formula. The measured γ-ray count rates were corrected for γ-ray abundance, efficiency of the detector, irradiation and measurement geometry, neutron flux fluctuation during the irradiations, and secondary neutrons.

Results and Discussion The experimental results of this work are shown graphically in Fig. 2. The experimental data in the threshold region are of particular importance since until recently those cross sections ware unmeasured. Our results agree with the ENDF/B-VII evaluation. The differences with the TUNL [8] data are as high as 10-20 %. The measurements recently made at Athens [9] are within 10 to 20 % agreement with our and TUNL data up to 10 MeV, however their results between 11 and 12 MeV incident neutron energy are considerably higher than those from TUNL. There are five sets of experimental data around 14 MeV namely, A. A. Filatenkov et al. [10], R. W. Lougheed et al. from 2002 [11], the cross-ection data

measured at LANL in 1983 and cited in ref. [12], and the data from TUNL [8]. The data of Filatenkov at al. are 5-10 % lower than the results from LLNL and LANL. The cross section at 13.2 MeV from this work better agree with the results from TUNL and Filatenkov. The experimental data above 15 MeV provide a valuable test for the preequilibrium modelling in the presence of fission. Our results are the only ones in this energy range and they agree with the ENDF/B-VII evaluation.

[1] *Motivation for new ^{241}Am Measurements*, JEF/DOC-931; and
O. Bouland, *Motivation for New Measurements on ^{241,242,243}Am Isotopes*, Prc. Int. Conf. on Nucl. Data for Science and Techn., Santa Fe, NM, Sept. 26 - 0ct. 1, 2004, American Institute of Physics (2005) 211

[2] A. Fessler, A. J. M. Plompen, D. L. Smith, J. W. Meadows, Y. Ikeda, Nucl. Sci. Eng. 134 (2000) 171-200.

[3] G. Lövestam, EnergySet, EC-JRC-IRMM, private communication (2004)

[4] M. Drosg, *DROSG-2000: Neutron Source Reactions, Report IAEA-NDS-87, v.2.2, Rev. 8*, IAEA, Vienna, Austria, www-nds.iaea.org (2003).

[5] J. F. Ziegler, SRIM 2003: The Stopping and Range of Ions in Matter, *www.srim.org* (2003)

[6] Nuclear Data Sheets; *http://www-nds.iaea.org/ensdf*; *http:/www.nea.fr*; *http://www.nndc.bnl.gov/nndc/endsf*

[7] X-5 Monte Carlo Team, *MCNP A General Monte Carlo N-Particle Transport Code, Version 5*, Los Alamos National Laboratory, New Mexico, April 24 (2003)

[8] A. Tonchev, Workshop on *Nuclear Reactions on Americium 2007, NRAM2007*, Santa Fe, September 2007 (unpublished)

[9] G. Perdikakis, C. T. Papadopoulos, R. Vlastou, A. Lagoyannis, A. Spyrou, M. Kokkoris, S. Galanopoulos,N. Patronis, D. Karamanis, Ch. Zarkadas, G. Kalyva and S. Kossionides, Phys. Rev. C73, 067601, (2006)

[10] A. A. Filatenkov and S. V. Chuvaev, Phys. At. Nucl. 63, 1504 (2000)

[11] R. W. Lougheed, W. Webster, M. N. Namboodiri, D. R. Nethaway, K. J. Moody, J. H. Landrum, R. W. Hoff, R. J. Dupzyk, J. H. Mcquaid, R. Gunnink, E. D. Watkins, Radiochimica Acta 90, 833 (2002)

[12] P. Talou, T. Kawano, P.G. Young, M.B. Chadwick, R.E. MacFarlane, Nucl. Sience Eng. 155 (2007) 84-95

Measurements of the total cross section of ^{241}Am

C. Sage , S. Kopecky , A. Plompen , P. Siegler

For burning minor actinides in reactor cores precise knowledge of their cross sections is of utmost importance, but at present the quality of some necessary data is insufficient, e.g. the cross section of ^{241}Am. It has been show that a disagreement between integral and differential measurements is caused by differences in the neutron capture in the low lying resonances of this isotope[1].
The majority of transmission measurements available in the literature have been performed using thin powder samples. In a recent paper [2] it has been shown, that such measurements can lead for a resonance with a capture width larger than the neutron width - as encountered for the low lying resonances of ^{241}Am - to an overestimation of the capture width and an underestimation of the neutron width. This effect is caused by sample inhomogenities inherent to a powder sample. As result the neutron capture in these resonances would be underestimated by these measurements. To address this problem a series of measurements using a novel sample type has been started. These samples are prepared by a sol-gel method [3], and they consist of a matrix of porous Y_2O_3 beads, that have a typical diameter of a few tens of μm. Into this matrix AmO_2 is infiltrated. The sample should be considered a two-phase material, i.e. a porous matrix with inclusions, for a transmission measurement the distribution of the americium should be sufficiently homogenous.

Transmission measurements were carried out at flight path 2 of GELINA, with the detector at a distance of 26.45 m from the neutron source. The sample station was located approximately half way between target and detector station. Air conditioning is installed at the measurement and sample stations, to reduce the drift in the electronics and to allow for a reliable calculation of the Doppler broadening. Two BF_3 proportional counters were used to monitor the neutron output of the accelerator and to normalise the spectra. For the measurements GELINA was operated with a repetition rate of 50 Hz, allowing for measurements down to thermal neutron energies, therefore no filters to reduce the neutron overlap were required. Only lead filters to suppress the gamma flash had to be inserted into the beam. The sample itself was a pellet of Y_2O_3 with a weight of 3.3 g and a diameter of 22 mm. Into this pellet approximately 325 mg of ^{241}Am had been infiltrated. The sample was then put into a aluminium container.

Measurements have been performed in March 2007, and the first analysis with the resonance shape analysis code REFIT [4], indicates that the new sample type fulfils the expectations, i.e. the homogeneity allows for a reliable extraction of the resonance parameters. Furthermore suggests this analysis a slightly smaller capture width and a slightly larger neutron width than the literature values. More measurements to reduce the statistical uncertainty and to investigate further the effects of the matrix material are planned for summer 2008.

[1] O. Bouland, *Motivation for New ^{241}Am Measurements*, JEF/DOC-931

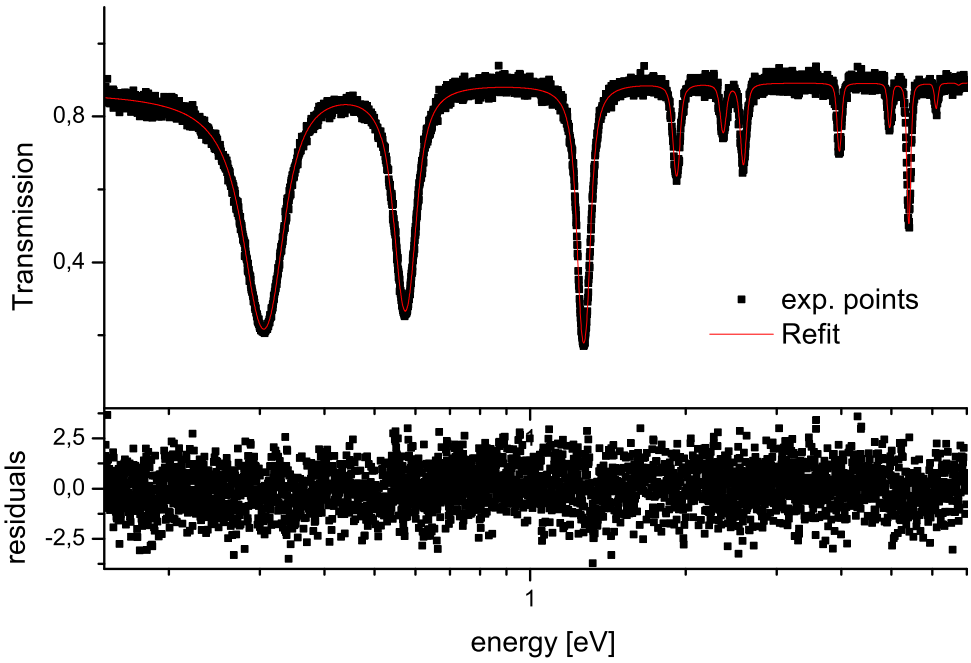

Fig. 1: Transmission of ^{241}Am

[2] S. Kopecky P. Siegler and A. Moens, *Low energy transmission measurements of ^{240,242}Pu at GELINA and their impact on the capture width*, in Proceedings of the International Conference on Nuclear Data for Science and Technology, Nice 2007, to be published

[3] C, Nästren, A. Fernandez, D. Haas, J. Somers and M. Walter, J. Nuc. Mat **362**, 350 (2007)

[4] M. C. Moxon, *REFIT - A least square fitting program for resonance analysis of neutron transmission and capture data*, AEA-InTec-0470, 1991

The 3^{rd} chance fission cross-section of ^{231}Pa

S. Oberstedt[1], *I. Fabry*[1], *F.-J. Hambsch*[1], *N. Kornilov*[1], *A. Oberstedt*[2]

[1] European Commission, JRC-IRMM, B-2440 Geel
[2] Institutionen för Naturvetenskap, Örebro Universitet, S-70182 Örebro

Beside the importance of the neutron-induced fission cross-section of ^{231}Pa for basic fission studies it is also of interest in the field of future reactor design based on the thorium-uranium fuel cycle [1]. The ^{232}Th/^{233}U breeder cycle, where the natural resources of the main fuel thorium are estimated to last for hundred thousands of years, is contemplated to provide "clean" and almost inexhaustible nuclear energy. Among the first priority isotopes the IAEA had pointed out ^{231}Pa and ^{233}Pa [2]. Both are of special interest being intermediate nuclei in the formation of the fissile $^{(232),233}$U from the fertile ^{232}Th. The latter one has been investigated in the recent years in great detail [3]-[6]. In particular, ^{231}Pa carries a similar risk as ^{239}Pu does in the standard uranium-plutonium cycle due to its comparable half-life and radio-toxicity.
Despite the wealth of existing experimental data important discrepancies exist, a scenario, which holds for the existing evaluated data files ENDF/B-VI and JENDL-3.3, too. This is shown in Fig. 1, where only the most instructive data are shown [6]-[11] together with data based on the above mentioned evaluations.
In the data a striking discrepancy exists for experimental data above E_n = 8 MeV. Towards the 3^{rd} chance fission the experimental data from Plattard et al. [9] show a very unusual behaviour, especially for energies above 16 MeV. Moreover, they are contradicting the data from Birgul et al. [10] by about 100%. Therefore, a new cross-section experiment had been performed at the VdG-driven neutron source of IRMM with neutrons in the energy range from 15 to 21 MeV [12].

The neutrons had been produced by using the reaction T(d, n)^{4}He using a solid-state TiT target. Due to secondary neutron-producing reactions of the deuterons on deuterons implanted in and on ^{16}O on the surface of the TiT sample the neutron beam is no longer mono-energetic at neutron energies higher than 17 MeV. Since no characterisation of the neutron beam profile could be performed at that time, appropriate corrections had to be based on data from Ref. [18]. However, since the properties of the neutron production target may change with time, the uncertainty was estimated by considering the most extreme variation of possible background scenarios. The deduced cross-section data are shown in Fig. 1 as up triangles (taken from Ref. [12]).

In order to validate the method of correcting for secondary neutron background the cross-section measurements have been repeated in 2006 at four different neutron energies, E_n = 16, 19, 20 and 21 MeV viz., with a measurement of the corresponding neutron energy distribution. For this purpose the source neutrons were measured with NE213 equivalent liquid scintillation detectors simultaneously at three different angles relative to the deuteron beam, at 0^o, 30^o and 60^o, viz. The pulse-shape discrimination technique was applied for efficient γ-ray suppression. The detector efficiency has been determined with neutrons from the spntaneous fission

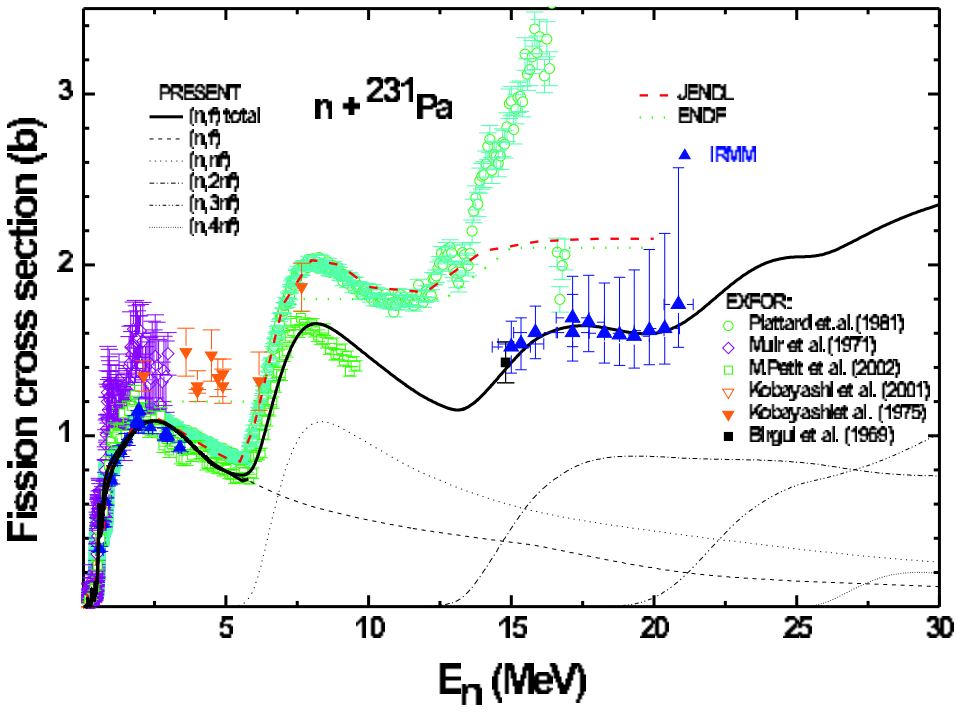

Fig. 1: Selection of the most relevant and characteristic experimental data of the neutron-induced fission cross-section of ^{231}Pa in energy range from 0 to 30 MeV [6]-[11] together with evaluations from JENDL and ENDF/B-VI; the up-triangles indicate the most recent cross-section data obtained at IRMM reaching for the first time beyond $E_n > 17$ MeV. The full line through the data are recent calculations based on Refs. [5]-[16].

of ^{252}Cf. Monte-Carlo simulation of the response function allowed to establish the efficiency curve for the whole neutron energy range [19]. In Fig. 2 all four obtained neutron energy distributions are shown. The increasing contribution of secondary neutrons with increasing neutron energy, i. e. increasing deuteron energy, is obvious exceeding 80 % of the total flux at $E_n = 21$ MeV. As a general result one can say, that the spectra confirm the basic input data used for correcting the previous data from Ref. [12]. However, the data will be analised again together with the new data collected in 2006.

The cross-section measurements were carried out by using a twin Frisch-grid ionization chamber, whose construction and operation is described elsewhere [17]. Since the detector can be operated in back-to-back geometry, the protactinium sample was mounted on one side of the chamber together with a known ^{238}U sample (132.2 μg/cm^2 as reference on the other side. The isotopic purity was given to be 99.9997 % [20]. Details about the measurement technique may be found in Refs. [12, 13, 14]. A detailed analysis of the experimental data is still ongoing.

[1] C. Rubbia et al., Conceptual design of fast neutron operated high-power energy amplifier, CERN report CERN/AT/95-44(ET) 1995

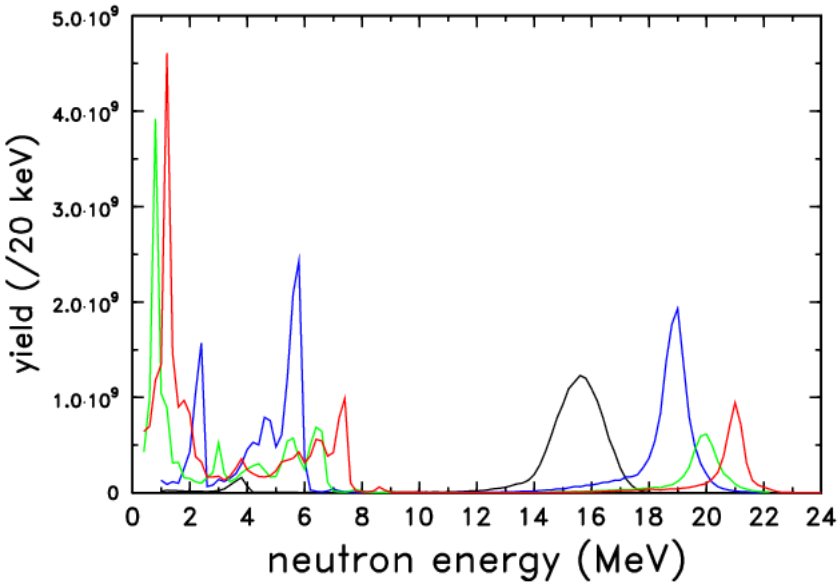

Fig. 2: Neutron energy spectra from the T(d, n)^{4}He reaction taken at 0^o relative to the deuteron beam: E_n = 16 MeV (black), 19 MeV (blue), 20 MeV (green) and 21 MeV(red).

[2] IAEA, CRP Evaluated nucler data for the Th-U fuel cycle

[3] F. Tovesson, F.-J. Hambsch, A. Oberstedt, B. Fogelberg, E. Ramström and S. Oberstedt, Phys. Rev. Lett. 88 (2002) 062502-1

[4] F. Tovesson, E. Birgersson, M. Flenéus, B. Fogelberg, V. Fritsch, C. Gustafsson, F.-J. Hambsch, A. Oberstedt, S. Oberstedt, E. Ramström, A. Tudora, G. Vladuca, Nucl. Phys. A 733 (2004) 3

[5] G. Vladuca, F.-J. Hambsch, A. Tudora, S. Oberstedt, A. Oberstedt, F. Tovesson, D. Filipescu, Nucl. Phys. A740 (2004) 3-19

[6] M. Petit et al., Nucl. Phys. A735 (2004) 345

[7] K. Kobayashi et al., Report Kurri-tr-8 10 (1975)

[8] D. W. Muir and L. R. Vessor, LA-4648 (1971)

[9] S. Plattard et al., Phys. Rev. Lett. 46 (1981) 633

[10] O. Birgul, S. J. Lyle, Radiochimica Acta 11 (1969) 108

[11] K. Kobayashi et al., Nucl. Sci. Eng. 139 (2001) 273

[12] S. Oberstedt et al., NP Scientific Report, EUR Report 22239 EN, ISBN 92-79-01939-2 (2006) 9

[13] S. Oberstedt et al., NP Scientific Report, EUR Report 21840 EN, ISBN 92-79-00310-0 (2005) 9

[14] S. Oberstedt, A. Oberstedt, F.-J. Hambsch, V. Fritsch, G. Lövestam, N. Kornilov, Ann. Nucl. Energy 32 (2005) 1867-1874

[15] G. Vladuca, A. Tudora, F.-J. Hambsch, S. Oberstedt, Nucl. Phys. A707 (2002) 32-46

[16] G. Vladuca, F.-J. Hambsch, A. Tudora, S. Oberstedt, NP Scientific Report, EUR Report 21840 EN, ISBN 92-79-00310-0 (2005) 12

[17] C. Budtz-Jørgensen, H.-H. Knitter, C. Stræde, F.-J. Hambsch, R. Vogt, Nucl. Inst. Meth. A258 (1987) 209

[18] A. Fessler, A. J. M. Plompen, D. L. Smith, J. W. Meadows, Y. Ikeda, Nucl. Sci. Engin. 134 (2000) 171-200

[19] I. Fabry and N. Kornilov, private communication, to be published

[20] F. Vivès, F.-J. Hambsch, H. Bax, S. Oberstedt, Nucl. Phys. A662 (2000) 63-92

The nuclear fission process

Ternary α and triton emission in the spontaneous fission of ^{244}Cm, ^{246}Cm and ^{248}Cm and in the neutron-induced fission of ^{243}Cm, ^{245}Cm and ^{247}Cm

S. Vermote[1], *C. Wagemans*[1], *O. Serot*[2], *J. Heyse*[1†], *J. Van Gils*[3], *T. Soldner*[4], *P. Geltenbort*[4]

[1] Dept. Subatomic and Radiation Physics, University of Gent, B-9000 Gent
[2] CEA Cadarache, DEN/DER/SPR/LEPh, F-13108 Saint-Paul-lez-Durance
[3] European Commission, JRC-IRMM, B-2440 Geel
[4] Institut Laue-Langevin, F-38042 Grenoble

Nuclear fission is essentially a binary process, but once every 300 - 400 fission events the two heavy fragments are accompanied by a light charged particle. In this so-called ternary fission process, mostly H and He isotopes are emitted. Due to the strong focusing effect of the Coulomb field, the particles are mainly emitted almost perpendicular to the fission axis and obviously their emission probability and energy distribution will be influenced by this field [1]. But also other parameters will have an impact on the emission probability: for instance, in a study of the ternary α emission probabilities for five spontaneously fissioning plutonium isotopes, Serot and Wagemans [2] demonstrated the dependence on the fissility parameter Z^2/A, the α cluster preformation probability factor S_α and the fission modes (or neutron shell effects).

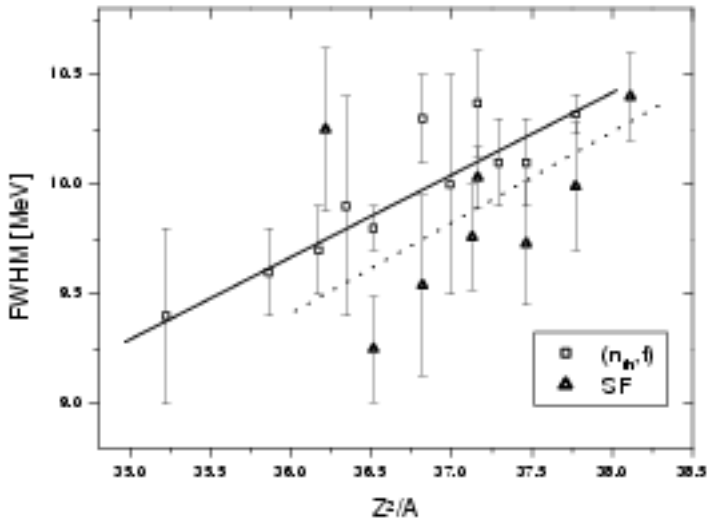

Fig. 1: FWHM for the ternary α energy distributions as a function of Z^2/A with a linear fit through the neutron induced fission data (full line) and the spontaneous fission data (dashed line)

Curium isotopes (proton number Z = 96) provide another excellent opportunity to investigate

†present address: SCK•CEN, B2400 Mol

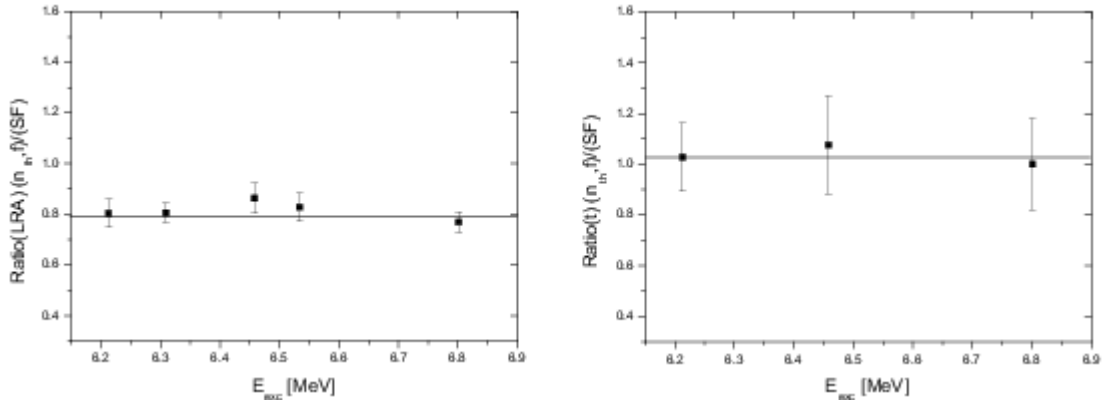

Fig. 2: Left: Ratio of the ternary α emission probabilities for neutron-induced and spontaneous fission of the curium isotopes, ^{240}Pu and ^{242}Pu as a function of the excitation energy. Right: Ratio of the ternary triton emission probabilities for neutron-induced and spontaneous fission of the curium isotopes as a function of the excitation energy. In both cases, the straight line corresponds to the weighted average of the results.

not only the influence of Sα and Z^2/A on the characteristics of ternary particle emission, but also of the excitation energy of the compound nucleus. Six curium isotopes have a sufficiently long half-life to permit the preparation of samples. Three of these isotopes (^{244}Cm, ^{246}Cm, ^{248}Cm) have a sufficiently small half-life for spontaneous fission to permit ternary fission measurements, three others (^{243}Cm, ^{245}Cm, ^{247}Cm) have a large fission cross section with thermal neutrons and a negligible spontaneous fission decay. Hence, ternary fission characteristics of the fissioning systems ^{244}Cm, ^{246}Cm and ^{248}Cm can be studied at zero excitation energy (spontaneous fission) and at an excitation energy of about 6.5 MeV (neutron induced fission).
In this work the emission probabilities and the energy distributions of the particles with the largest emission probability, i.e. ^{3}H and ^{4}He, have been studied for two reasons:

a. a different behaviour of ternary α and triton emission was observed in a systematic study by Wagemans [3];

b. triton emission yields are requested by nuclear industry for safe manipulations of radioactive waste [4].

The particle identification was done with suited ΔE-E telescope detectors, at the IRMM (Geel, Belgium) for the spontaneous fission and at the ILL (Grenoble, France) for the neutron-induced fission measurements. The present work provides for the first time experimental data on the ternary α and triton emission for the fissioning systems ^{244}Cm, ^{246}Cm and ^{248}Cm in the ground state and at an excitation energy of about 6.5 MeV. These results significantly enlarge the available data base and permit a few important observations:

- As shown in Fig. 1, the FWHM for the ternary α energy distribution is about 0.3 MeV smaller for spontaneous than for neutron-induced fission. Moreover it linearly increases with increasing Z^2/A. This confirms the well-known phenomenon already observed for fission fragments, that excitation energy enlarges kinetic energy distributions.

- Fig. 2 demonstrates that, despite an excitation energy of about 6.5 MeV, the ternary α emission probability is about 20 % lower in neutron-induced than in spontaneous fission. The triton emission on the other hand is hardly affected by this excitation energy. This can be explained by the strong impact of the α cluster preformation probability on ternary α emission.

A detailed discussion of the results can be found in [5].

[1] C. Wagemans, The Nuclear Fission Process, CRC Press, Boca Raton, Florida (USA) (1991)

[2] O. Serot and C. Wagemans, Nucl. Phys. A641 (1998) 34

[3] C. Wagemans, Proc. Seminar on Fission Pont d'Oye II, Habay-la-Neuve, Belgium (1991) 61

[4] *Compilation and evaluation of fission yield nuclear data*, IAEA-TECDOC-1168 (2000)

[5] S. Vermote, C. Wagemans, O. Serot, J. Heyse, J. Van Gils, T. Soldner, P. Geltenbort, Nucl. Phys. A (2008) http://dx.doi.org/10.1016/j.nuclphysa.2008.03.006

Left-right and angular asymmetry of fission neutron emission

N. Kornilov[1], *F.-J. Hambsch*[1], *I. Fabry*[1], *S. Oberstedt*[1], *S. P. Simakov*[2]

[1] European Commission, JRC-IRMM, B-2440 Geel
[2] Forschungszentrum Karlsruhe, Institute for Reactor Safety, D-76021 Karlsruhe

Following a recommendation of the NEA Working Party on Evaluation cooperation (WPEC) the prompt fission neutron spectrum (PFNS) was measured at $\approx$ 0.5 MeV incident neutron energy [1].
Three experiments were carried out at the 7 MV Van de Graaff accelerator of the IRMM in Geel, Belgium, using the fast neutron time-of- flight technique. A pulsed proton beam of about 1.0 - 1.5 ns FWHM at 1.25 - 2.5 MHz repetition rate and 0.2 - 0.8 μA average current was used. Mono- energetic neutrons of 0.52 MeV average energy were produced using the ^{7}Li (p, n) reaction. A metallic ^{235}U sample (93.15 % enrichment, 161.28 g) and a similar sized lead sample were applied for foreground and background measurements, respectively.
In a first run (Jul06) an angular dependent effect was found. The neutron yield is $\approx$ 10 % higher and the average secondary neutron energy about 80keV higher at 120^o compared to 90^o. The result was discussed at the Nice ND2007 conference [2]. This unusual finding stimulated new investigations to verify and to identify the nature of this effect. In a second experiment (Apr07) we used three identical neutron detectors at a flight path of 2.24 $\pm$ 0.01 m placed at 90, 150 and 120^o. The distance from the neutron production target to the sample was $\approx$ 8 cm.
In a third experiment (Jan08) the same detectors were applied. Two of them were placed at 90^o to the left (L90) as well as to the right (R90) side relative to the proton beam direction. The third detector was placed at 150^o to the right side (R150). Flight paths had a length of (2.25 $\pm$ 0.01) m. The sample was placed at (8.5 $\pm$ 0.2) cm from the neutron target (position 0) and displaced also along the axis between detectors R90 and L90 at $\pm$3 cm and $\pm$7 cm. The plus sign means, that the sample was moved towards the R90-detector, and the minus sign, that it was moved in opposite direction towards detector L90. The third detector can see the sample only in the 0-position. Results for the sample in the 0-position only are discussed in this report. In each experiment neutron detectors were shielded against direct and room-scattered neutrons.
The traditional pulse-shape analysis was applied to reduce the γ-ray background. A small Pilot-U scintillation detctor was used as proton pulse-shape monitor. The data were collected in list mode for further off-line analysis. The detector efficiency was measured relative to the ^{252}Cf standard neutron spectrum. A specially designed low mass, fast ionization chamber [3] was put at the place of the U-sample keeping the same geometry as during the experiments. The energy spectra were corrected for detector efficiency, for neutron multiple scattering in the sample, and for time resolution. A detailed description of the experimental procedure will be published elsewhere [4].
The pulse mode operation of the VdG was not the same during all experiments. The FWHM was between 1 - 1.5 ns in all experiment. However, some tailing is observed, which could not

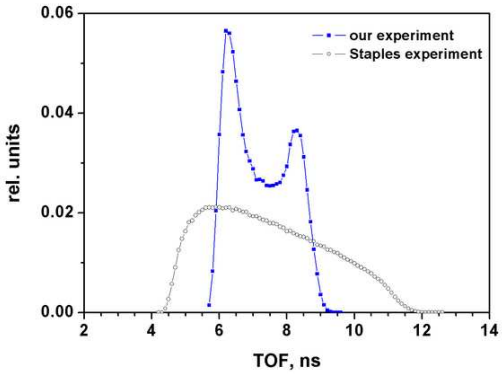

Fig. 1: Comparison between the TOF distribution of the input neutrons inside the sample for the present experiment (full symbols) and the one from Ref. [6](open symbols). The data are from a Monte Carlo simulation.

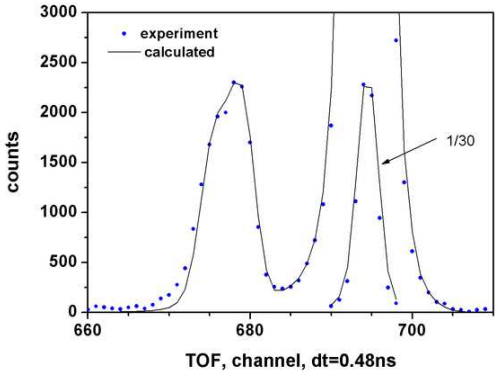

Fig. 2: Prompt γ-rays peaks measured with the detector at 90^o (R90, Jan08 run). The detector threshold is 1.2 MeVee. The channel width is 0.47 ns. The convoluted result is also given. The target γ-rays (right peak) give detector resolution and proton pulse-width. The prompt fission γ-rays give the total timing resolution including the neutron spread inside the sample (Fig. 1)

be removed completely. The worst tailing existed during the Jul06 experiment. The best beam quality was eventually realized during the third experiment, with a FWHM around 1 ns and a FW(1/1000)M $<$ 10 ns. We re-calculated the time resolution correction for the measured spectra from the Jul06 run published before [3, 5]. An additional energy dependence in the neutron detector efficiency at E $>$ 4 MeV has been taken into account, too. This factor slightly reduced the PFNS in the energy range between 5 - 8 MeV and the average secondary neutron energy by up to about 15 keV in the first run.

The time resolution of the neutron TOF spectrometer consists of the following components: detector resolution, shape of the pulse from the accelerator and neutron distribution inside the sample. The latter factor is very important. Fig. 1 shows the TOF intensity distribution of the incident neutrons inside the sample for our experiment compared to the one in Ref. [6]. Clearly the double peaked intensity structure of our ring shaped sample is visible in contrast to the very broad distribution of the very large sample (7.7 cm diameter) of Ref. [6]. This factor together with a shorter flight path length of only 1.63 m and despite of a very short proton burst of 0.6 ns is very important for data comparison. Consequently, the experimental data of Ref. [6] were corrected for time resolution assuming the same contribution of the detector resolution as in the present experiment. The measurered time resolution together with the calculated one, taking all above mentioned factors into account, are compered in Fig. 2. The experimental PFNS were normalized to unity and the average secondary neutron energy was calculated. A Maxwellian spectrum was fitted in the energy range of 0.7 - 1.5 MeV and 9 - 11

Tab. 1: Average energies of the PFNS for all angles and runs. The letters shows left-L and right-R sides of the detector relative to the proton beam, ΔE = 0.010 MeV.

detector orientation relative to beam axis (^{o})	$< E >_{jul'06}$ (MeV)	$< E >_{apr'07}$ (MeV)	$< E >_{jan'08}$ (MeV)
R90	2.004	2.002	2.021
L90	-	-	2.007
L120	2.076	2.050	-
R150	-	2.026	1.975

Tab. 2: Average spectral ratios $< R > =$ N$(E, R90)$/N$(E, L90)$ and their respective errors for different energy intervals

E_1 - E_2 (MeV)	$< R > \pm \delta R$	E_1 - E_2 (MeV)	$< R > \pm \delta R$
0.8 - 2	0.999 ± 0.003	5 - 6	1.009 ± 0.005
2 - 3	1.010 ± 0.002	6 - 8	1.051 ± 0.006
3 - 4	1.020 ± 0.005	8 - 10	0.970 ± 0.032
4 - 5	1.034 ± 0.004		

MeV to the measured spectrum, and an extrapolation to zero and to 20 MeV was performed. Based on our detailed analysis of all incorporated corrections and possible uncertainties we conclude that the average energy is estimated with an accuracy of $\pm$ 0.010 MeV. The average energy for all measurements are given in Table 1.
The PFNS at all investigated angles and for all runs are shown in Fig. 3 as a ratio to a Maxwellian distribution with the average energy $< E > =$ 2.002 MeV.
The following pecularities are highlighted:

a. The data demonstrates the variety of the prompt neutron spectrum shape. The difference exists not only for various detector angles but for detectors placed at 90^o left and right of the proton beam axis (see Jan08 R90, L90 in Fig. 2 and Tabs. 1 and 2).

b. The normalized spectra are fixed at low and high energies (see Fig. 3). The yields integrated between 1.3 - 2.3 MeV and 8 - 10 MeV are constant. The standard deviations of 8 spectra are 0.6 % and 3 %, respectively.

c. Among the data one may find a result which agrees perfectly with one of the old

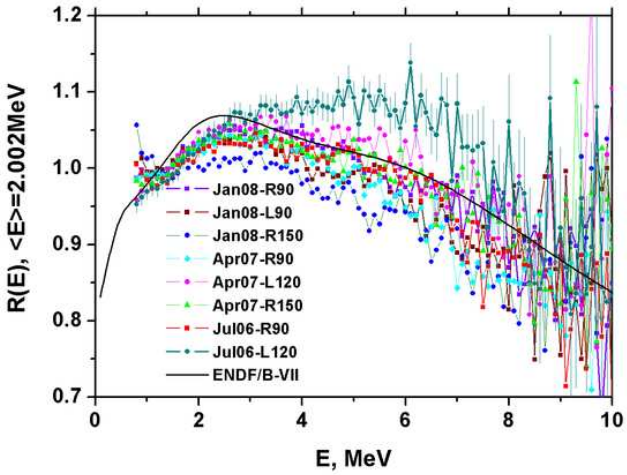

Fig. 3: Comparison between all our results (full symbols). ENDF/B-VII spectrum is given as full line

experiments or evaluations.

A comparison between the present experiments and literature values are given in Figs. 4-8. The spectra measured at thermal energy were normalized to a Maxwellian with reduced average secondary energy, i. e. $< E_{th} > = 0.995 \times < E_{0.5MeV} >$.
Before starting any scientific discussion about the nature of this strange behavior of the PFNS one should answer the main question: is this a real effect or an experimental artifact?
The experiments were carried out relative to the standard ^{252}Cf spectrum measured in the same experimental conditions. Therefore, a lot of mistakes such as flight path differences, uncertainties in the time channel width, a possible time reference shift (T_0 value) connected with the detector operation, a distortion of the spectrum due to scattering in the collimator were drastically reduced or even cancelled. The shift of T_0 versus pulse height was investigated. After application of an additional correction as a function of pulse height, the residual peak shift was smaller than 0.1 ns (ADC channel width was 0.117 ns).

We investigated a possible change of the ^{252}Cf spectrum due to different emission angles of the neutrons relative to the electrode plates in the ionization chamber. The ionization chamber was rotated relative to its vertical axis and the neutron spectra were measured by two detectors at 90, and 120^o [4]. No influence was found.
The spectrum shape may be distorted due to the proton pulse shape (VdG pulse mode operation) and a possible mistake in the time resolution correction. In this case the high energetic part of the spectrum (most sensitive to the time resolution) should be distorted. Since we observe the same integrals for the energy interval 8 - 10 MeV this argument is not valid. In addition, this factor is common for all detectors and can not explain the observed difference between them.
So the most sensitive factor is the stability of the detectors and the correct estimation of the T_0 value. The detector efficiency might be arbitrary changed in between the Cf and U measurements. As one can see in Fig. 2 the prompt fission γ peak (the zero time (T_0

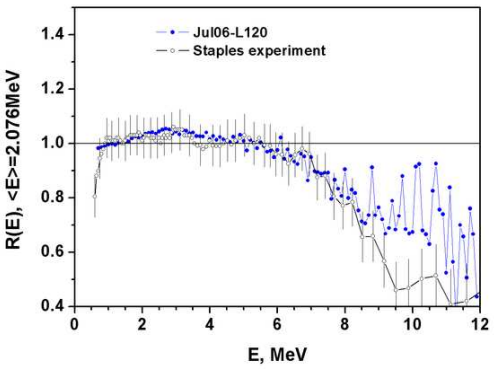

Fig. 4: Comparison between our result (Jul06, L120 detector) and data from Ref. [6]

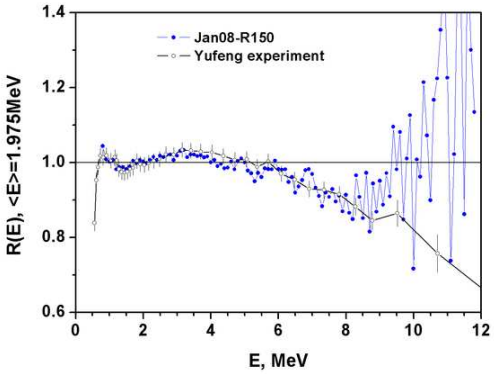

Fig. 5: Comparison between our result (Jan08, R150 detector) and data from Ref. [7]

is determined relative to this prompt peak position) is very well separated from the main component due to prompt gamma rays from the target and T_0 can be deduced with an accuracy of 0.1 ns. In addition to provide a measured difference between the spectra we should shift T_0 in the opposite direction depending on the neutron detector.

We simulated the influence of both factors. The results are given in Fig. 9. We calculated the spectrum with the nominal parameters, with a shifted T_0 by 1 ns and with a distorted detector efficiency by the function 1.0 $\pm$ 0.1 (1.7 - E), E $<$ 1.7 MeV. The influence of these factors may provide an effect comparable with the data spread shown in Fig. 3, the average secondary energy varied by $\pm$ 70 keV. However, a shift of T_0 by 1 ns changed the integral in the energy range 8 - 10 MeV by 28 % which is about 10 times higher then the real data spread in Fig. 3, so we can also exclude this. Another possibility would be that the distortion factor is connected with instabilities of the threshold and neutron-gamma discrimination parameters. The detector efficiencies were measured before, in the middle, and after the U run in each experiment. The U-spectra shown in Fig. 3 are sums of several (5 - 7) runs measured during 10 - 20 hours, so the direct comparison of the separate spectra may answer this question about the detector stability. According to the results given in Figs. 10 and 11 there is no evidence for a detector instability which may provoke the change in the measured results. In addition the detector efficiencies are in very good agreement with calculated results using the NEFF7 code [12], see Fig. 12.
These arguments are valid for each of the experiments, and the present conclusion is that we measured a real effect and no experimental artifact!

On the basis of the above discussion one may conclude that a factor exists which has a rather strong influence on the PFNS shape and asymmetry effects but was not fixed in our investigations and in all available experiments performed during the long history of fission investigations. One may assume that this factor is the neutron polarization. In the preparation stage of any PFNS experiment it was assumed that this factor is not important or by definition should be equal to zero. If this explanation is true, the transmission mechanism of the information from

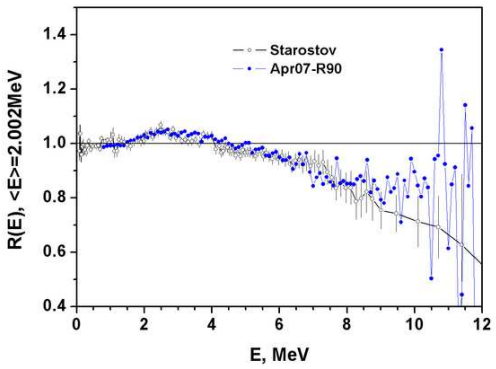

Fig. 6: Comparison between our result (Jul06, R90 detector) and data from Ref. [8]

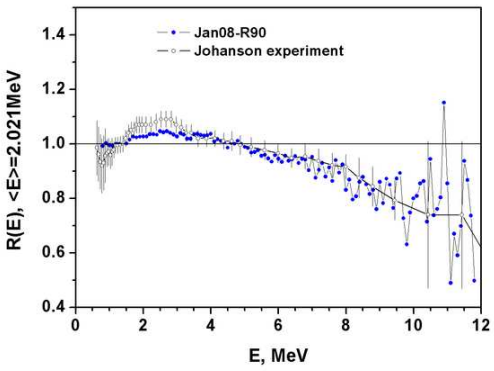

Fig. 7: Comparison between our result (Jan08, R90 detector) and data from Ref. [9] corrected with multiple scattering and angular distribution from the T(p, n) reaction taken from Drosg's evaluation [10]

the incident neutron to the secondary fission neutron should be found. The only possibility might be scission neutron emission, a fast process without formation of the compound nucleus. This may provide the link between the incident neutron and the secondary fission neutron. We should have in mind that three particles (two fission fragments and a scission neutron) are emitted at the same time which complicates the problem a lot.
The information about scission neutron emission is very poor. It was estimated in Ref. [13] that the probability of fission with scission neutron emission is $\approx$ 40 %, that the spectrum of scission neutrons consists of a low ($\sim$ 0.8 MeV) and a high energy component ($\sim$ 2.5 MeV). In Ref. [14] evidence was given that scission neutrons are emitted by fission fragments with high total kinetic energy (TKE) (compact system). From the results of this paper we estimate a high energy limit for scission neutron emission of $\sim$ 8.5 MeV. The questions is now, which parameters should be changed to provide the variety of results given in Fig. 3.

In case of scission neutron (SCN) emission, fission neutrons should be emitted from three sources:

a. Neutrons from fragments after fission of the compound nucleus A+1

$$N_{A+1}(E) = (1-\alpha)\, W_{A+1}(E) \quad , \tag{1}$$

where α is the share of scission neutrons emitted, and W_{A+1} is the spectrum which describes the neutron emission from accelerated fragments;

b. Neutrons from accelerated fragments after fission of the nucleus A, which is formed after the emission of one SCN:

$$N_A(E) = \alpha(\nu-1)\, W_A(E)/\nu \quad . \tag{2}$$

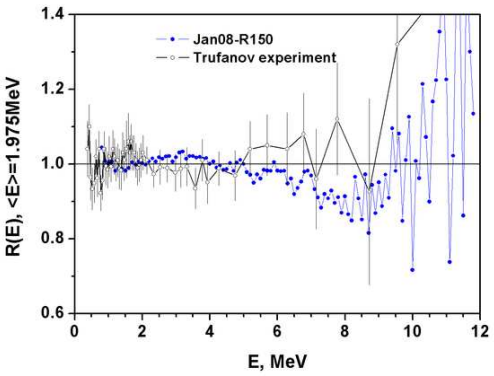

Fig. 8: Comparison between our result (Jan08, R150 detector) and data from Ref. [11]

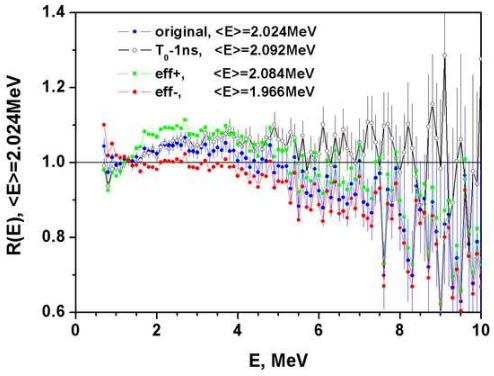

Fig. 9: The original spectrum and the ones estimated using different perturbation factors as given in the legend

c. Scission neutrons itself:

$$N_{SCN} = \frac{\alpha}{\nu} E \left(\frac{\zeta}{T_1^2} exp(-E/T_1) + \frac{1-\zeta}{T_2^2} exp(-E/T_2) \right) \quad , \tag{3}$$

where ζ is the share of the low energy component and ν is the neutron multiplicity.

The spectra W_A, W_{A-1} were calculated with a Watt distribution for light and heavy fragments with masses A_h = 140 and A_l = A -140. The ratio of the neutron multiplicity for light and heavy fragments was $\nu_l/\nu = \nu_h/\nu$ = 0.5. Temperature parameters were found based on the Fermi-gas relation and the thermal-equilibrium assumption with an additional correction of cor = 0.9 for the excitation of the heavy fragment $U_h = U_{0h}$ cor [13]. The level density parameter was calculated as a = A/c, c = 8.4, TKE = 170.5 MeV, ν = 2.45.
The equation for N_{scn}(E), and the corresponding parameters α, T_1 and T_2 were taken from Ref. [13] introducing minor corrections: α = 0.4, T_1 = 0.4 MeV, T_2 = 1.35 MeV. Changing only ζ from ζ = 0.2 to ζ = 0.6 allowed us to describe the spectrum shape with reasonable accuracy from the highest average secondary neutron energy $< E >$ = 2.070 MeV to the lowest $< E >$ = 1.967 MeV (Fig. 13). The spectrum with ζ = 0.31 extrapolated to thermal energy describes the integral experiments. The average ratio of the calculated cross sections to the experimental ones (Ref. [15], IRDF-2002) is $< R >$ = C/E = 0.997 $\pm$ 0.008. The average energy of the PFNS at thermal energy is $< E >$ = 2.038 MeV.
In conclusion, a very unusual result, not observed before was found in the present investigation. Presently, there is no model, able to explain this result. We may assume that a different mechanism of the fission process and of neutron emission should be incorporated.
For the moment we may only conclude, that the measured effect is not an experimental artifact. We should assume the existence of an additional factor (parameter), for example the neutron polarisation which may be responsible for the measured peculiarities. However, we did not demonstrate the direct link between this unknown parameter and the fission neutron spectrum, the left-right and angular asymmetry. At present we can not answer the very

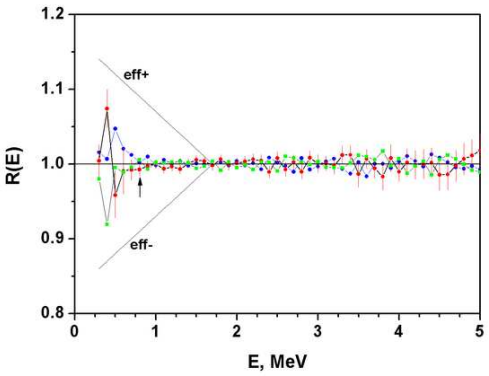

Fig. 10: The ratio of the detector efficiencies to the average value measured during the Jan08 experiment at the beginning, in the middle and at the end of the experiment. The distortion factors are shown by the full line. An arrow shows the cut-off energy in the data analysis.

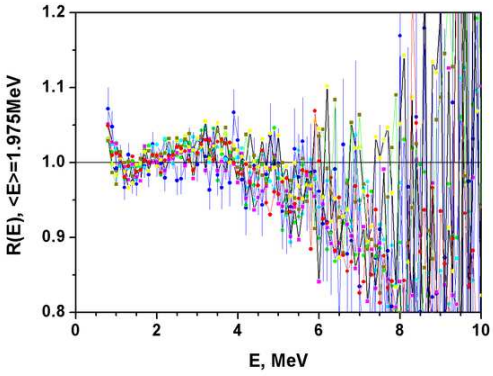

Fig. 11: The spectra measured with the 150R detector during the Jan08 run

important question, why the parameters of prompt fission neutrons changed so drastically and what is happening inside nuclear reactors. Evidently, a new type of experiments are urgently needed. In this respect, experiments with polarised thermal neutrons might be very interesting.

[1] D. G. Madland, ISBN-92-64-02134-5, NEA/WPEC-9, 2003

[2] N. V. Kornilov, F.-J. Hambsch, I. Fabry, et al., *Proc. of the Int. Conf. on Nucl. Data for Sci. and Tech.*, ND2007, Nice, France, April 2007, to be published

[3] N. V. Kornilov, F.-J. Hambsch, S. Oberstedt et al., JRC-IRMM, Neutron Physics Unit, Scientific report 2005, (2006)67

[4] N. V. Kornilov, F.-J. Hambsch et al., Internal report GE/NP/01/2007/02/14

[5] N. V. Kornilov, F.-J. Hambsch, S. Oberstedt et al., JRC-IRMM, Neutron Physics Unit, Scientific report 2006, (2007) 37

[6] P. Staples, J. J. Egan, G. H. R. Kegel, A. Mittler and M. L. Woodring , Nucl. Phys. A591 (1995) 41

[7] W. Yufeng et al., Chin. J. Nucl. Phys. 11 (1989) 47 EXFOR32587.

[8] B. I. Starostov et al., Nejtronnaja Fizika (6^{th} Conf. for Neutron Phys., Kiev. 1983), 1984, T.2. C.285, 290, 294, EXFOR 40871, 40872, 40873

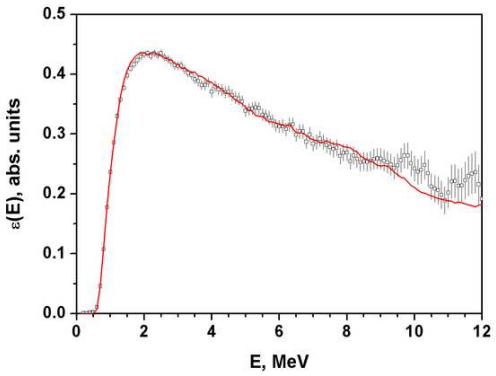

Fig. 12: The efficiency of one detector (Jan08, R150 detector) measured relative to ^{252}Cf and calculated with the NEFF7 code (full line).

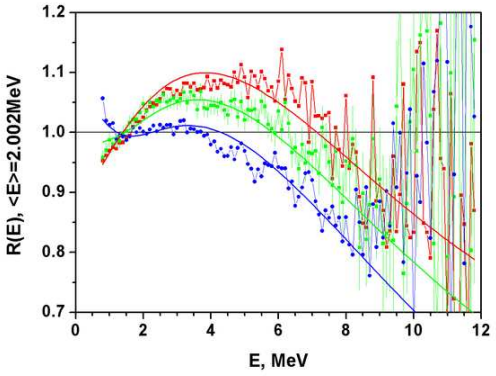

Fig. 13: Selection of experimental data and their description with a "3 source model" (full lines); blue: $\zeta = 0.6$; green: $\zeta = 0.4$; red: $\zeta = 0.2$ (for details see text)

[9] P.I. Johansson, B. Holmqvist, Nucl. Science Eng. 62 (1977) 695

[10] M.Drosg, http://www-nds,org/drosg2000.html

[11] A. M. Trufanov et al., J. Nucl. Phys. 57 (1994) 606

[12] G. Dietze, H. Klein, PTB-ND-22 Report (1982)

[13] N. V. Kornilov et al., Phys. At. Nucl. 62 (1999) 209 and Nucl. Phys. A686 (2001) 187

[14] N. V. Kornilov, F.-J. Hambsch, A. S. Vorobyev, Nucl. Phys. A789 (2007) 55-72

[15] K. I. Zolatorev, INDC(NDC)-448, 2003, 25

Test experiment on photo–induced fission of ^{238}U at the superconducting Darmstadt electron linear accelerator S–DALINAC

M. Köhler[1], *J. Enders*[1], *P. von Neumann–Cosel*[1], *A. Oberstedt*[2], *S. Oberstedt*[3], *S. Rathi*[1], *A. Richter*[1], *A. Shevchenko*[1]

[1] Institut für Kernphysik, TU Darmstadt, D-64289 Darmstadt,
[2] Institutionen för naturvetenskap, Örebro universitet, S-70182 Örebro,
[3] European Commission, JRC-IRMM, B-2440 Geel

Even 70 years after its first observation by Hahn and Strassmann [1], nuclear fission remains a topic of ongoing research. Besides studying fission channels and the structure of intermediate states (e. g., shape isomers) in the fission process, one has also observed parity violation, i. e., the influence of the weak interaction on the nuclear fission process. Parity violation effects of the order of a few times 10^{-4} have been observed following fission induced by polarized thermal neutrons [2, 3]. The effects are thus much stronger than one would anticipate from the ratio of the weak and strong interaction coupling constants. Enhancement factors – that are also observed in the helicity–dependent transmission of polarized neutrons in heavy nuclei (see [4] for an overview) – have first been discussed by Sushkov and Flambaum [5], but open questions persist and may be answered by using different experimental probes.

In order to study the feasibility of an experiment searching for parity violation in fission induced by polarized bremsstrahlung photons, a test experiment was set up, carried out, and analyzed at the superconducting Darmstadt electron linear accelerator S–DALINAC [6]. An early account of this test was given in last year's scientific report [7]. During the feasibility study, the performance of a double ionization chamber in an intense photon beam was to be studied, and a data analysis procedure was to be established in which the drift times of the fission fragments were used for the first time to extract the emission angle of the fragments.

The experiment was carried out at the experimental bremsstrahlung site [8] behind the superconducting injector linac of the S–DALINAC where electron beams with energies up to 10 MeV can be stopped completely in a copper radiator target and be converted into bremsstrahlung. Endpoint energies of 6.0 MeV through 8.5 MeV have been chosen, in steps of 500 keV, and electron beams (unpolarized) with currents of 10 μA were available at the time of the experiment. At the central cathode of a double ionization chamber [9], a 130 μg/cm^2 $^{238}UF_4$ sample was mounted, backed on one side by a polyimide foil and a gold layer to provide conductivity, and the two fission fragments were measured in coincidence of the two opposite anodes that were shielded from the cathode using Frisch grids. Drift times and anode and cathode pulse heights were measured and digitized.

In order to reconstruct the energy and emission angle of the fission fragments, the anode pulse heights have been plotted as a function of the time difference between the anode and the cathode signal. Figure 1 shows an intensity plot of the raw data for the example of the sample side. The data for the backing side look similar, but have slightly smaller pulse heights and the distributions are broader due to straggling in the backing material. The figure also shows that the heavier fragments with lower kinetic energy have shorter average drift paths $\overline{X}$ so that the

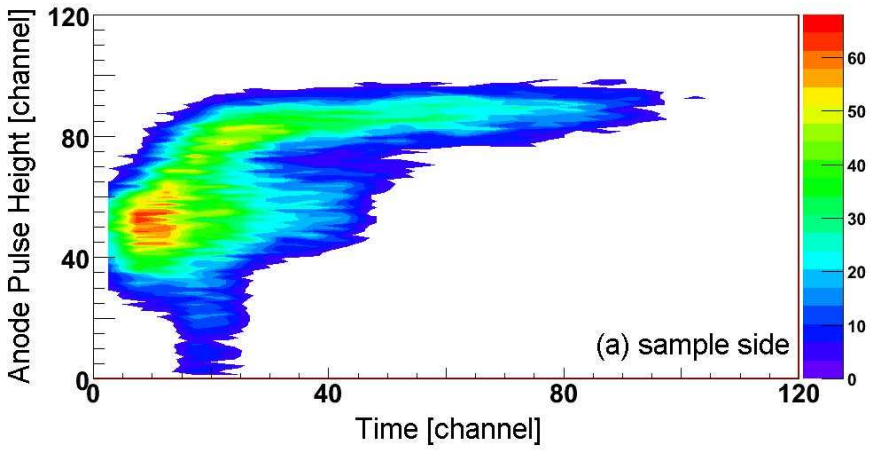

Fig. 1: Uncorrected anode pulse height versus drift time to the anode for the example of the sample side.

drift times t span a shorter interval. With distance D between cathode and Frisch grids and emission angle θ with respect to the perpendicular to the target plane, the proportionality

$$t \propto \frac{\overline{X}}{D} \cos\theta$$

holds.

Besides correcting for the pulse–height dependence of the drift times for extraction of the emission angle, the following corrections have been applied to the data. (i) The detection inefficiency due to the Frisch grids was taken into account. This depends on the geometry, pulse heights, and drift times [10, 11]. (ii) The pulse heights were corrected for angular–dependent energy loss. This was done for the sample and the backing side separately. (iii) The pulse–height defect results primarily from scattering off the nuclei in the detector gas so that the measured pulse height is not fully proportional to the kinetic energy of the fragments. The defect depends on the energy, charge, and mass of the fragments (after neutron evaporation). To correct for the effects of the pulse–height defect, the approach by Lindhard et al. [12] was used with the parameters for P–10 gas as derived by Budtz–Jørgensen and co–workers [9]. This is done in an iterative procedure starting with an approximation of the preneutron energies. For the determination of the postneutron energies and the pulse–height defect as a function of the postneutron energies and masses, the average number of evaporated neutrons was taken from the work of Pommé et al. [13].

Following the corrections, the anode pulse height as a function of the cosine of the emission angle was extracted as is shown in Fig. 2. A detailed description of the analysis of the present data can be found in the Thesis of M. Köhler [14]. Already Fig. 2 demonstrates that the emission angle of the fragments can be determined from the measured drift times.

Following these corrections, mass distributions and total kinetic energy distributions have been deduced. For this analysis only fragments emitted at angles smaller than 30° have been included. While some inconsistencies persist with the extracted mass distributions, the average total kinetic energy is in reasonable agreement with literature values [13] as is indicated in Fig. 3. Deviations might originate from the still limited statistical accuracy of the data sets.

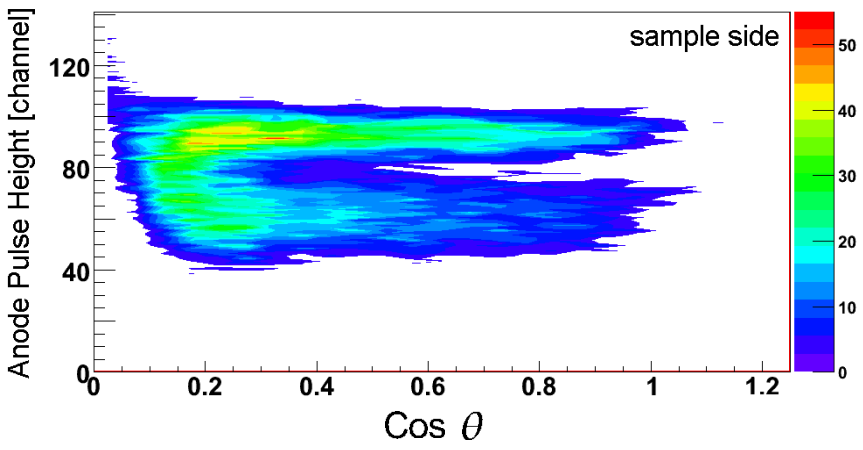

Fig. 2: Corrected anode pulse height versus the cosine of the fragment emission angle for the example of the sample side.

The extracted angular distribution (Fig. 4) is minimal at 0°, in good agreement with the expectations for fission following electric dipole excitations (with K quantum number 0), see [15]. However, as only emission angles $\theta < 30^\circ$ are trustworthy in the analysis, fit parameters for the angular distribution can be extracted with limited reliability only. Even in the literature [16, 17] there are contradictory results so that a precise measurement – especially as a function of the average excitation energy – would be desirable.

For estimating the feasibility of an experimental search for parity–violation effects in photo–induced fission, the yield of analyzable events is important. This quantity is shown in Fig. 5, including events emitted at angles below 60° only. An investigation of the data with endpoint energies of 8.0 MeV and 8.5 MeV showed that apparative asymmetries disturbing a dermination of forward–backward differences due to parity violation are smaller than 0.5% for emission angles below 30° while at larger angles deviations as high as ∼2% have been observed. The accuracy for determining intrinsic asymmetries is limited by statistics.

A future improved experiment should take the following aspects into account: (i) The setup should be rotated to include more analyzable results as the angular distribution is maximal at 90° with respect to the incident beam direction. (ii) Longer runs and higher beam intensities will help gathering enough data for a precise analysis of apparative asymmetries and determining mass and kinetic energy distributions for various endpoint energies. (iii) Optimizing the data analysis should resolve the discrepancies between the present mass distributions and the literature. (iv) While an experimental sensitivity of a few times 10^{-4} could be reached for a future parity–violation experiment based on an optimization of the present experimental setup, i.e., a twin ionization chamber, increasing the number of target atoms while keeping the present experimental mass and energy resolution would prove extremely helpful (e.g., an active target containing UF_6 gas).

We are indebted to M. Chernykh, Y. Poltoratska, and I. Pysmenetska for assistance with the data taking and to J. Hasper for the simulations of the bremsstrahlung spectrum using the code GEANT. The Darmstadt group acknowledges funding by the Deutsche Forschungsgemeinschaft through SFB 634.

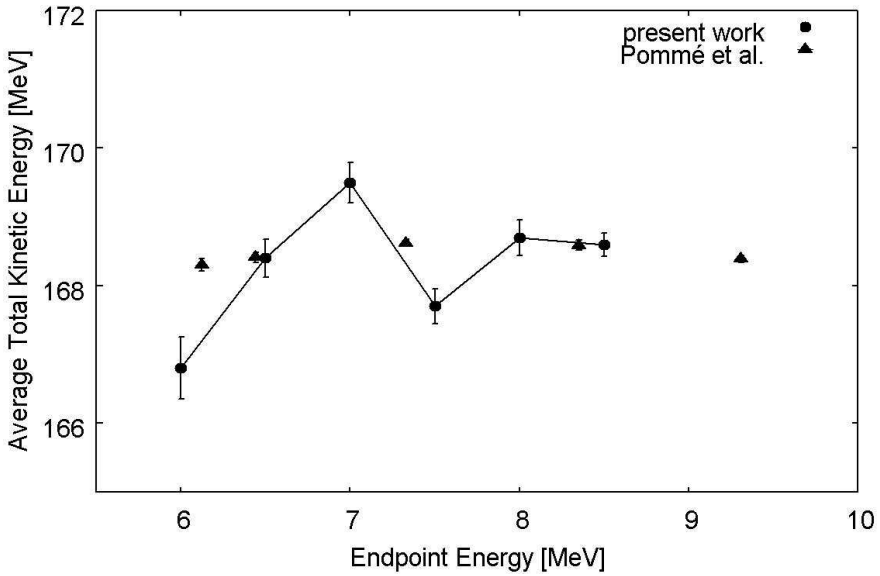

Fig. 3: Extracted centroid of the total kinetic energy distribution as a function of the bremsstrahlung endpoint energy.

[1] O. Hahn, F. Strassmann, Naturwissenschaften 27 (1939) 11

[2] G. Danilyan et al., JETP Lett. 26 (1977) 186

[3] V. P. Alfimenkov et al., Nucl. Phys. A 645 (1999) 31

[4] G. E. Mitchell, J. D. Bowman, S. I. Penttilä, E. I. Sharapov, Phys. Rep. 354 (2001) 157

[5] O. Sushkov, V. Flambaum, JETP Lett. 32 (1980) 352

[6] A. Richter, in S. Myers et al. (Eds.), Proc. 5th Eur. Part. Accel. Conf, Sitges, IOP Publishing, Bristol, Philadelphia (1996) 110

[7] J. Enders et al., Neutron Physics Unit Scientific Report 2006, p. 33

[8] P. Mohr et al., Nucl. Instrum. Methods in Phys. Res. A 423 (1999) 480

[9] C. Budtz–Jørgensen et al., Nucl. Instrum. Methods in Phys. Res. A 258 (1987) 209

[10] O. Bunemann et al., Canadian J. Research A 27 (1949) 191

[11] P. Siegler, Dissertation, Technische Hochschule Darmstadt (1994), D 17

[12] J. Lindhard et al., Kgl. Dansk. Vidensk. Selsk. Mat.–Fys. Medd. 33 (1963) 455

[13] S. Pommé et al., Nucl. Phys. A 572 (1994) 237

[14] M. Köhler, Bachelor Thesis, Technische Universität Darmstadt (2007)

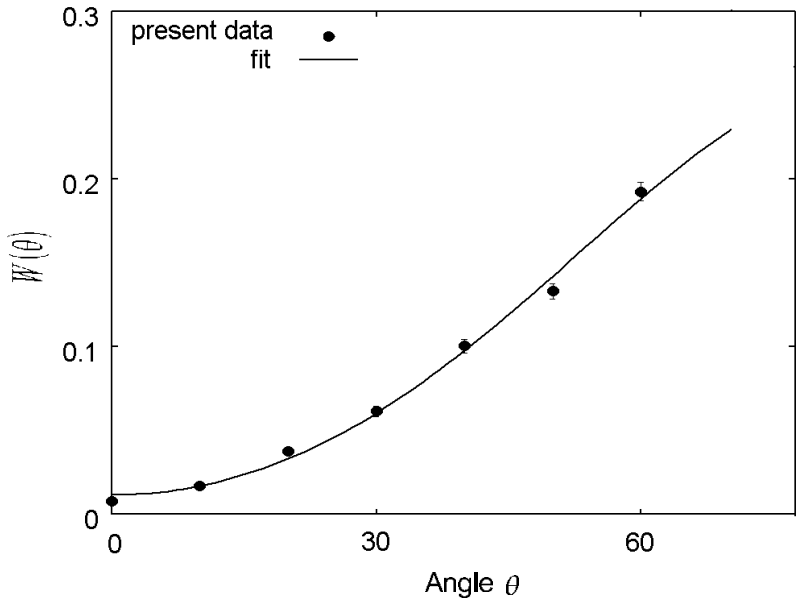

Fig. 4: Angular distribution of the average fragment emission angle.

[15] E. Jacobs, U. Kneissl, in: C. Wagemans (Ed.), *The nuclear fission process*, CRC Press, Boca Raton, ISBN 0-8493-5434-X (1991) 103

[16] N. S. Rabotnov et al., Yad. Fiz. 11 (1970) 508

[17] S. Kuniyoshi et al., Rev. Bra. Fis. 3 (1973) 441

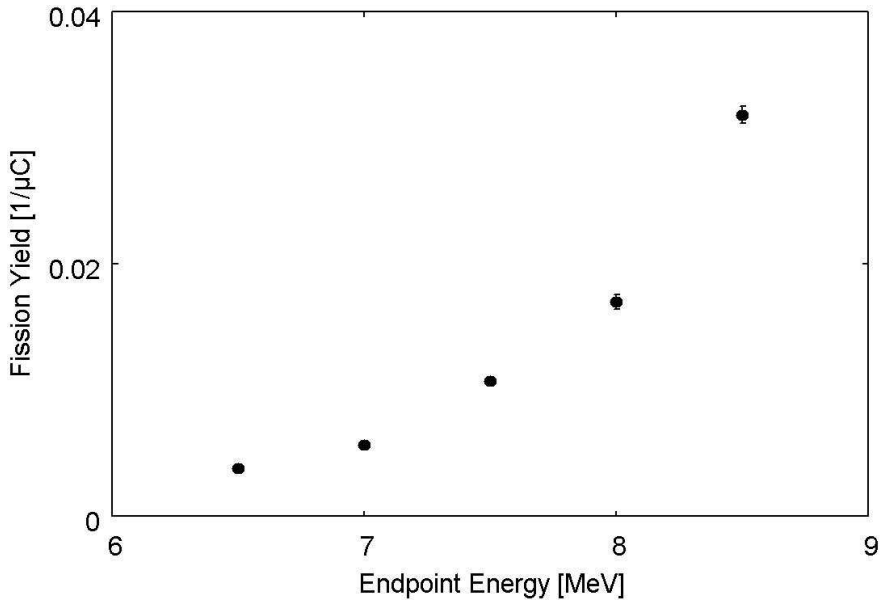

Fig. 5: Fission yield normalized to the total charge of the electron beam. Online fragment with emission angles $< 60^{\circ}$ have been included.

Search for the shape isomer in ^{239}U

S. Oberstedt[1], *A. Oberstedt*[2]

[1] European Commission, JRC-IRMM, B-2440 Geel
[2] Institutionen för Naturvetenskap, Örebro Universitet, S-70182 Örebro

Since the early 1960s many fission isomers have been discovered in nuclei ranging from ^{236}U to ^{245}Bk [1]. Their existence is a consequence of the appearance of a second minimum in the potential energy surface of actinide nuclei, as firstly described by Strutinsky [2] as the superposition of microscopic shell corrections in a nuclear potential to the nuclear binding energy, varying periodically with deformation, and the unstructured macroscopic part of the deformation energy usually described by the liquid-drop model. One of the persisting problems still recently was the lack of any shape-isomer half-life data for odd-N uranium and neptunium isotopes. Only for ^{239}U the apparent population of the super-deformed (SD) ground state in a neutron-induced capture experiment was observed [3, 4]. Since for these isotopes fission half-lives are expected to be in the order of several hundreds of μs or even longer, the detection with commonly used pulsed particle beams is very difficult. It is even more difficult in neutron-induced reactions, where the environmental background created from sub-sequent pulses is extremely disadvantageous. Together with the extremely low production cross-section for shape isomers, typically of the order of a few μb, as well as half-life predictions ranging in some cases over five orders of magnitude leaves the measurement of shape-isomer decay data to a challenging venture for the experimentalist.

A recent experiment performed at the pulsed neutron beam facility NEPTUNE [†)] of the IRMM led to the first observation of a fission-decaying shape isomer in the odd-N uranium isotope ^{235}U via the reaction ^{234}U + n. The deduced cross-section for shape isomer population of about 10 μb demonstrated the high sensitivity of the NEPTUNE facility [6] to detect rare decay processes. This motivated a measurement campaign to search for a fission-decaying shape isomer in ^{239}U for which the apparent population had been reported earlier [3, 4]. Predicted half lives range from 10 μs up to more than 100 ms [7, 8, 9]. The present experiment was sensitive to half lives roughly between 1 ms and several hundreds of ms depending on the population cross-section of the shape isomer in ^{239}U.

The 7 MV Van de Graaff accelerator of the IRMM created neutron beams with E_n = (1.8 $\pm$ 0.2) MeV, that were used at a pulse repetition frequency of 50 and 5 Hz. In all cases the duty cycle was chosen to be 50 %. The working principle of the NEPTUNE facility is explained in Ref. [5]. The neutrons impinged on the targets, placed in the center of a twin Frisch-grid ionization chamber with common anode (cf. Fig. 1). On the side closest to the beam a 0.9136 mg ^{238}U sample was mounted, whose contamination with ^{235}U was less than 3×10^{-6}. On the backside a ^{235}U sample with mass 2.38 mg was placed in order to serve as monitor for room-scattered and thermalized neutron induced fission. For the monitoring of direct and scattered neutrons a NE213 scintillator was placed in beam direction, allowing for

[†)] NEutron Pulses with TUNEable pulse structure

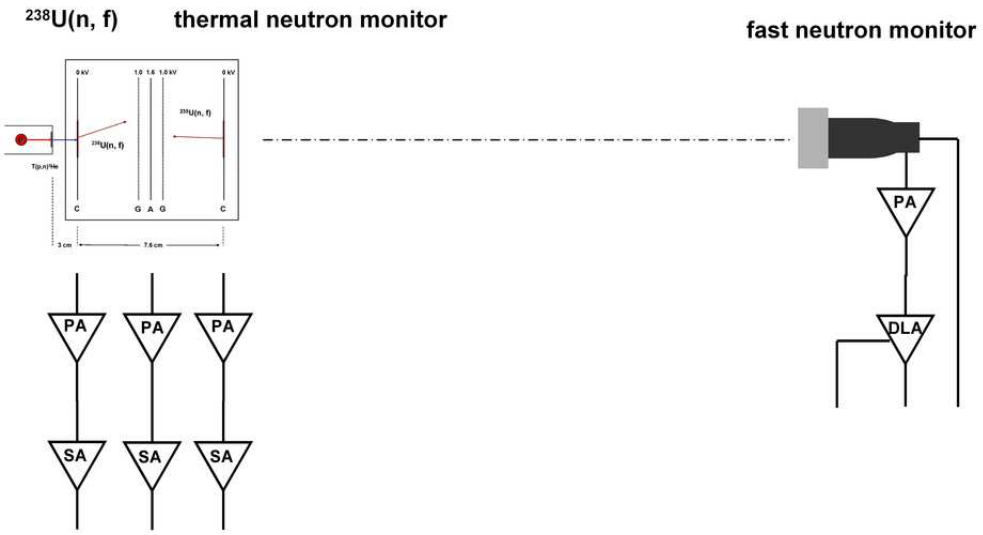

Fig. 1: Sketch of the experimental set-up: a twin Frisch-grid ionisation chamber with common anode was loaded with a 0.9136 mg ^{238}U sample (close to the neutron source) and a 2.38 mg ^{235}U sample serving as a monitor for room-scattered and thermalised neutrons. A NE213 equivalent liquid scintillator detector served as fast neutron monitor.

neutron-gamma separation by employing the pulse-shape discrimination technique.

In Fig. 2 the time of event relative to the start of the neutron pulse versus pulse height for neutron pulse repetition frequency of 50 Hz (left) and of 5 Hz (right) is shown. On both screen shots regular α-decay is visible at low pulse height values as atime-independent distribution. The lower half of the spectra corresponds to prompt neutron-induced fission. For both settings delayed events are observed, i. e. when the proton beam is deflected onto the beam dump and neutron production is inhibited, for which the pulse height is compatible with that of fission events. A detailed analysis will reveal, whether these events are due to room-sacttered neutrons or induced by cosmic radiation or, whether they correspond to true delayed fission from the decay of a shape isomer in ^{239}U.

From a first inspection of the raw data, however, the population cross-section of the shape isomer in ^{239}U seems to be considerably lower than the corresponding one in ^{235}U [6].

[1] B. Singh, R. Zywina and R. B. Firestone, Nuclear Data Sheets 97 (2002) 241

[2] V. M. Strutinsky, Nucl. Phys. A95 (1967) 420

[3] S. Oberstedt, F. Gunsing, Nucl. Phys. A589 (1995) 435

[4] S. Oberstedt, F. Gunsing, Nucl. Phys. A636 (1998) 129

[5] 'Exploratory Research at IRMM 2004', Final report, comp. by the IRMM scientific Committee, Internal Report GE/SCIRMM/ER/2005 (2005)

[6] A. Oberstedt, S. Oberstedt, M. Gawrys, and N. Kornilov, Phys. Rev. Lett. 99, 042502 (2007)

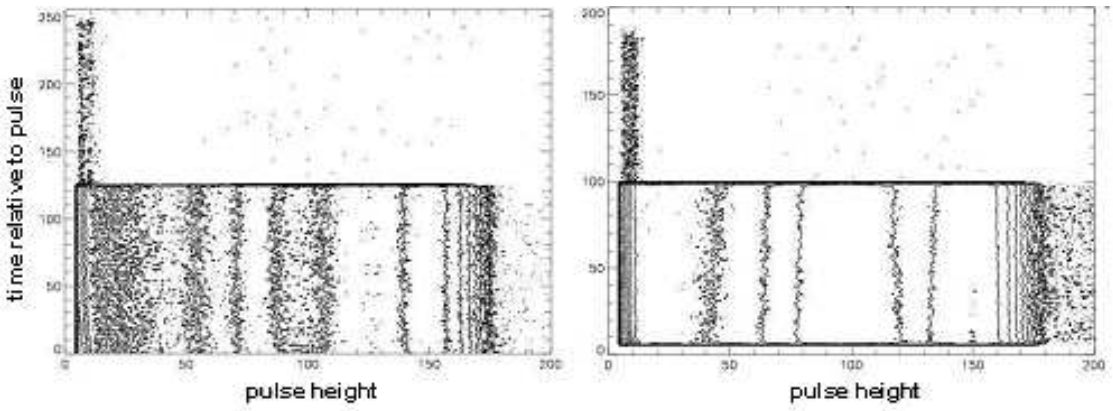

Fig. 2: Time of event relative to the start of the neutron pulse versus pulse height for a neutron pulse repetition frequency of 50 Hz (left) and for 5 Hz (right). In both cases the duty cycle is 50 %. On the left part of both spectra (screen shot) the events from regular α-decay are visible as a time-independent distribution. The lower half of the spectra corresponds to prompt fission. For both settings delayed events are observed for which the pulse height is compatible with fission events (see text).

[7] H. Weigmann and J. P. Theobald, Nucl. Phys. A187 (1972) 305

[8] S. Oberstedt, J. P. Theobald, H. Weigmann, J. A. Wartena, C. Bürkholz, Nucl. Phys. A (1994)

[9] V. Metag, Dissertation 1974, in S. Bjørnholm and J. E. Lynn, Rev. Mod. Phys. 52 (1980) 725

Nuclear reaction mechanisms and standards

Measurement of the ^{16}O(n, α_0)^{13}C cross section in the range 3.9 to 9.0 MeV

G. Giorginis[1], *V. Khryachkov*[1,2], *V. Corcalciuc*[1,3], *M. Kievets*[1]

[1] European Commission, JRC-IRMM, B-2440 Geel
[2] IPPE, RU-249020 Obninsk
[3] Horia Hulubei NIPNE, P. O. Box MG-6, RO-76900 Bucharest

First measurements of the ^{16}O(n, α)^{13}C cross section were performed in 2006 at IRMM in the energy range 4.9 to 7.4 MeV in response to a data request created in the High Priority Nuclear Data Request List (HPRL) of the Nuclear Energy Agency [1, 2]. Additional measurements in the energy intervals 3.9 - 4.4 MeV and 7.4 -9.0 MeV were performed in 2007 in order to investigate the most relevant structures of the ^{16}O(n, α)^{13}C excitation function in the energy range of the HPRL data request which is 2.5 - 10 MeV [2]. Mono-energetic neutrons below 4.4 MeV and above 4.9 MeV were produced at the 7 MV Van-de-Graaff accelerator of the IRMM by using T(p, n)^{3}He and D(d, n)^{3}He reactions, respectively. A 214 μg/cm^2 TiT layer with a silver backing was used in the former case. A deuterium gas target with a 5 μm molybdenum entrance window, 4 cm gas volume length, and a tantalum beam stop was used in the latter case. In all measurements deuterium pressures of 20 and 50 kPa were used below and above 7.5 MeV neutron energy, respectively. The 2006 and 2007 results obtained at IRMM are shown in Fig. 1 together with data from the ENDF/B-VI.8 [3] and ENDF/B-VII.0 [4] evaluations. There is good eye agreement with ENDF/B-VII.0 in the 3.9-4.4 MeV range but there is disagreement between 4.9 and 9.0 MeV.

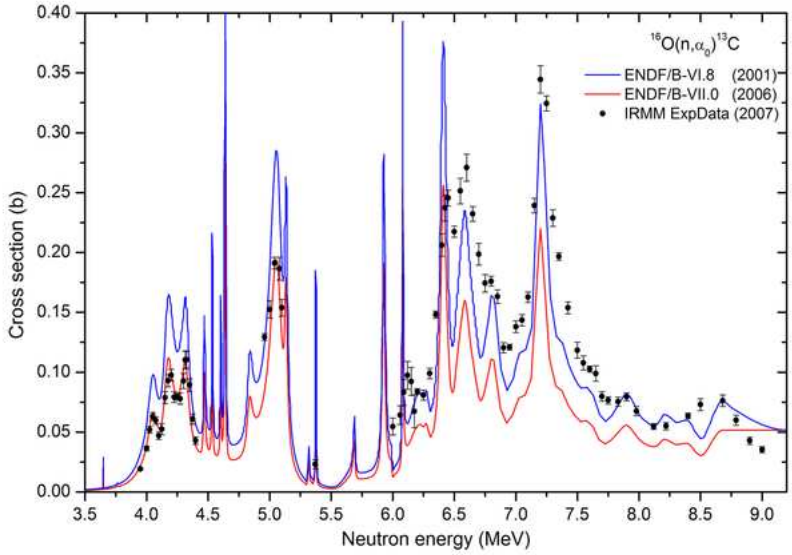

Fig. 1: Preliminary results of the 2006 and 2007 cross section measurements of ^{16}O(n, α_0)^{13}C at IRMM compared with the ENDF/B-VI.8 and ENDF/B-VII.0 evaluations

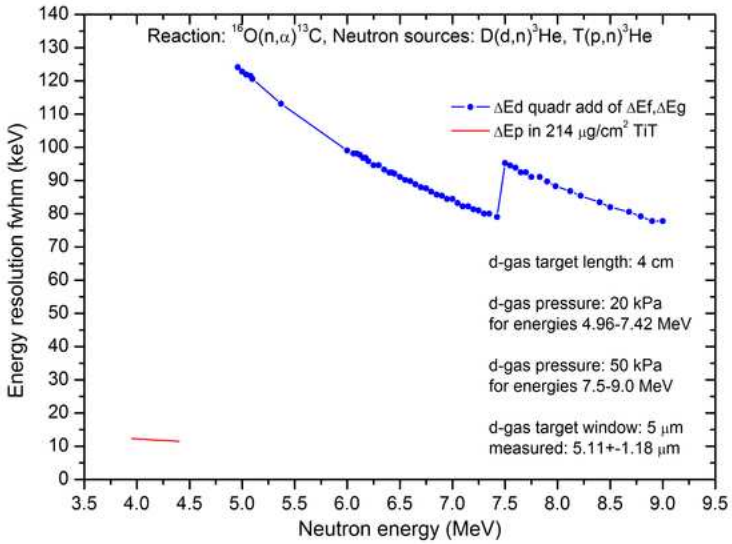

Fig. 2: Experimental energy resolution of the ^{16}O(n, α)^{13}C measurements at IRMM in terms of energy width of the charged projectile beams used for neutron production (protons and deuterons)

The broadening and shift of resonances in the 4.9 - 9.0 MeV range measured at IRMM is due to the low energy resolution of the D(d, n)^{3}He neutrons, which for the small neutron emission angle of the IRMM measurements ($\theta \approx 4^o$) is mainly determined by the energy width of the deuteron beam. Thickness inhomogeneities of the molybdenum foil window was the main reason for the poor energy resolution of the deuteron beam. Their effect was determined by transmission of monoenergetic α particles from a thin ^{241}Am source. The fwhm broadening of the α particle beam was equivalent to 1.18 μm of molybdenum. The energy broadening ΔE_f caused by this thickness to the deuteron beam was calculated and combined with the energy loss in the deuteron gas ΔE_g in order to obtain the energy resolution of the deuteron beam ΔE_d. The energy resolution of the neutrons in the 3.9 - 4.4 MeV range, which is determined by the energy loss of the protons ΔE_p in the TiT layer, was much higher than that of the D(d, n)^{3}He neutrons in the 4.9 - 9.0 MeV range as it can be seen in Fig. 2.

The neutron energy resolution of the IRMM measurements was on average 3 % and 2 % larger than the corresponding proton and deuteron energy resolution in the 3.9 - 4.4 MeV and 4.9 - 9.0 MeV ranges, respectively.

A correction of the IRMM cross sections for energy resolution was done by indirect deconvolution using the shape of the ENDF/B-VII.0 excitation function and the energy resolution of the charged projectile beams used for neutron production (protons and deuterons). Assuming that the ENDF evaluation is free of energy resolution effects the ENDF/B-VII.0 excitation function was convoluted with the distribution of the experimental energy resolution shown in Fig 2. Then the convolution curve was piecewise adjusted in height in order to fit to the IRMM data. The agreement of the eye-fitted convolution curve with the experimental data is very good as it can be seen in Fig. 3. A normalisation function was obtained from the height adjustment (not shown). Finally the ENDF/B-VII.0 excitation function was multiplied by the normalisa-

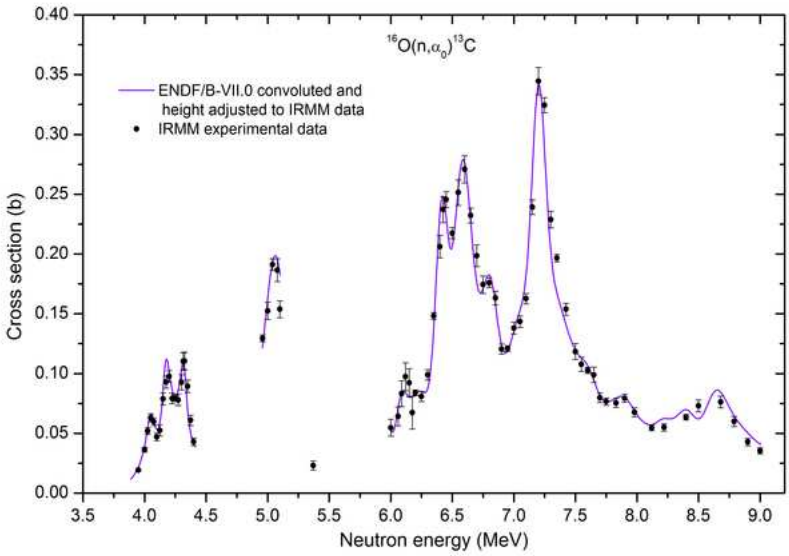

Fig. 3: Convoluted ENDF/B-VII.0 excitation function with the experimental energy resolution after height adjustment to the ^{16}O(n, α_0)^{13}C cross section which was measured at IRMM.

tion function and ENDF/B-VII.NEW was obtained in the energy regions of our measurement as shown in Fig. 4. The name ENDF/B-VII.NEW means a renormalisation of ENDF/B-VII.0, which in turn is a renormalisation of ENDF/B-VI.8 but not a new evaluation [1, 4].
From a comparison between ENDF/B-VI.8, -VII.0, and -VII.NEW the following cross-section ratios were obtained at the 4.32, 5.05, 6.42, and 7.2 MeV resonance positions: $\sigma_{VII.NEW}/\sigma_{VI.8}$ = 0.68, 0.90, 1.02 and 1.28, respectively, and $\sigma_{VII.NEW}/\sigma_{VII.0}$ = 1.0, 1.32, 1.50 and 1.88, respectively. ENDF/B-VII.NEW is in very good agreement with ENDF/B-VII.0 in the 3.9 - 4.4 MeV range and with ENDF/B-VI.8 at 6.42 MeV. Disagreement with ENDF/B-VII.0 occurs in the 4.9 - 9 MeV range, with substantially larger ENDF/B-VII.NEW values, and with ENDF/B-VI.8 below and above 6.42 MeV, with smaller and larger ENDF/B-VII.NEW values, respectively, except in the range 7.9 -8.25 MeV, where the agreement is very good.
The validity of the 32 % reduction of the ENDF/B-VI.8 values, which was applied to produce ENDF/B-VII.0 for the ^{16}O(n, α_0)^{13}C cross section in the neutron energy region 2.4 - 8.9 MeV [1, 4] is confirmed by the IRMM measurements only for energies below 4.4 MeV.
A measurement of the ^{16}O(n, α_0)^{13}C cross section in the region of 5 MeV resonance by using T(p, n)^{3}He neutrons is planned in 2008 in order to check the cross section scale by a comparison with the results obtained in 2006 using D(d, n)^{3}He neutrons in the same energy region. Cross section measurements of the excited states ^{16}O(n, $\alpha_{1,2,3}$)^{13}C are also planned at IRMM.

[1] G. Giorginis, V. Khriatchkov, V. Corcalciuc, M. Kievets, *Measurement of the ^{16}O(n, α)^{13}C cross section*, Neutron Physics Unit, EC-JRC IRMM Scientific Report, EUR 23039

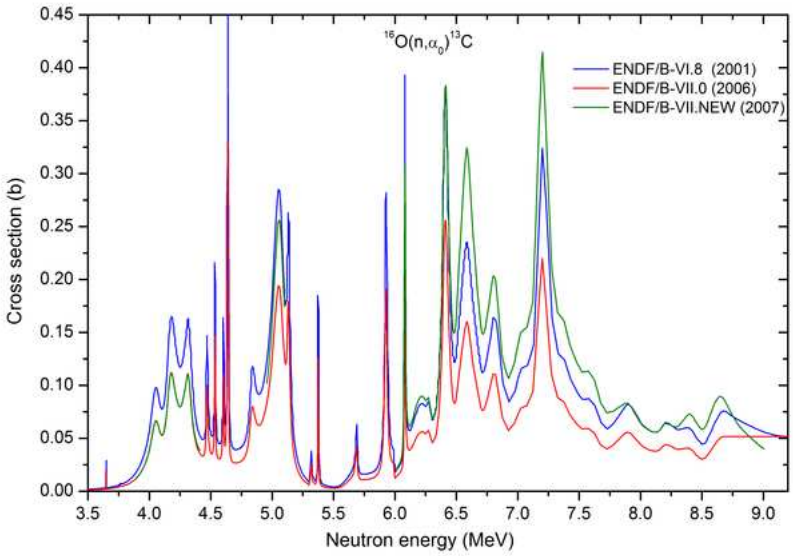

Fig. 4: ENDF/B-VII.0 and ENDF/B-VI.8 in comparison with ENDF/B-VII.NEW for the ^{16}O(n, α_0)^{13}C cross section. ENDF/B-VII.NEW is the result of the correction of the IRMM data for energy resolution by using the shape of the ENDF/B-VII.0 excitation function and the experimental energy resolution

EN, ISBN 978-92-7905365-8 (2007) 47

[2] A. Courcelle, 2005, *http://www.nea.fr/html/dbdata/hprl/hprlview.pl?ID=417*

[3] P. G. Young, G. M. Hale, Chadwick, E. Caro, C. R. Lubitz, 2001, *http://www.nndc.bnl.gov/exfor/servlet/E4sGetIntSection?SectID=114968&req=14432*

[4] P. G. Young, G. M. Hale, Chadwick, E. Caro, C. R. Lubitz, P. R. Page, 2006, *http://www.nndc.bnl.gov/exfor/servlet/E4sGetIntSection?SectID=13381&req=14432*

^{10}B(n, α)^{7}Li cross section measurements by means of a double twin ionization chamber with Frisch grids

F.-J. Hambsch, I. Ruskov

At the last standards evaluation of the IAEA [1], the ^{10}B(n, α)^{7}Li standard got a large attention due to its improved database and its extension from 100 keV up to 1 MeV incident neutron kinetic energies, mainly based on results obtained at IRMM [2, 3]. For the first time, also the full angular distribution for both alpha-particle transitions (α_0 - ^{7}Li ground state transition and α_1 - ^{7}Li first excited state transition) has been measured [3] and used in a multi-level, multi-channel R-matrix calculation [4].
With the present experiment we will try to extend the incident neutron energy range so far reported [2, 3] up to about 3 MeV, and, additionally, to measure the reaction cross-section, in order to have an overlap with the measurements performed at the Van de Graaff accelerator [5].
A Multiplate Ionization Chamber (IC) with Frisch-grids [6] was set-up for measurements at GELINA flightpath 16, at a distance of about 60 m from the neutron producing target.
After testing several arrangements of the mechanical and electronical set-up, the measurements were started with a double twin Frisch-grid ionisation chamber (Fig. 1).

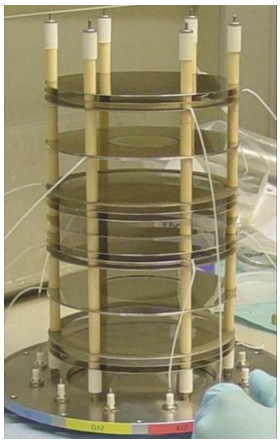

Fig. 1: Present ionisation chamber set-up: the uranium-boron samples are mounted in back-to-back geometry on the common electrodes (cathodes). The Frisch-grids are at a distance of 4 cm followed by the electron-collecting anodes at a distance of 0.7 cm and shielding electrodes. The outer length of the 1 mm thick cylindrical vessel is about 35 cm.)

By means of a remotely controlled fast neutron scanner, the neutron beam hitting the chamber was measured and observed to be uniform (in its statistical fluctuation limits) across both the uranium and boron samples (Fig. 2).
In view of the long time consuming experiment, due to the very low counting rate, some improvements have been made in the stabilization of the room temperature ($= 20 \pm 2^{o}$C) and noise reduction (pump, ventilators) in the measuring station, which are the main sources of the electronical instability.

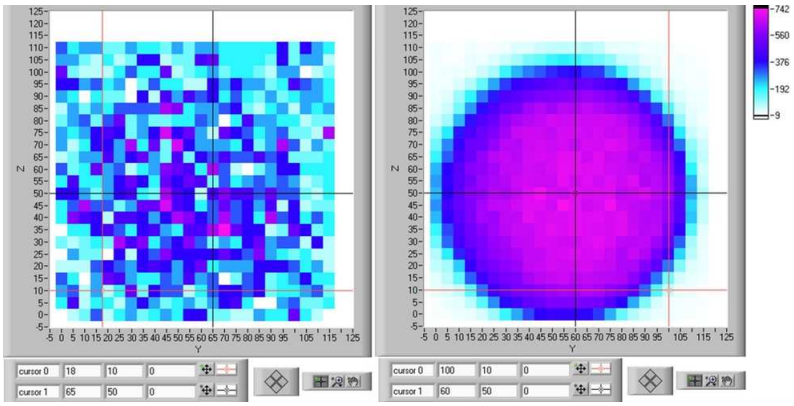

Fig. 2: The neutron beam profile at the FP16/60 m measuring station about 1 m behind the ionisation chamber: the left panel shows the background measurement with beam status OFF; the right panel shows the neutron (and γ-ray) distribution when the beam status is ON.

In Tables 1 and 2 some characteristics of the IC and the Samples used are given.

Tab. 1: Ionisation chamber parameters

component	vessel	cathodes	grids		anodes/shields	separators
type	cylinder	annular disc	wires	ring	foil	cylinder
material		stainless steel			Al	ceramics
thickness (mm)	1	1	0.11	1	0.05	4
pitch (mm)			1.00			
inner ø (mm)	228	100		152		6
outer ø (mm)	230	178				10
height (mm)	173.5					6, 10, 30

Because of different diameters of the uranium and boron samples, the neutron beam was collimated to a diameter of about 95 mm to ensure the uniform irradiation of both types of samples.
As detector gas a mixture of 95 % Ar + 5 % CO2 is used at 63-64 kPa. This pressure is sufficient to stop alpha-particles with kinetic energies up to 4.5 MeV before reaching the grids. The samples are mounted in a back-to-back geometry (Uranium/Boron, Boron/Uranuim) on the cathodes both in forward and backward position relative to the direction of the incident neutron beam. The signals from the Frisch-grids were used to trigger the timing information of the neutron interactions with the samples nuclei.
The block diagram of the twin ionisation chamber with its standard electronic chains is shown in Fig. 3. It is the same as in Ref. [2], except that the present set-up records twice the number of spectra (8 amplitudes + 2 time signals) requiring the use of multiplexer modules (MMPM) developed at IRMM. All the 16 outputs of the 4 MMPM modules were fed to the first slot of the MPI8100 data acquisition system and stored via the LISA software in list-mode on the

Tab. 2: Physical characteristics of the boron and uranium samples

characteristics	boron support		uranium support		
material	inox				
thickness (mm)	0.3		0.5		
thickness (mm)	100		70		
samples characteristics	boron		uranium		
composition	B_4C		UF_4		
purity	98 %		specific α-activity	(3.913±0.016) dps/μg	
isotope composition	94 % ^{10}B 6 % ^{11}B		1.6653% ^{234}U, 97.663% ^{235}U 0.14912% ^{236}U, 0.5229% ^{238}U		
deposit ø (mm)	84		45		
twin chamber	sample	density (μg/cm^2)	weight (μg)	sample	density (μg/cm^2)	weight (μg)
1	№ 3	14.5±0.8	804±44	№ 2	193.1±2.9	3071±46
2	№ 4	15.7±0.8	870±44	№ 1	193.7±2.9	3081±46

harddisk for further off-line analysis. By setting appropriate low-level thresholds in the ADCs and CFDs the number of events from the spontaneous alpha-decay of the uranium samples was significantly reduced. The experimental set-up at FP16/60m is shown in Fig. 4.
The gamma-flash from the GELINA neutron producing target was attenuated with a number of in-beam filters (bismuth and lead), situated at a distance of about 1 m in the front of the chamber. Data taking is ongoing since October 2007. Data analysis is in progress.

[1] IAEA CRP on *Improvement of the Standard Cross Sections for Light Elements*, http://www.iaea.org/programmes/ripc/nd/crps/standcrosect_of_lightelem.htm

[2] F.-J. Hambsch, and I. Ruskov, *The $^{10}B(n, \alpha_0)/^{10}B(n, \alpha_1\gamma)$ Branching Ratio*, Nucl. Sci. Eng. 156 (2007) 103

[3] F.-J. Hambsch, and I. Ruskov, *The $^{10}B(n, \alpha)$ angular distributions for $E_n < 1$ MeV*, submitted to Phys. Rev. C

[4] G. M. Hale, private communication (2007)

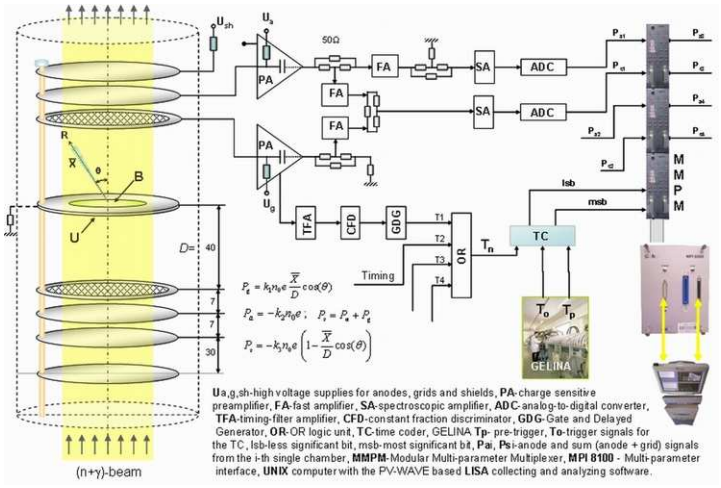

Fig. 3: Scheme of the twin ionisation chamber and associated electronics

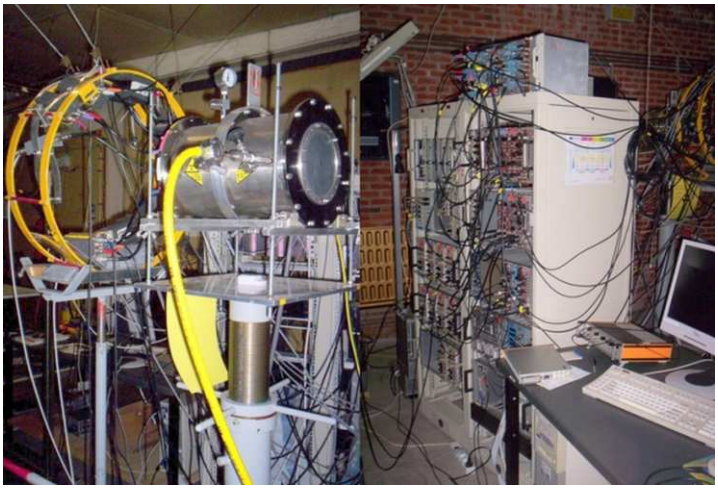

Fig. 4: The ^{10}B(n, α)^{7}Li experimental set-up at the GELINA flight-path station FP16/60 m

[5] G. Giorginis, and V. Khryachkov, *The cross-section of the $^{10}B(n, \alpha)^{7}Li$ reaction measured in the MeV energy range*, Nucl. Instr. Meth. A562 (2006) 737

[6] I. Ruskov, F.-J. Hambsch, *Multi-section ionization chamber for charged particle spectrometry - a status report*, Report EUR 22239 (2005) 74

NUDAME -
NUclear DAta MEasurements

NUDAME - EURATOM Trans-national Access programme

The distinctive research capabilities offered at the two IRMM accelerator facilities create excellent opportunities for trans-national collaborations. The facilities are ideal tools for a number of high-priority neutron measurements. A EURATOM specific support action for trans-national access at our facilities was launched in order to endorse the neutron data requirements in the field of the management of radioactive waste, radiation protection and other fields of nuclear technologies and safety. Measurements are necessary to obtain improved accuracy and consistency in the evaluated nuclear data libraries. The trans-national access project, called NUDAME, is running from April 1, 2005 until March 31, 2008. Within 3 years a total of 3000 supplementary data-taking hours is made available to external users. Selection of the supported experiments is based on peer review by a Programme Advisory Committee (PAC). Approved experiments get the necessary beam time and the same scientific, logistical and technical support provided to all researchers of the Institute. A limited number of the participating researchers are supported for their travel and subsistence costs during the time required for conducting the experiment.

There were three calls for proposals. 22 proposals have been submitted. The majority of the proposals were guided by the high priority request list (HPRL) edited by the Working Party of Evaluation Co-operation (WPEC) of the OECD/NEA Nuclear Science Committee. The total requested beam time was 7456 hours. The requested beam time largely exceeded the time that could be made available. Within the budget, the PAC could endorse a maximum 3170 beam hours. This was 43 % of the beam time requested by the external users. As a result, out of 22 proposals 18 experiments have been approved, but with a drastically reduced beam time.

The following experiments have been supported by NUDAME.

At GELINA there were 9 NUDAME experiments:

- High-resolution capture and transmission measurements of ^{nat}Hf
  Spokesperson: G. Noguère, CEA Cadarache
  20/02/06 - 03/03/06
- Capture and Transmission on ^{nat}Cd
  Spokesperson: A. Trkov, IAEA Vienna
  06/03/06 - 17/03/06
- Test of data acquisition with C_6D_6 detectors using fast signal digitisers
  Spokesperson: GTagliente, INFN Bari
  23/10/06 - 27/10/06 and 11/12/06 - 15/12/06
- ^{235}U(n, 2n)
  Spokesperson: Ph. Dessagne, IReS Strasbourg
  04/06/07 - 08/06/07

- ^{235}U(n, n'γ) and ^{235}U(n, 2nγ) reaction cross sections
  Spokesperson: Ph. Dessagne, IReS Strasbourg
  19/11/07 - 23/11/07 and 04/02/08 - 08/02/08

- Population of the superdeformed ground state in ^{235}U
  Spokesperson: A. Oberstedt, Örebro University
  21/01/08 - 08/02/08

- Accurate measurements of neutron cross sections of tungsten isotopes
  Spokesperson: S. Marrone, INFN Bari
  10/02/08 - 22/02/08

- Capture Measurements on enriched Hf samples
  Spokesperson : C. Dean, Winfrith Technology Centre
  17/02/08 - 29/02/08

- ^{233}U capture-to-fission ratio
  Spokesperson: B. Jurado, CENBG Bordeaux
  20/02/08 - 04/03/08

Also at the Van de Graaff there were 9 NUDAME experiments:

- Experimental validation of a multi-sphere spectrometric system used for radiation protection applications around high-energy electron accelerators and medical linacs
  Spokesperson: R. Bedogni, INFN Frascati
  21/01/06 - 28/01/06

- ^{243}Am(n, f) in the 0.7 10 MeV energy range
  Spokesperson: B. Jurado, CENBG Bordeaux
  20/03/06 - 31/03/06

- Fission decay of shape isomer in ^{235}U
  Spokesperson: A. Oberstedt, Örebro University
  11/09/06 - 22/09/06

- Short-lived activation cross-sections on ^{206,207}Pb
  Spokesperson: A. Pavlik, University of Vienna
  09/10/06 - 15/10/06

- Leakage spectrum measurements on Pb and Bi
  Spokesperson: J. Csikai, Debrecen University
  27/01/07 - 11/02/07

- ^{241}Am(n, 2n) measurements
  Spokesperson: O. Bouland, CEA Cadarache
  26/02/07 - 02/03/07 and 18/06/07 - 22/06/07

- Validation of ^{3}He counter and Bonner spheres
  Spokesperson: C. Domingo, University of Barcelona
  05/03/07 - 11/03/07

- Testing and calibration of neutron dosemeters for radiation protection in the nuclear industry and space applications
  Spokesperson: F. Vanhavere, SCK, Mol
  05/11/07 - 09/11/07

- Very short-lived activation cross-sections from inelastic scattering on ^{206,207}Pb
  Spokesperson: A. Pavlik, University of Vienna
  12/11/07 - 23/11/07

A general user meeting was organised on February 21-22, 2008. The meeting was intended to finalise and close the NUDAME project. The external users that were supported by the project gathered to present results, to discuss open issues and to foster future collaborations. There were 57 participants.

The value of the NUDAME project can be exemplified by the fact that the requested beam time widely exceeded the available beam time, that a high proportion of external researchers were first-time users and that several new collaborations with IRMM researchers evolved. In view of the success of this project and the positive appreciation by our own researchers and by the members of the Programme Advisory Committee, we submitted to EURATOM a new proposal for a Trans-national Access project, entitled: "European facility for innovative reactor and transmutation neutron data" (acronym: EUFRAT). During the evaluation process the EUFRAT proposal was very well appreciated by the external referees. In their evaluation they highlighted the scientific value of the IRMM accelerators for the neutron data research community. The project is now in the status of the contract negotiations with RTD- URATOM. Compared to NUDAME we enlarged substantially the scale of the new project. The duration will be four years and the beam that will be made available to the external users is 1000 hours/year at GELINA and 400 hours/year at the Van de Graaff facility.

Measurement of short-lived activation cross-sections from inelastic neutron scattering on lead

A. Pavlik[1], *E. Jericha*[2], *P. Baumann*[3], *Ph. Dessagne*[3], *R. Jaime Tornin*[4], *M. Kerveno*[3], *G. Lövestam*[4], *S. Oberstedt*[4], *A. Plompen*[4], *G. Rudolph*[3], *V. Semkova*[4]

[1] Universität Wien, Fakultät für Physik, AT-1090 Wien
[2] TU Wien, Atominstitut der Österreichischen Universitäten, AT-1020 Wien
[3] Institut Pluridisciplinaire Hubert Curien, F-67037 Strasbourg
[4] European Commission, JRC-IRMM, B-2440 Geel

Neutron inelastic scattering and (n, xn) cross sections are of importance to lead cooled reactors and subcritical accelerator driven systems. Such reactions have been investigated with the (n, xnγ) technique at the GELINA facility for several target isotopes [1, 2], amongst them ^{206}Pb and ^{207}Pb [1]. For inelastic neutron scattering isomers in ^{206}Pb and ^{207}Pb play important roles. In ^{206}Pb this is the 11^{th} excited state (E_x = 2200 keV, $J^\pi = 7^-$, $t_{1/2}$ = 125 μs) and in ^{207}Pb the third excited state (E_x = 1633 keV, $J^\pi = 13/2^+$, $t_{1/2}$ = 0.805 s). Partial level schemes are given in Fig 1. The production cross section of these isomers cannot be measured by the technique of detecting promptly emitted γ-rays.

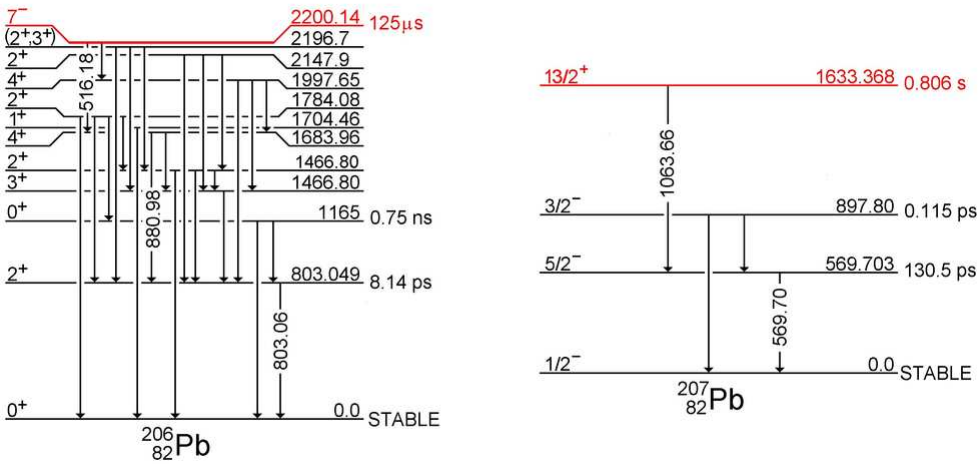

Fig. 1: Partial level schemes of ^{206}Pb and ^{207}Pb

As these isomers carry a significant part of the inelastic cross section we performed an experiment to measure the ^{206}Pb(n, n')^{206m}Pb and ^{207}Pb(n, n')^{207m}Pb cross sections at the IRMM Van-de-Graaff facility to complement the prompt γ-ray emission measurements done at the GELINA facility. Due to the short half-life of only 125 μs for ^{206m}Pb it is not possible to transport the activated sample from the irradiation position to the detector. Leaving the sample in place and using the beam chopper [3] at the Van-de-Graaff facility, measurement cycles consisting of activation periods followed by periods for activity measurement are possible. The activity measurement is performed when the accelerated particle beam is deflected

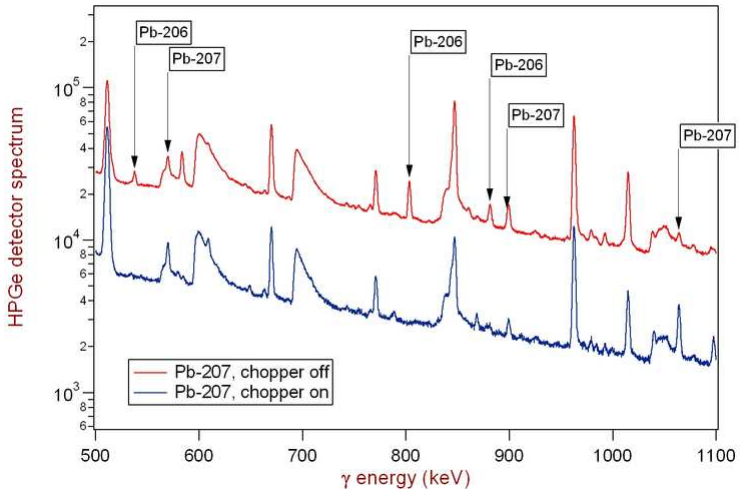

Fig. 2: Gamma-ray spectra during the activation cycles (chopper off) and the deflected-beam cycles (chopper on)

off the neutron production target. Neutrons were produced via the D(d, n)^{3}He source reaction using a deuterium gas-cell as neutron production target. Measurements were performed for deuteron energies of 2.0, 2.5, 3.0, 3.5, 4.0 and 4.5 MeV, resulting in average neutron Energies of 4.43, 5.14, 5.74, 6.30, 6.84 and 7.37 MeV at the chosen irradiation angle of 0 degree. A lead sample of natural isotopic composition could be used, as interfering (n, 2n) reactions are not present at these energies. The sample was a stack of 5 to 10 disks of 10 cm diameter and 1 mm thickness each, positioned at a distance of 44 cm from the neutron production target. A 40 % relative efficiency HPGe detector was placed at 47 cm distance from the sample at 90 degree with respect to the deuteron beam axis and shielded by a copper shadow bar. Different beam chopper settings were used for measuring the ^{206m}Pb and ^{207m}Pb decay. Activation periods of two half-lives length (250 μs and 1.6 s, respectively) were followed by periods for activity measurement of four half-lives length with deflected deuteron beam. Conventional electronics was employed for these measurements. The detector pulse height and the time relative to the beginning of the irradiation (as defined by the chopper control signal) were recorded in list mode. Gamma-ray pulse-height spectra as shown in Fig. 2 can be derived from these data. The red curve shows the spectrum accumulated during all activation periods in a measurement lasting about 15 hours, the blue curve is the spectrum accumulated during the periods with the deuteron beam deflected. In this run an activation period of 1.6 s and a decay period of 3.2 s were chosen to measure the production of the 0.8 s isomer in ^{207}Pb. Prompt γ-ray transitions from ^{206}Pb and ^{207}Pb as well as lines from the decay of the isomer in ^{207}Pb can clearly be identified in the spectra.

The intensity distribution of the net peak contents of the 569.7 keV line in ^{207}Pb as a function of the time during the irradiation cycles is shown in Fig.3. Data accumulated during all cycles of an experiment run are shown. The time scale starts when the chopper is turned off, i. e. at the begin of the irradiation. During the 1.6 s of irradiation the sum of the intensities from prompt emission and from the activity build-up of the isomer is observed. When the beam is deflected, only the exponential decay of the isomer can be seen. A least-squares fit to the shown raw data results in a half-life of (0.761 $\pm$ 0.059) s. The neutron fluence was determined with the IRMM proton-recoil telescope [4] in separate runs at the same neutron energies. In-

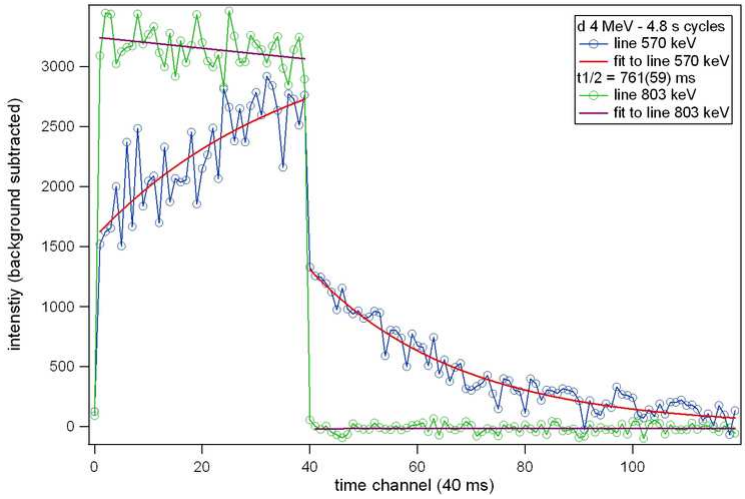

Fig. 3: Intensity distribution of the 570-keV and the 803-keV gamma lines as a function of the time after the start of the irradiation cycle

dium activation foils were used as well in the telescope runs as in the Pb sample runs for normalization and as an additional neutron fluence monitor. The long-term time distribution of the neutron fluence was measured by a BF_3 long counter. Gas-out runs were performed for all deuteron energies to check for possible contributions of neutrons from deuteron break-up or possible D(d, n) neutron sources in beam line elements upstream the gas target. For some deuteron energies also runs without a Pb sample or the beam always in the deflected position were performed to determine background contributions to the γ-ray spectra. The efficiency of the HPGe detector was measured using a calibrated ^{152}Eu source at the sample position. A detailed analysis of the measurement is in progress, especially for the higher deuteron energies a careful check of the background is necessary.

[1] L. C. Mihailescu, *Neutron (n, xnγ) cross-section measurements for ^{52}Cr,^{209}Bi and ^{206,207,208}Pb from threshold up to 20 MeV*, Doctoral Thesis, University of Bucharest 2006

[2] L. C. Mihailescu et al., *High resolution measurement of neutron inelastic scattering and (n, 2n) cross-sections for ^{209}Bi*, Nucl. Phys. A799 (2008) 1

[3] S. Oberstedt, G. Lövestam, C. Chaves, W. Geerts and R. Jaime Tornin, *Identification of the shape isomer in ^{239}U with the electrostatic beam-chopping device* (European Report GE/SCIRMM/ER/2005) pp D1-D12, European Communities 2005.

[4] G. Lövestam, *The recoil proton telescope in non-coincidence mode for neutron fluence measurements*, Nucl. Instr. Meth. A 566 (2006) 609

Measurement of the ^{235}U(n, 2nγ) reaction cross sections

P. Baumann[1], Ph. Dessagne[1], H. Karam[1], M. Kerveno[1], G. Rudolph[1], J. C. Thiry[1], C. Borcea[2], A. L. Negret[2], A. Plompen[2], M. Stanoiu[2], A. Pavlik[3], E. Jericha[4],

[1] Institut Pluridisciplinaire Hubert Curien, F-67037 Strasbourg
[2] European Commission, JRC-IRMM, B-2440 Geel
[3] Universität Wien, Fakultät für Physik, AT-1090 Wien
[4] TU Wien, Atominstitut der Österreichischen Universitäten, AT-1020 Wien

The elaboration of the next generation nuclear reactors requires the measurement of (n, xn) reactions. One of the possible experimental methods is the prompt γ-ray spectroscopy which allows identifying nuclei produced by these reactions in very short-lived excited states. The success of our measurement on lead isotopes (A = 206 - 208) at the 200 m detection station of GELINA has encouraged us to investigate the ^{235}U(n, 2n) reaction, having in mind to perform the study of the ^{233}U(n, 2n) reaction which is of crucial importance in the fast thorium-cycle. Due to the available quantity of material and the γ-ray absorption at low energy, the ^{235}U sample has to be much thinner than the Pb ones and the measurement has to be performed with a shorter flight path (30 m). A 8 g ^{235}U sample 93 % enriched in ^{235}U has been provided by IRMM. The γ-rays emitted by the sample are detected by HPGe planar detectors and a fission chamber (IRMM) is used for the neutron flux determination. In a first step, several tests have been performed to adjust our experimental technique (prompt γ-ray spectroscopy coupled to time of flight measurement for the determination of the neutron energies) based on a fast digital acquisition system. A very important effort has been devoted to obtain a well collimated neutron beam, and the smallest possible rate of γ-rays from the flash. In a second step data taking has been performed during a few weeks. Preliminary results are mentioned in this contribution.
The neutron flux has been obtained at 30 m with a fission chamber containing two foils of ^{235}U (UF_4 and U_3O_8 deposits of 323 μg/cm^2 and 387 μg/cm^2, respectively). The neutron flux is shown in Fig. 1 as a function of incident neutron energy.

For each γ-ray detected in the HPGe crystals the energy and the time were registered by the digital data acquisition system. Figure 2 presents the two dimensional distribution (time as a function of γ-ray energy) of the events collected by one germanium detector. We can clearly see the contribution of the radioactivity of the sample and also a set of gamma transitions corresponding to the (n, n'γ) reactions. In that case the events are present in the 0.5 to 6 MeV neutron energy window. We observe in the 6 to 20 MeV energy range events related to the (n, 2nγ) reaction, in particular the 152 keV and 201 keV gamma transitions.

The present data (beam time of 12 weeks) have been obtained in 3 different experimental conditions (various beam diameter, target positions, parameters of the digital cards...). For one germanium counter Fig. 3 shows the γ-ray energy distribution related to the (n, n'γ) and

(n, 2nγ) channels and to the radioactivity of the sample. For the (n,n'γ) channel (blue curve) the indicated gamma transitions of 129 keV and 146 keV correspond to the de-exciation of excited levels located in ^{235}U at respectively 129 keV and 249 keV excitation energy. For the (n, 2nγ) reaction channel (red curve) the 152 keV and 201 keV transitions are associated in ^{234}U to the states located at respectively 296 keV and 497 keV excitation energy.
For these two last transitions we have extracted some preliminary results as the cross sections shown in Fig. 4.

The data analysis is in progress in order to improve the precision on several quantities (γ-ray efficiency, neutron flux...). The results will be compared to theoretical approaches as e. g. the TALYS code.

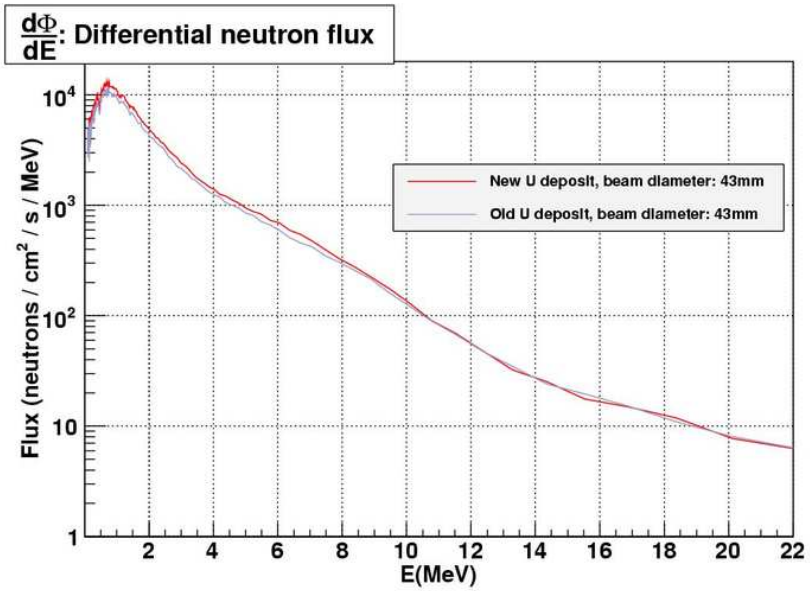

Fig. 1: Differential neutron flux obtained at 30 m with two ^{235}U foils (red and grey curve are respectively for the UF_4 and the U_3O_8 deposit)

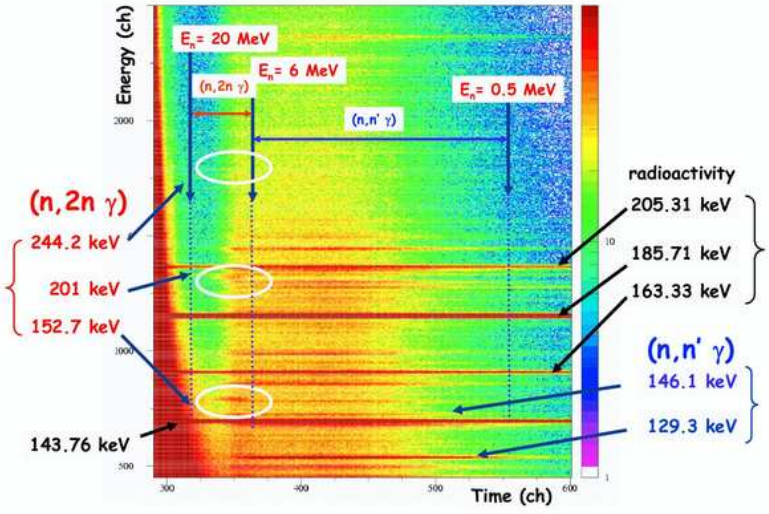

Fig. 2: Gamma energy distribution in function of time obtained in four weeks for one germanium counter. The gamma transitions corresponding to different reaction channels are clearly identified.

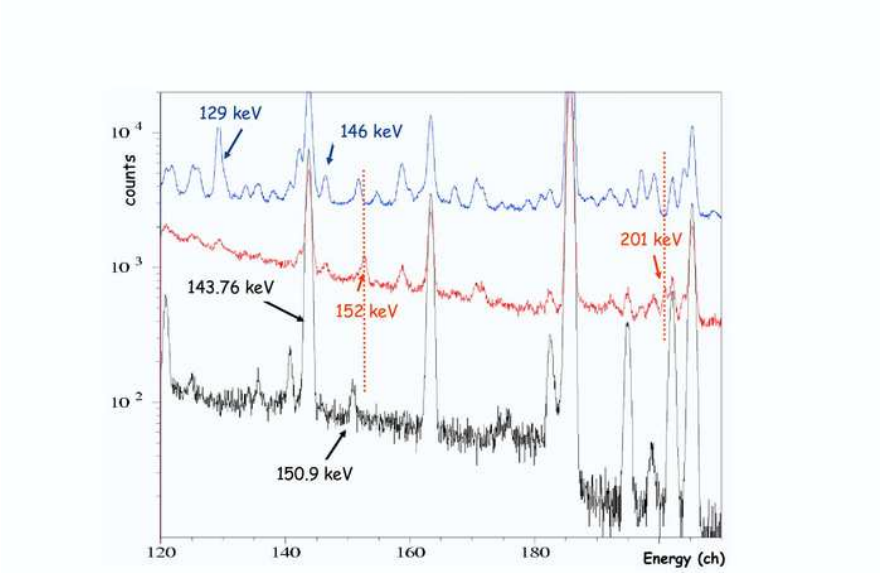

Fig. 3: Gamma energy distributions corresponding to : the (n, n'γ) channels (blue curve), the (n, 2nγ) channels (red curve) and the radioactivity of the ^{235}U sample (black curve)

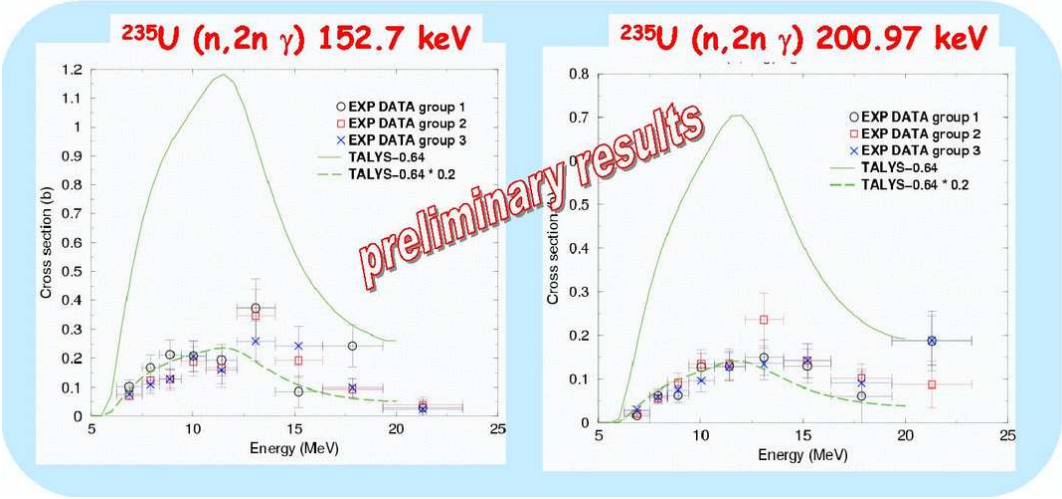

Fig. 4: Cross sections for three sets of data relative to two gamma transitions in the ^{234}U nucleus produced by the ^{235}U(n, 2n) reaction channels

Population of the super-deformed ground state in ^{235}U - a feasibility study

A. Oberstedt[1], *J.-C. Drohé*[2] *F.-J. Hambsch*[2], *R. Jaime Tornin*[2], *S. Oberstedt*[2], *P. Schillebeeckx*[2], *M. Vidali*[2], *R. Wynants*[2]

[1] Institutionen för Naturvetenskap, Örebro Universitet, S-70182 Örebro
[2] European Commission, JRC-IRMM, B-2440 Geel

With the recent discovery of the fission isomer in 235U and the determination of its half-life for isomeric fission, $T_{1/2}$=(3.6 $\pm$ 1.8) ms [1], one has come a huge step towards the precise knowledge of the distinct structure of the fission barrier in this nuclide. However, for the determination of the outer fission barrier height E_B, and the penetrability $\hbar\omega_B$ also the SD ground state energy E_{II}, needs to be known. This paper reports about a feasibility study for the search of γ-rays populating the shape-isomeric ground state in ^{235}U via neutron-capture in ^{234}U, from which E_{II} may be determined directly by measuring γ-rays following neutron capture in the energy region of the intermediate structure (IS) in the sub-threshold region of the fission cross-section.

Following the experimental approach in Refs. [2, 3], the determination of E_{II} is possible by measuring γ-rays following neutron capture in the energy region of the IS in the sub-threshold region of the fission cross-section. The population of the SD ground state in slow neutron-capture reactions proceeds through γ-decay of an excited quasi class-II state, which is mainly located above the SD minimum. As a consequence additional γ-rays, which appear exclusively in resonances belonging to an IS, are candidates for a possible decay towards the SD ground state. Best-suited candidates are neutron resonances with a low neutron width Γ_n, and a large fission width Γ_f, indicating a high fraction of a class-II state. In case of the target nucleus ^{234}U two resonances exhibit a ratio Γ_f / $\Gamma_n > 2$, as shown in the Fig. 1. In analogy with the IS in the fission cross-section of ^{238}U the fission resonance at E_n = 1092.5 eV appears to practically coincide with a class-II state, therefore, being essentially of class-II nature.

The experiment was performed at the Geel linear accelerator facility (GELINA) of EC-JRC IRMM in Belgium. The population of the SD ground state was achieved by irradiating a thick ^{234}U sample (2.12 g with about 2 cm in diameter) with a pulsed white neutron spectrum, whose neutron pulse width and a repetition frequency was 1 ns and 800 Hz, respectively. The neutron energy of interest was between 50 and 1500 eV (cf. Fig. 1) and coincides with the region of intermediate structures in the neutron-induced fission cross-section of ^{234}U. The experiment was set up at flight path FP5 with a distance from the neutron source of about 10 m. With the available sample the expected number of measured γ-rays populating the shape isomer was relatively low within the requested beam time of two weeks. Hence, the detection had to depend strongly on the general experimental conditions, e. g. environmental background radiation and detector resolution. Therefore, this experiment was considered as a feasibility study to establish precise γ-ray spectra for clearly identifying decay from excited ^{235}U as well as from the radioactive decay of the target material and to estimate the amount

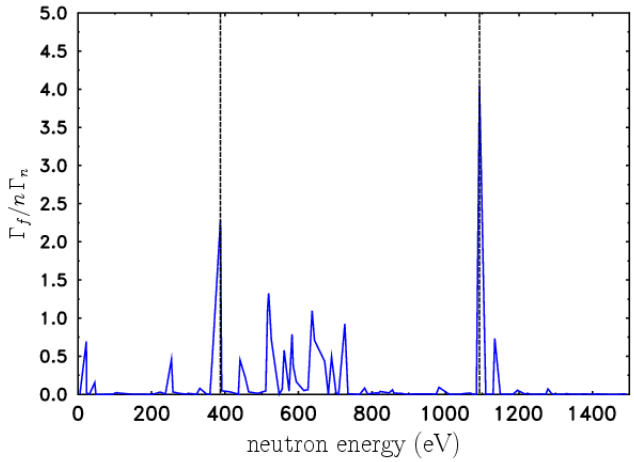

Fig. 1: Possible resonances at E_n = 387.6 and 1092.5 eV in ^{235}U with considerable class-II contributions, indicated by dashed lines.

of sample material and/or total beam time needed to identify γ-decay towards the SD shape-isomeric ground state.

The γ-rays were detected with two high-purity Germanium detectors (ORTEC HPGE with X-coolers, n-type) and two planar Germanium detectors (Canberra LEGe, n-type), whose relative efficiency was 45 % and 7 %, respectively. The detectors were placed at a distance of 23 cm (one at 17 cm) from the target, at angles of 110^o and 150^o, which in principle allows for the determination of the multipole order of the γ-radiation.

Although two weeks of beam time were applied for, only a couple of days had effectively been available for running the experiment. Naturally, problems occurred basically due to the high γ-count rates, caused by the highly radioactive ^{234}U sample ($A_\alpha \approx 4.9 \times 10^8$ Bq) and the short distance between the source and the detectors. Since these distances could not be increased at the experimental setup that was available due to a lead wall at FP5, we had to switch off the closest of the four detectors and cover the entrance windows of the others with a 5 mm thick lead shielding. An additional coincidence condition between a γ-ray and the pulsed neutron beam was imposed, which on the one hand reduced the count rate also for events of our interest, but on the other hand increased the signal-to-background ration due to the higher neutron capture γ-multiplicity (n-capture is followed by the emission of about 5 γ-rays, compared to about 1 γ-ray in α-decay). Nevertheless, the Germanium detectors were calibrated with known ^{60}Co and ^{22}Na sources as well as with the 511 keV annihilation radiation, and considering the high activity of the sample, an impressive energy resolution of the Ge-detectors was achieved. Despite the little time that was available for actual data taking, neutron time-of-flight spectra were eventually recorded. Fig. 2 shows such a neutron spectrum, however converted to neutron energy. The grey-shaded areas indicate the regions for resonances with largest neutron width Γ_n [4] and, actually, the position of the resonances may be anticipated.

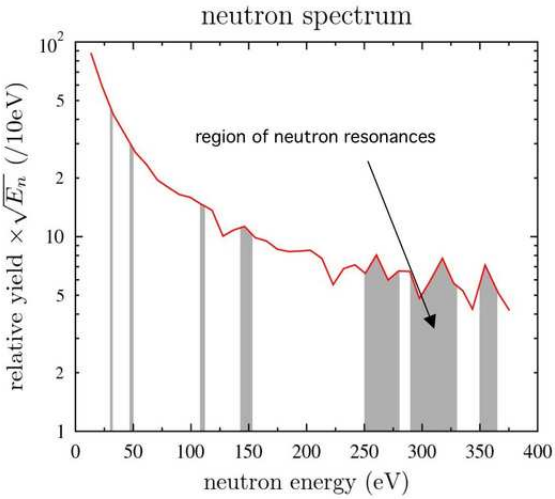

Fig. 2: Neutron energy spectrum indicating the regions of resonances (see text for details).

In conclusion, we have reported on a feasibility study of an experiment dedicated to the population of the super-deformed ground state in ^{235}U. As expected, several problems were encountered, but they were also identified and partially already resolved. We reckon that a serious experiment may be successful under certain circumstances. Necessary improvements concern basically an increased distance between the sample and the detectors as well as more beam time. With these conclusions in mind we consider that the aim of this study was reached.

[1] A. Oberstedt et al., Phys. Rev. Lett. 99, 042502 (2007)

[2] S. Oberstedt and F. Gunsing, Nucl. Phys. A589 (1995) 435

[3] S. Oberstedt and F. Gunsing, Nucl. Phys. A636 (1998) 129

[4] S. F. Mughabghab, Atlas of Neutron Resonances: Thermal Cross Sections and Resonance Parameters. Amsterdam: Elsevier (2006)

Measurement of the ratio between the capture and the fission cross sections of ^{233}U

M. Aiche[1], G. Barreau[1], G. Boutoux[1], S. Czajkowski[1], D. Dassiè[1], B. Haas[1], B. Jurado[1], G. Kessedjian[1], P. Schillebeeckx[2], A. Borella[2], F.-J. Hambsch[2]

[1] CENBG, F-33175 Gradignan Cédex
[2] European Commission, JRC-IRMM, B-2440 Geel

The Th-U fuel cycle presents two important advantages with respect to the current fuel cycle: a minimized proportion of heavy, long-lived radiotoxic nuclei in the spent fuel and the capability of breeding either in a thermal or a fast neutron spectrum. Recent sensitivity studies [1] of the impact of the cross section uncertainties on the breeding capability of this fuel cycle have shown that fissile regeneration is dominated by the uncertainty in the ratio between the capture and the fission cross sections of ^{233}U. Indeed, the available data for this ratio [2, 3, 4, 5, 6] present a dispersion of 25 %. Consequently, the calculated uncertainty for the breeding capability of thorium reactors is about 4 %, whereas the breeding potential itself is expected to be of the same order. Therefore, it is not yet possible to ensure that this cycle is self-sufficient in the regeneration of the fissile element ^{233}U. The sensitivity results are relatively independent of the neutron energy. However, the most critical region is the epithermal area because it is the spectrum proposed for some graphite moderated Molten Salt Reactors [7]. The aim of this experiment is the precise measurement of the ratio of the capture to fission cross sections of ^{233}U in the 1 to 100 eV neutron energy range.

First experiment C_6D_6 liquid scintillators have been successfully utilised in high resolution neutron capture cross-section measurements at time-of-flight facilities, using the total energy detection principle in combination with the pulse height weighting technique [8, 9]. One of the biggest difficulties one has to face when applying this technique to a fissile nucleus such as ^{233}U is to disentangle the gamma rays coming from a capture event from those coming from fission. To overcome this problem we added to the C_6D_6 array a high-efficiency fission detector that allows one to mark the gamma rays originating from the fission fragments. The ratio of the capture to fission cross section is then given by:

$$\frac{\sigma_c}{\sigma_f} = \frac{n_c\,\epsilon_f}{n_f\,\epsilon_c} \quad , \tag{1}$$

where n_c (n_f) and ϵ_c (ϵ_f) correspond to the number of capture (fission) events and the efficiency of the capture (fission) detector, respectively. The quantity n_c has to be corrected for fission γ-rays not "tagged" by the fission detector:

$$n_c = n_c^{tot} \; - \; n_f\,\frac{\epsilon_{cf}\,(1-\epsilon_f)}{\epsilon_f} \quad , \tag{2}$$

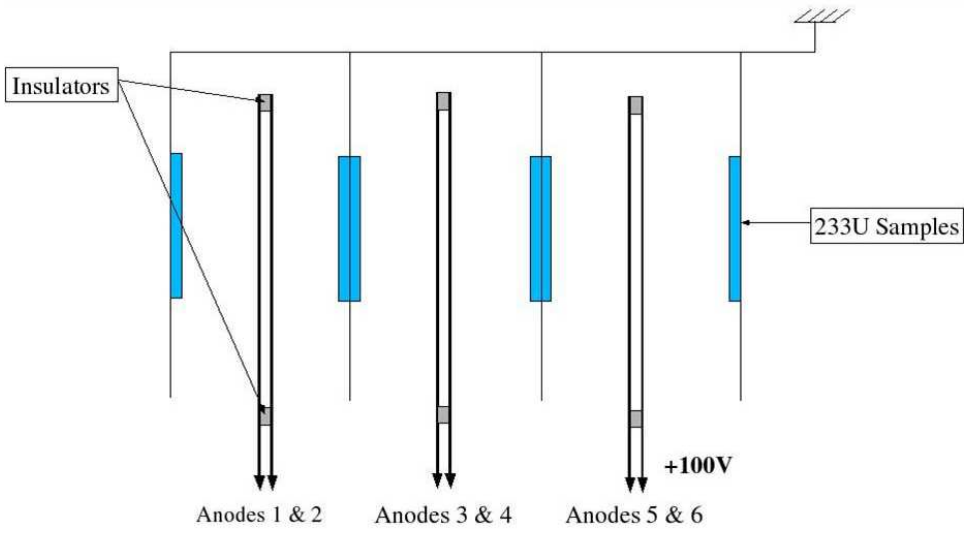

Fig. 1: Schematic view of the interior of the multiplate ionisation chamber

where n_c^{tot} is the total number of capture events detected by the C_6D_6 array and ϵ_{cf} is the efficiency of the C_6D_6 array for detecting gammas coming from fission fragments.
The advantage of measuring simultaneously capture and fission events is that there is no need to measure the neutron flux and the number of target atoms per surface unit, quantities for which a precise measurement is rather difficult.

We have performed a first test experiment at the neutron time-of-flight facility GELINA in February 2008. Our fission detector was a multiplate Ionisation Chamber (IC). The neutron flight path was 12 m. The complete set-up consisted of a 10B IC for beam monitoring and the multiplate IC surrounded by four C_6D_6 γ-ray detectors. The multiplate IC contained six ^{233}U samples of approximately 450 μg/cm^2 each. The samples were electrodeposited on the chamber cathodes by the target laboratory of the IRMM. The anodes of the IC were biased to 100 V and the ionisation gas was a mixture of Ar-Methane (10 % Methane). Figure 1 shows a side view of the interior of the multiplate IC.

In this first experiment at GELINA the multiplate IC showed a very high stability with respect to the gamma flash. The good performances of the multiplate IC are reflected by the fission spectrum as a function of neutron energy shown in Fig. 2. The arrows indicate some well known resonances between 1 and 23 eV. These resonances will be used to determine the efficiency ϵ_f of the IC.
In this test experiment we also coupled for the first time the IC and the C_6D_6 detector array. Figure 3 illustrates the number of γ-rays detected by the C_6D_6 scintillators in coincidence with the multiplate IC. This spectrum was accumulated simultaneously with the spectrum of Fig. 2, the difference in number of counts between the two spectra reflects the difference in efficiency of the fission IC and the C_6D_6 array.

Unfortunately, in this first experiment the γ-ray background originating from neutron reactions in the Al of the target supports was too high to observe the capture events from neutron-induced reactions in ^{233}U.

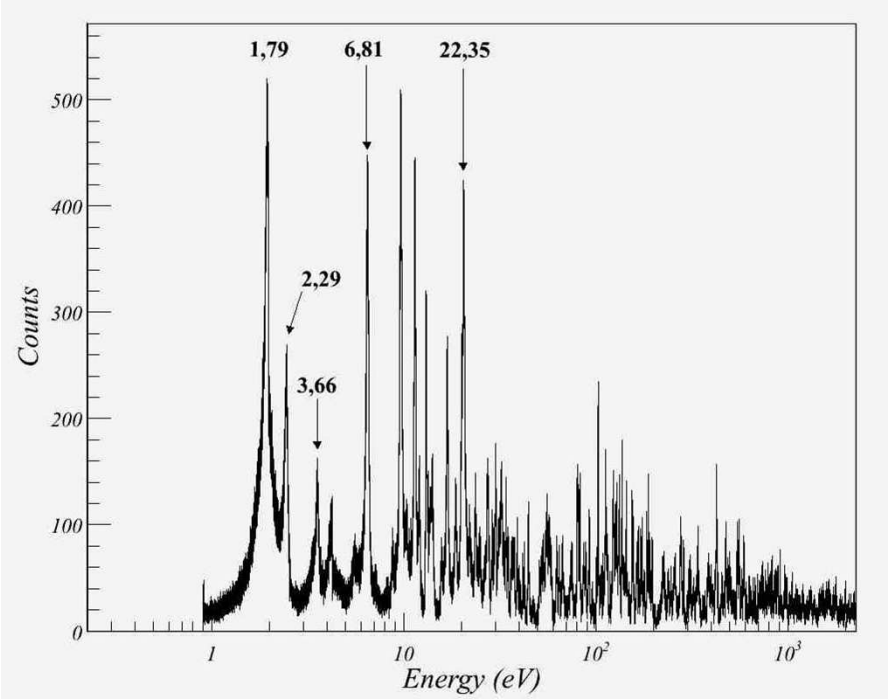

Fig. 2: Number of fission events detected by the ionisation chamber as a function of neutron energy. The arrows indicate the mean neutron energy of various well-known fission resonances of ^{233}U.

Perspectives An analysis of the spectra of Figs. 2 and 3 with the code REFIT [10] will allow to extract the fission resonance parameters of ^{233}U. In order to increase the signal to noise ratio for capture events in future experiments we will reduce by a factor 30 the thickness of the ^{233}U supports. The quantity of ^{233}U will be increased by a factor 10 and we will use six C_6D_6 detectors. A stronger beam collimation would also be helpful to reduce the γ-ray background.

[1] A. Bidaud, PhD Thesis, Université Paris-XI, Orsay, 2005

[2] J. Halperin et al., Nuclear Science and Engineering 16 (1963) 245

[3] J. C. Hopkins et al., Nuclear Science and Engineering 12 (1962) 169

[4] M. S. Moore et al., Phys. Rev. 18 (1959) 714

[5] O. D. Simpson et al., Nuclear Science and Engineering 7 (1960) 187

[6] L. W. Weston et al., USAEC Report ORNL-TM-1751, Oak Ridge National Laboratory, 1967

[7] L. Mathieu, PhD Thesis, Institut National Polytechnique de Grenoble, 2005

[8] J. N. Wilson et al., Nucl. Instr. Meth. A 511 (2003) 388

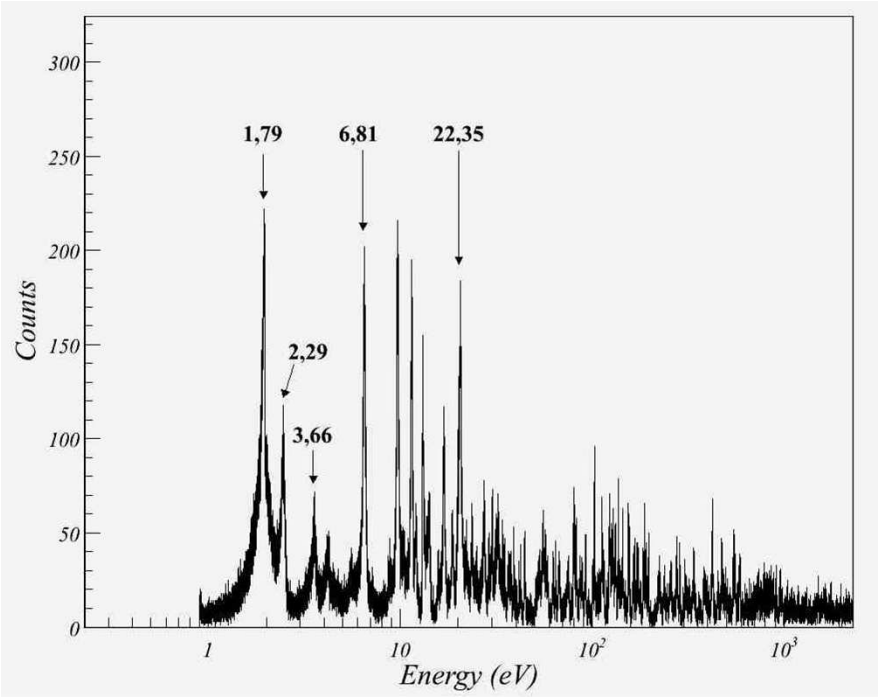

Fig. 3: Number of γ-ray events detected by the C_6D_6 detectors in coincidence with the ionisation chamber. The arrows indicate the mean neutron energy of various well-known fission resonances of ^{233}U.

[9] A. Borella et al., Nucl. Instr. Meth. A 577 (2007) 626

[10] M. C. Moxon et al., AEA-InTec-0630, AEA Technology, October 1991

Validation of the response functions of the active (^{3}He detector) and passive (^{197}Au foils activation) UAB Bonner Sphere Spectrometers

C. Domingo[1], *F. Fernandez*[1], *M. Garcia*[1], *G. Lövestam*[2]

[1] Department of Physics, Universitat Autònoma de Barcelona, E-08193 Bellaterra
[2] European Commission, JRC-IRMM, B-2440 Geel

The neutron group from 'Grup de Fsica de les Radiacions' (GFR) of 'Universitat Autònoma de Barcelona' in Spain performs neutron dosimetry and spectrometry of neutron fields, applied to radiation protection mainly in nuclear power plants and medical premises (LINAC electron accelerators and PET cyclotrons). For spectrometric purposes, they are equipped with a Bonner Spheres System formed by 8 polyethylene spheres, 2.5", 3", 4.2", 5", 6", 8", 10" and 12" diameters (Centronic), plus a Cd shell which can be used with the three smallest spheres, allowing a total of 11 different configurations. Located at the center of the spheres, there is the sensible part of a ^{3}He cylindrical proportional counter, 0.5NH1/1KI type, manufactured by Eurisys Mesures. This active system was calibrated and validated in the past at primary neutron reference installations.
This spectrometric system is not suitable for use in mixed fields with high photon intensity, such as those encountered at medical LINACs above 10 MeV, as the contribution of the photon component may completely hide the signal form the neutron one. There is also the saturation and pile-up effect that make the active system not useful in very intense neutron or mixed fields, such as those obtained in PET cyclotrons. In order to overcome these difficulties, a passive system has been developed using the same polyethylene spheres (11 configurations in total), but placing at its centre 300 mg gold foils as passive detectors based on neutron activation. This system eliminates the saturation and pile-up effects and allows differentiating the neutron contribution from the photon one, as ^{197}Au + n $\longrightarrow$ ^{198}Au and ^{197}Au + γ $\longrightarrow$ ^{196}Au + n. Both ^{198}Au and ^{196}Au are γ-ray emitters with short a half life and with basically only one γ-line each and, hence, it is possible to distinguish how much of the activation is due to incident neutrons and how much due to incident photons. The response functions of this Bonner Sphere + gold foil system have been calculated using the Monte Carlo code MCNPX 2.4.0. When an unknown neutron field is measured, the unfolding code MITOM, developed by the Barcelona group, makes use of the calculated response functions to obtain the neutron spectra, neutron fluences and neutron dose equivalents H*. At present, the response functions of the complete passive spectrometer (11 configurations with Bonner Spheres plus Cd shell + gold foils) have not yet been validated at any primary neutron reference installation to (quasi)-monoenergetic neutron beams. Only Am-Be and Cf sources have been used so far. Obviously, in order to make the system usable as a reference neutron spectrometer it is necessary to have it calibrated and its response functions validated in a neutron reference laboratory also to (quasi)-monoenergetic neutron beams.

For this, the spectrometer was irradiated at the EC-JRC IRMM Van-de-Graaff accelerator laboratory with quasi-monoenergetic neutron beams of 300 keV, 800 keV, 3 MeV, 7.5 MeV,

16 MeV and 19.5 MeV. The irradiation took place at 4 distances to the neutron producing target (2 m, 2.5 m, 3 m and 3.5 m) to correct for scattered component (except for the 300 keV). A total of 231 irradiations (21 sets of 11 spheres) were performed during 5 working days.

Testing and calibration of neutron dosemeters for radiation protection in the nuclear industry and space applications

F. Vanhavere[1], *J.-L. Genicot*[1], *F. Mastroleo*[1], *G. Lövestam*[2]

[1] SCK•CEN, B-2400 Mol
[2] European Commission, JRC-IRMM, B-2440 Geel

Radiation protection dosimetry in mixed neutron/photon fields is still far less established than for photon radiation alone. In practice, personal dosimetry is carried out using passive devices with high dose threshold and not ideal energy characteristics. Recently some electronic dosimeters with direct reading became commercial available for neutron dosimetry. Within the EC 5^{th} Framework Programme, the project EVIDOS (EValuation of Individual DOSimetry in mixed neutron and photon radiation fields at workplaces of the nuclear fuel cycle, with special regard to neutrons) showed that the electronic neutron personal dosemeters can lead to an improvement in radiation protection dosimetry, but still need characterisation of field specific correction factors.

The energy and angular dependence of three types of commercially available electronic personal neutron dosemeters were determined using the IRMM quasi mono-energetic neutron fields. The energies used were 0.2, 0.5 1.0, 3.5, 7.0, 15.9 and 19.5 MeV. These measurements are indeed lacking since the detectors are new, and several improvements have been introduced lately in their design and, thus, the literature data available is not always correct. The results of the measurements will be used to determine how to introduce these dosemeters as official neutron personal dosemeters at the SCK•CEN.
The effects of the complex radiation field in space, consisting of neutrons, electrons and high-energy heavy charged particles, on biological samples are of high interest in the fields of radiobiology and exobiology. Radiation doses absorbed by biological samples must be quantified to be able to determine the relationship between observed biological effects and the radiation dose. For radiation protection purposes the effective doses to astronauts needs to be assessed, while in dosimetry for biological experiments the absorbed dose and the equivalent doses to the samples need to be known. Special techniques and correction methods combining luminescence detectors and track etched detectors are required due to the presence of particles with a wide range of LET (Linear Energy Transfer) values. Within the DOBIES project (Dosimetry for Biological Samples in Space), the objective is to develop a standard dosimetric method (as a combination of different techniques) to measure accurately the absorbed doses. A measurement and calculation procedure for such measurements is in development. This objective can be achieved by studies of the LET dependencies of the different types of detectors. This requires irradiations in standard high energy particle fields on earth. Knowing the responses of the different types of detectors to radiation of different LET, their responses from space exposures can be combined to give the true absorbed doses.

Two types of optically stimulated luminescence material, six types of thermoluminescent material and two types of track etch detectors were exposed at the EC-JRC IRMM to mono-energetic neutrons from the same energies as above. The responses will be part of the full characterisation of the materials to different particles from different LET's. The TEPC measurements can partly serve as a reference for the LET of the beam.

EFNUDAT European Facilities for NUclear DATa Measurements

F.-J. Hambsch, W. Mondelaers on behalf of the EFNUDAT collaboration

The EFNUDAT project is an Integrated Infrastructure Initiative within the EURATOM FP6 program. It is a four years project, which started November 1, 2006 and will run until end of October 2010.
The objective of the project is to provide a convenient platform to integrate all scientific efforts needed for high-quality nuclear data measurements in support of waste transmutation and design studies of GEN IV systems. The EFNUDAT consortium consists of 10 of the leading European institutes in the field of nuclear data measurements. The aim of EFNUDAT is to integrate all infrastructure-related aspects of nuclear data measurements. The project is organised in three network activities, 9 different Trans-national Access Activities (TAA) and three Joint Research Activities (JRA).
IRMM is a partner in EFNUDAT, but not involved in the transnational access activities, due to our own TAA project NUDAME (and EUFRAT). IRMM is however, engaged in the management Board of EFNUDAT with F.-J. Hambsch as the scientific coordinator and W. Mondelaers the TAA coordinator. The project coordination lies with G. Barreau, CNRS, Bordeaux, France. IRMM is also participating in all the three JRA's, A. Plompen being the responsible for the activities within JRA1 (Development of novel acquisition and analysis methods for nuclear data). JRA2 deals with "Quality assurance for nuclear data measurements" and JRA3 tackles the problem on "Nuclear target upgrade for improved nuclear data measurements". In each of those several partners are involved. Within the framework of its TAA the consortium offers a total of 4015 h additional beam time for external users at the EFNUDAT facilities. Each 6 months (deadline March 15 and September 15) a project advisory committee is evaluating the TAA proposals received. In addition short scientific visits are also possible at one of the institutes of the EFNUDAT partners. Information about applications for both the TAA scheme and the short term visitors is given at the EFNUDAT website.
EFNUDAT is also organising workshops and scientific meetings at different partner sites. Those meetings are announced also via the ENUDAT website. The last meeting both giving general information as well as the progress of the project was held in Feb. 2008 at Forschungszentrum Dresden/Rossendorf. Detailed information on all aspects about the project is given on the EFNUDAT website www.efnudat.eu.

New instruments and methods

Support to the Ancient Charm project

A. Borella, J. C. Drohe, J. Gonzalez, L. C. Mihailescu, P. Schillebeeckx, J. Van Gils, R. Wynants

During 2007 the support to the Ancient Charm project concentrated on the identification of the optimum gamma-ray detector and the development of a prototype position sensitive neutron detector (PSND) for NRCI and NRTI measurements in the epi-thermal region below 1 keV at ISIS.
The Neutron Resonance Capture Analysis (NRCA) technique has been developed at the time-of-flight facility GELINA of the IRMM in collaboration with the University of Delft. At GELINA C_6D_6 liquid scintillators are used to detect the capture events. These detectors are preferred due to their good time resolution, low sensitivity to neutrons and the possibility to apply the total energy detection principle in combination with the weighting function technique. The latter feature is needed when absolute quantitative measurements are required without performing additional calibration measurements with representative reference samples. The drawback of the C_6D_6 detectors is their low intrinsic detection efficiency and bulky detectors are needed for NRCI. Due to space limitations these detectors can not be used for imaging measurements at ISIS.

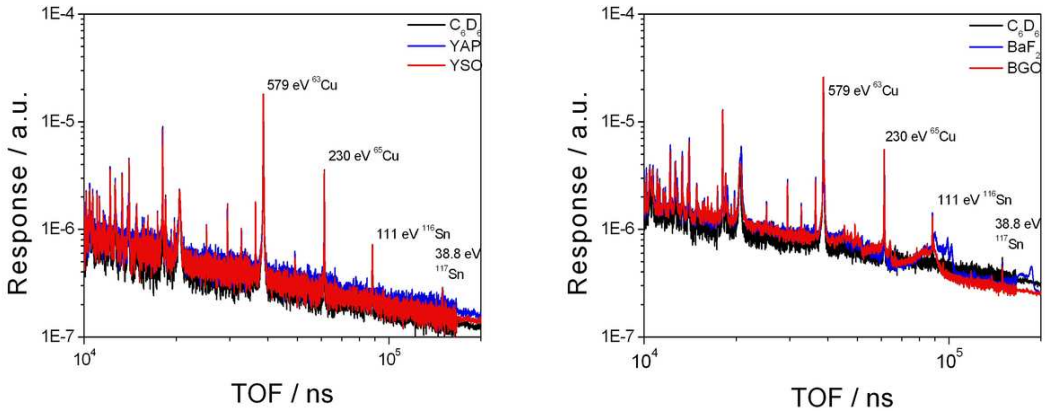

Fig. 1: The response of a YAP and YSO (left) and a BaF_2 and BGO (right) detector for NRCA measurements of a 0.4 mm Cu disc

In order to choose the γ-ray detector technology for the NRCI system, tests on BGO, BaF_2, YAP (Yttrium Aluminum Perokvsite) and YSO (Yttrium OrthoSilicate) detectors and associated electronics were carried out at GELINA. The performance of these detectors was compared with the performance of C_6D_6 detectors which are commonly used in neutron capture measurements, e.g. C_6D_6. The performance indicators of interest were: energy differential linearity, time resolution, sensitivity to neutrons in the epi-thermal energy region below 1 keV and peak to background conditions for NRCA measurements on reference samples such as Cu and Sn. From the results of these measurements we can take the following conclusions:

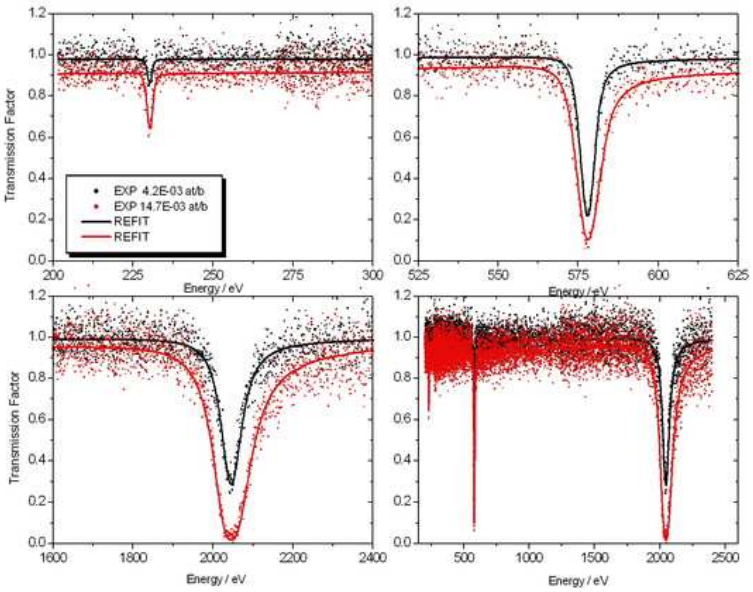

Fig. 2: The transmission factor obtained from transmission measurements with the prototype PSND developed at ISIS for Cu-samples with different thicknesses (4.22×10^{-3} at/b and 1.47×10^{-2} at/b)

- the energy differential linearity for all detectors is sufficient to define reliable energy discriminator levels
- the time resolution of all the detectors is sufficient for NRCI measurements in the epi-thermal energy region around
- in contrast to YAP and YSO detectors, BGO and BaF_2 detectors suffer from the impact of neutron sensitivity in the epi-thermal region below 1 keV
- in the epi-thermal region below 1 keV the YAP and YSO detectors have a comparable performance as compared to the C_6D_6 detector.

The latter two conclusions can be deduced from a comparison of the response of the different capture detectors for NRCA measurements of a 0.4 mm thick Cu sample. The response of a BGO and BaF_2 detector is compared with the one of C_6D_6 in Fig. 1 and the response of a YAP and YSO is compared with the one of a C_6D_6 in Fig. 2 . To obtain the same intrinsic detection efficiency the size of the YAP and YSO detector can be reduced by a factor 10 compared to a C_6D_6 detector. Therefore, the choice of the γ-ray detector was determined by the availability and cost of YAP and YSO detectors.
A prototype position sensitive neutron detector (PSND) was developed at the Science and Technology Facilities Council (STFC). The detector is a 4 $\times$ 4 array of 16 Li-glass crystals (1.8 $\times$ 1.8 $\times$ 9.0 mm), resulting in a 10 $\times$ 10 mm active area.
The performance of the detector was tested at the INES measurement station and at a 13 m flight path station of GELINA. The detector was characterized in terms of cross talk, time-of-flight response and peak to background. In Fig. 2 the performance of the PSND detector for Neutron Resonance Transmission Analysis (NRTA) is shown. This figure shows the transmission in different energy regions for two Cu-samples with a different thickness 4.22×10^{-3} at/b

and 1.47 $\times$ 10^{-2} at/b. The thickness of the Cu-samples was determined from a resonance shape analysis using the REFIT code. The result of such an analysis is also shown in Fig. 1. The values deduced from the data obtained with the PSND (4.29(5) $\times$ 10^{-3} at/b and 1.49(1) $\times$ 10^{-2} at/b) are in good agreement with the declared values, confirming the good performance of the prototype PSND developed at ISIS for NRTA.

GENDARC: The GEel Neutron physics Data acquisition, Analysis and Run Control program

I. Fabry, F.-J. Hambsch, S. Oberstedt, Sh. Zeynalov, N. Kornilov

A new graphical data analysis and data acquisition computer program package called GENDARC (GEel general Nuclear physics Data Acquisition, Analysis and Run Control Program) has been developed at the IRMM. This software provides both capabilities within a unified framework.
The measurement of neutron data is one of the priority areas of the IRMM. The IRMM Neutron Physics Unit has a long-standing expertise of more than 30 years to provide accurate neutron data for basic scientific research and applications like future nuclear energy systems both fission and fusion, nuclear waste management, or medicine, being a major contributor to nuclear databases like ENDF/B-VII and JEFF3.1.
The measurement process requires specialised equipment in the form of analogue and digital measurement hardware, as well as modern data acquisition and data analysis software. Increasing computer power, with quickly growing storage possibilities, allows the introduction of new advanced Digital Signal Processing (DSP) methods, which is becoming the main technology in nuclear physics experiments, into the measurement equipment, resulting in improved data quality. The recording of complete waveforms allows repeated data analysis without the need to repeat the experiments, by imposing different experimental conditions (thresholds, coincidence time windows, etc.). However, with the use of waveform digitisers, but also with experimental setups using multiple detectors, the amount of data recorded per event grows rapidly. Hence, the use of state-of-the-art data analysis tools becomes a must, too. At IRMM, this approach is currently being implemented [1].

On the one hand, GENDARC is a data acquisition system for an analogue-electronics based data logger like the MPI8100 Multi-parameter-interface [2], providing online monitoring and run control capabilities. It is suited for the processing and monitoring of list-mode data, for example generated by analogue-electronics experiments. The data input stream of the program is also suited for waveform digitisers.
On the other hand, GENDARC is also a data analysis program with state-of-the-art data analysis tools, providing the capability to handle large amounts of data efficiently. The program is written in the programming language C++ and is based on the object-oriented open-source software framework ROOT [3]. It allows for the generation, manipulation and offline visualization of an arbitrary number of 1- and 2-dimensional histograms. GENDARC possesses state-of-the-art features to analyse and visualize list-mode data and store them either in list-mode or in spectral mode to a data file in native ROOT- format. This data format, containing at the same time spectral data (histogram objects) as well as n-tuple data, provides the functionality to make sophisticated n-dimensional analytical cuts within the data. In the program, the definition of regions of interest in the n-tuple data using 2-dimensional graphical cuts is implemented. An additional benefit is that the n-tuple data need less disc space than binary data due to the built-in compression algorithm. The program provides the possibil-

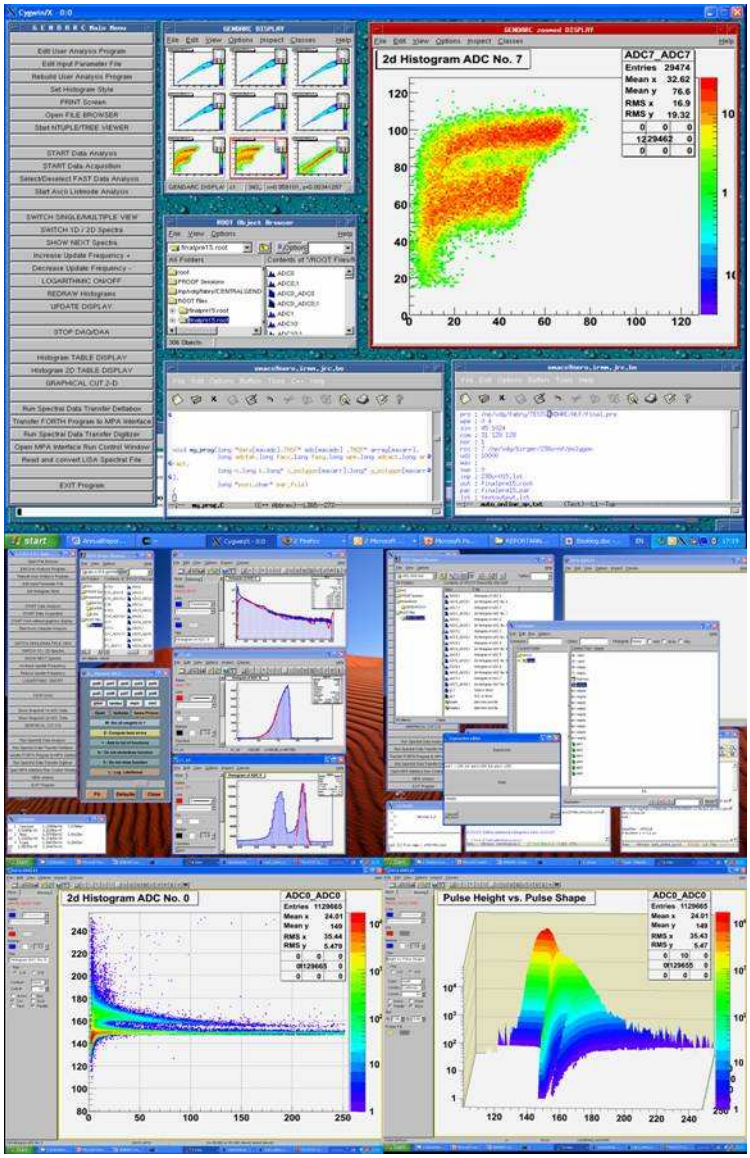

Fig. 1: Screenshots of GENDARC, the new ROOT-based data acquisition and analysis program, giving an overview of some of the possibilities of the program

ity for implementing modern Digital Signal Processing methods, which are presently under development [4].

A platform-independent Graphical User Interface (GUI) was implemented into the new program with a rich set of widgets and a great variety of user routines in order to give the user numerous possibilities to handle the program and visualize the data. This includes zooming-in/out of spectra, selecting regions of interest and thumbnail-viewing of histograms with zooming function, as well as numerous other functions. The GUI also allows for the possibility of fitting mathematical functions to the data. Using shared libraries invoked from within ROOT, the program code is structured as a compiled program. With this measure, a high performance can be achieved, since a compiled program is up to 10 times faster than an interpreted one, simultaneously retaining the advantages of an interpreter.

Our new program supersedes the existing data acquisition and analysis software LISA [5], based on the commercial PV-WAVE software from Visual Numerics Ltd. [6], which has been in use

at the Van-de-Graaff group for more than a decade. Due to the development of a specialised C++ interface GENDARC is fully compatible to LISA. This feature allows not only to create experiment-dependent user code in exactly the same easy way as in the former software, but also allows re-using tested source code developed over decades for numerous experiments.

The development is also contributing to the deliverables of the EFNUDAT (European Facilities for Neutron Measurements) project, in which IRMM is taking part. It is running on UNIX and Linux operating systems, using only open- source ingredients (libaries, compilers etc.). The program was presented at the IRMM2007 Research Fellows workshop and at the ROOT2007 international conference at CERN, Geneva [7]. Currently, the program is being utilised for data taking in neutron physics experiments at the IRMM 7 MV Van-de-Graaff accelerator [8].

[1] F.-J. Hambsch, S. Oberstedt, I. Fabry, N. Kornilov, Sh. Zeynalov, *Digitisation techniques applied in nuclear physics experiments*, International Workshop on fast neutron detectors, Capetown, Proceedings of Science (FNDA2006) 090

[2] Send Electronics Gmbh, Hamburg, Germany, *http://www.send.de*

[3] R. Brun, F. Rademakers, *ROOT - An Object Oriented Data Analysis Framework*, Proceedings AIHENP'96 Workshop, Lausanne, Sep. 1996, Nucl. Inst. Meth. in Phys. Res. A 389 (1997) 81-86. and *http://root.cern.ch/*

[4] Sh. Zeynalov, F.-J. Hambsch, I. Fabry, Development of DSP routines for the acquisition of nuclear data. See this report, p. 91

[5] A. Oberstedt, F.-J. Hambsch, *LISA - a powerful program package for LIstmode and Spectral data Analysis*, Nucl. Instr. Meth. A340 (1994) 379-383

[6] Visual Numerics Incorporation, Boulder CO, USA

[7] ROOT2007, March 26-28 2007, CERN, Geneva. See: http://root.cern.ch/root/R2007/

[8] N. V. Kornilov, F.-J. Hambsch, I. Fabry, S. Oberstedt, S. P. Simakov, *New experimental results for the ^{235}U fission neutron emission*, EC-JRC IRMM Scientific Report, EUR 23039 EN, ISBN 978-92-7905365-8 (2007) 37

Fast digitizers for (n, γ) cross-section measurements at GELINA

L. C. Mihailescu[1], *A. Borella*[1], *C. Massimi*[1,2], *P. Schillebeeckx*[1]

[1] European Commission, JRC-IRMM, B-2440 Geel
[2] Università di Bologna; INFN Sezione di Bologna, Italy

Radiative capture cross-section measurements are performed at GELINA using the total energy principle in combination with the pulse height weighting technique [1]. Liquid scintillators with deuterated benzene (C_6D_6) are used for the detection of the γ-rays from the neutron capture reaction. The pulse height weighting technique needs both the time and the pulse height information for each detected event. Conventional data acquisition systems used at GELINA are able to provide simultaneously the time and the pulse height information of the event, but with a dead time between 2.5 and 5 μs. The dead time correction procedures used routinely in time-of-flight measurements introduces uncertainties to the reaction yield and even worse they fail when the correction exceeds 30 %. For capture cross-section measurements with radioactive samples (^{241}Am) and with thick samples of materials that have strong resonances (^{197}Au, ^{113}Cd) the average counting rate can be of the order of 4000 counts/s/detector and the correction can easily exceed 30 %. Therefore, we investigated the possibility to use new data acquisition system with a much sorter dead time.
The solution for a much shorter dead time is a data acquisition system based on a fast digitizer. Two different digitizers have been investigated: the Acqiris DC282 and the CAEN N1728B. Both digitizers are commercially available.
Acqiris DC282 card is a 10-bit and 2 GSample/s digitizer housed in Compaq PCI create. The card has 4 input channels and one common external trigger input. New data acquisition software was written for this card starting from the drivers provided with it. The DC282 card does not perform any signal processing on-board, therefore the digitized signal from the detector is first transferred to the computer via a PCI/PXI bus and then analyzed online.
The CAEN N1728B digitizer is a 4 channels, 100 MHz and 14 bits flash ADC with an on-board signal processing done with a Filed Programmable Gate Array (FPGA). In addition to the 4 input channels, the module has another 4 digital (or NIM) inputs channels which can be used to record the T_0 and the pre-trigger signals from GELINA. The CAEN N1728B card is delivered with acquisition software that is able to pilot the acquisition and to process online the digitized signals. For both digitizers, after the online signal processing, the time and the pulse height values of the event were saved in list mode files.
The two digitizers were tested with C_6D_6 detectors using γ-ray calibration sources and performing capture measurements on ^{197}Au and natural Cd samples. The pulse height resolution of both systems is comparable with the resolution of the conventional data acquisition system. The large difference between the two digitizers is the time resolution: 2 ns was easily achieved with the Acqiris DC282 module, while for the CAEN N1728B module the time resolution was limited to 15 ns. The total dead time of 350 ns and 560 ns was found for the DC282 and for the N1728B module, respectively. The effect of the dead time was clearly observed in a (n,γ) measurement with a ^{197}Au samples of 1 mm thickness. The signals from 4 C_6D_6

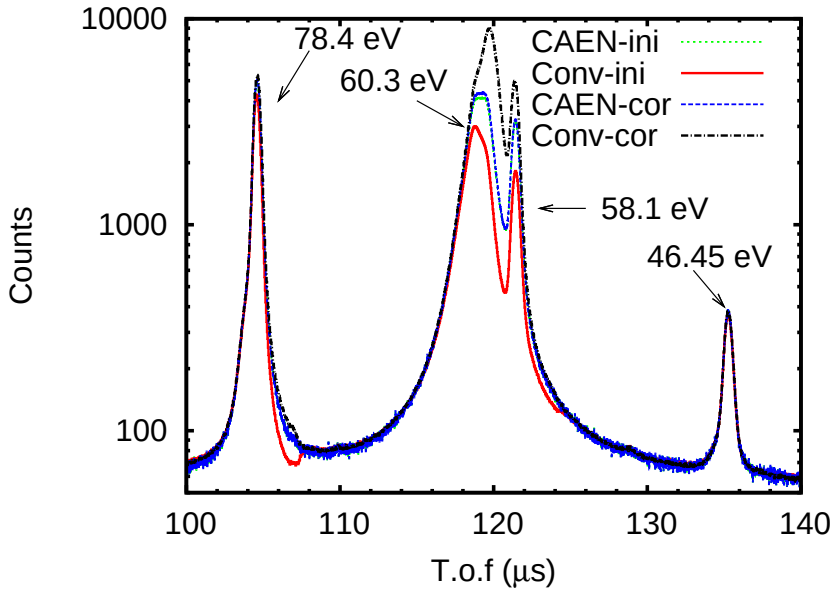

Fig. 1: T.o.f. spectra recorded with the CAEN digitizer and with the conventional system for a ^{197}Au sample of 1 mm thickness. The corresponding dead time corrected spectra are shown as well. All the four spectra are normalized to the maximum of the 46.45 eV resonance. The energy of each resonance is indicated.

detectors were recorded simultaneously with the conventional acquisition system and with the two digitizers. The time-of-flight spectra are shown in Fig. 1. The spectrum recorded with the DC282 digitizer was similar with the one recorded with the N1728B module. The shape and the maximum of the resonances at 58.1 eV, 60.3 eV and 78.4 eV were affected by the long dead time of the conventional system. For these resonances the correction for the dead time failed: a correction factor 8 was obtained for the resonance at 60.3 eV.
Using any of the two digitizers presented here, such corrections for dead time become very small and in many cases even negligible. Both digitizers can be used for (n,γ) cross-section measurements at GELINA. The choice of the fast digitizer to be used can be done depending on the time resolution needed for the studied nucleus. Time resolution of 15 ns is sufficient for resonance shape analysis for many nuclei of interest for nuclear applications. But for nuclei with low level density, time resolution of few ns is needed especially at incident neutron energies of few keV. For the majority of measurements the CAEN N1728B digitizer can be preferred due to the fact that no additional electronic modules are needed. For nuclei with low density levels the Acqiris DC282 module has to be used.

[1] A. Borella, G. Aerts, F. Gunsing, M. Moxon, P. Schillebeeckx, R. Wynants, *The use of C_6D_6 detectors for neutron induce capture cross-section measurements in the resonance region*, Nucl. Instrum. Methods Phys. Res. A577 (2007) 626

Development of DSP routines for the acquisition of nuclear data

Sh. Zeynalov, F.-J. Hambsch, I. Fabry

The resonance neutron induced fission of ^{235}U and ^{239}Pu was intensively investigated for decades because of the great importance of these actinide nuclei for nuclear power production on the one hand and for understanding of the fundamental aspects of the nuclear fission process on the other hand. Experimental investigations of prompt neutron distribution for resonance neutron induced fission carried out in the 70-ies for both uranium and plutonium detected small fluctuations of the prompt neutron multiplicities between resonances [1, 2]. The nature of these fluctuations is still not clearly understood and that fact stimulated further elaborated investigations. In the 80-ies at IRMM fission fragment mass fluctuations were first observed in resonance neutron induced fission of ^{235}U [3] and in the late 90-ies similar fluctuations were reported in Ref. [4] for ^{235}U and for ^{239}Pu in Ref. [5]. The magnitude of the prompt fission neutron fluctuations was correlated with the fluctuations observed in the fission fragment (FF) average total kinetic energy (TKE). As an obvious next step simultaneous measurements of the FF TKE and prompt neutron yields were envisaged. One of the main experimental difficulties in resonance neutron induced fission experiments is the very low event rate demanding the development of elaborated detector systems providing maximum possible information from a single measurement. The trend to use digital pulse processing technology in experimental nuclear physics brings also digital signal processing (DSP) into nuclear particle spectroscopy [6, 7, 8, 9]. Applications of DSP to both FF and prompt fission neutron spectroscopy improves the quality of the final results. An electronic snapshoot of the fission event containing timing and pulse shape information based on the digital waveforms of the detector signal becomes available. Prompt neutron registration requires a multi detector system as a consequence of the small counting rate of the FF leading to further complication of the data acquisition electronics and software.

The first experimental setup developed at JRC-IRMM in 2005-2006 (Fig. 1) was mainly based on analogue signal processing modules. This setup was used for measurements of ^{252}Cf(sf) and ^{235}U(n$_{res}$, f) at the GELINA accelerator. A double Frisch-gridded ionisation chamber was used as the fission fragment spectrometer and as trigger for the neutron detection. The neutron detector (ND) array consisted of eight DEMON modules each containing four litre of NE213 liquid scintillator. For each fission event the following information was recorded: two pulse heights of correlated fission fragments, the angle between the fission and chamber axis, eight prompt neutron time-of-flight (pTOF) and pulse shape values and the incident neutron time-of-flight (rTOF).
The data acquisition software allowed real time digital signal processing and real time data monitoring during the measurement and had a user friendly graphical user interface (GUI). The data are acquired event by event and stored on the local hard disk of a PC for further off-line data analysis.

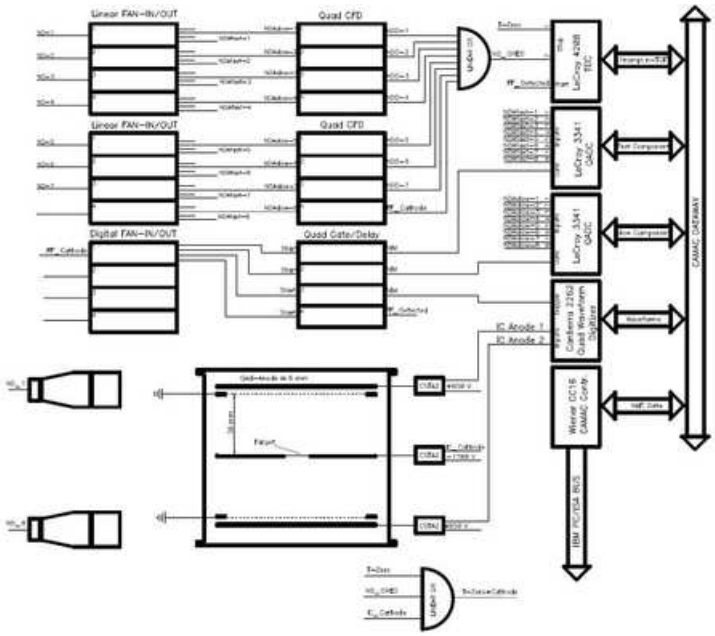

Fig. 1: Experimental setup for prompt fission neutron emission in resonance neutron induced fission (mixed analogue/digital signal processing modules)

A new fully digital signal processing data acquisition system was developed in 2007. The heterogeneous data acquisition system (Fig. 2) consisted of waveform digitisers (WFD) from two manufacturers: one four channel DC282 module from the Acqiris, Agilent Technologies Inc., and four double channel MI3025 modules from Spectrum GmbH. Because of the large power consumption of the WFD modules, they were used in autonomously powered separate racks and PCI-to-PXI and PCI-to-PCI bus extension units as shown in Fig. 2. A temporary solution for the synchronization between two (Acqiris and Spectrum) sets of digitizers was made using an analogue OR mixer and one of the Acqiris channels. A more sophisticated synchronization module is a field programmable gate array (FPGA) based device with a USB 2.0 interface to the data acquisition PC developed at JINR, Dubna. This synchronization (here call *Trigger Master* - TM) device will replace the two linear OR modules shown in Fig. 1 providing a common trigger signal for all digitizer modules. In addition, the TM provides the encoded ND number, hit by the prompt fission neutron and the rTOF value measured with 20 nsec precision. The synchronization currently in use, although providing confidence on the validity of the acquired data, can not be considered as a universal solution for every heterogeneous data acquisition system. The TM module was developed as a universal and flexible solution (because of use of the FPGA).
The output of the data acquisition software are waveforms, which are passed trough the DSP software to provide the list mode data. The further list mode data analysis can be performed using programs like GENDARC [7] the recently developed data analysis program. The DSP software procedure library is under development [8, 9]. The library will be used both in data acquisition and data analysis.

[1] J. Fréhaut, D. Shackleton, *Mesure du nombre moyen de neutrons prompts émis lors de la fission induite par neutrons de resonance dans l'^{235}U et l'^{239}Pu*, in Proc. 3rd Symp.

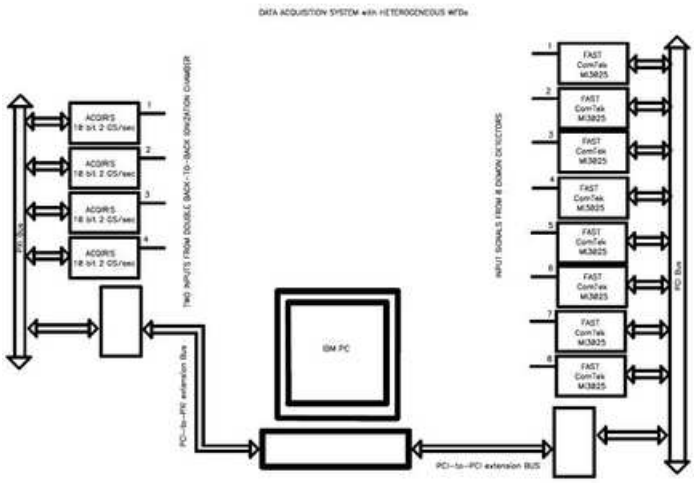

Fig. 2: Further evolution of the experimental setup for prompt fission neutron emission in resonance neutron induced fission (full digital signal processing approach)

Physics and Chemistry of Fission, IAEA Vienna (1974) 201

[2] R. E. Howe, T. W. Philips, and C. D. Bowman, Phys. Rev. C13 (1976) 195

[3] F.-J. Hambsch, H.-H. Knitter, C. Budtz-Jørgensen, J.P. Theobald, Nucl. Phys. A491 (1989) 56

[4] Sh. Zeinalov, M. Florek, W. I. Furman, V. A. Kriatchkov, Yu. S. Zamyatnin, Proc. VII Int. Seminar on Interaction of Neutrons with Nuclei (ISINN-7), Dubna, Russia, May 25-28 (1999 258

[5] L. Demattè, F.-J. Hambsch, H. Bax, in: C. Wagemans, O. Serot, P. D'Oye IV, October 6-9, 1999, Habay-la-Neuve. World Scientific, Singapore (2000) 135

[6] L. Bardelli, G. Poggi, M. Bini, G. Pasquali, N. Taccetti, Nucl. Instr. And Meth. A 521 (2004) 480

[7] I. Fabry, F.-J. Hambsch, S. Oberstedt, S. Zeynalov, N.Kornilov, *GENDARC, the GEel Neutron physics Data acquisition, Analysis and Run Control program*, EC-JRC IRMM Scientific Report, EUR 23039 EN, ISBN 978-92-7905365-8 (2006) 88

[8] Sh. Zeynalov, F.-J. Hambsch, S. Oberstedt and I. Fabry, submitted to Nucl. Instr. Meth. A

[9] O.V. Zeynalova, Sh. Zeynalov, F.-J. Hambsch, S. Oberstedt, submitted to Nucl. Instr. Meth. A

Prototype of a novel type of neutron detector

G. Lövestam, A. Fessler, J. Gasparro, M. Hult, P. Kockerols, G. Marissens, E. Wieslander

The developed neutron detector, the DONA (DOsimetry using Neutron Activation) neutron spectrometer, is based on the measurement of neutron induced activity in a series of small metal disks that have been exposed to a neutron field. The neutron spectrum is calculated by means of an unfolding technique, using the neutron excitation functions of the included disk materials and a library of known neutron spectra.
The novelty of the approach lies in the concept as such, including usage of carefully selected metal disks arranged in a holder, high performance γ-ray spectrometry and spectrum unfolding using a library of neutron spectra. Starting in 2004, a first study was carried out within the frame of IRMM exploratory research projects. Several prototype detectors were developed and successfully tested in laboratory neutron fields. The results showed that the detector could be very well used as a low-level neutron spectrometer and as such, serve as a good complement or alternative to existing more cumbersome techniques. The project was awarded the JRC 2007 Innovation Project Competition launched by the ISR/TTSC unit.

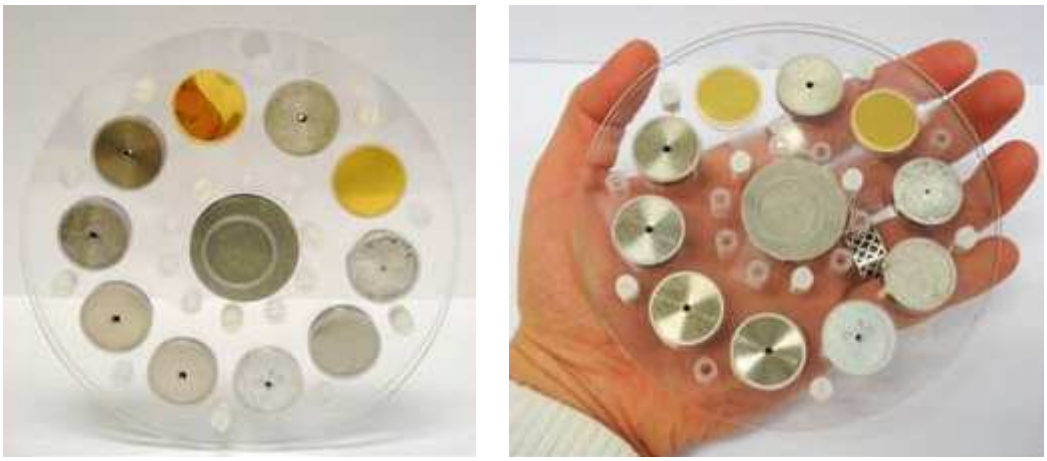

Fig. 1: The DONA prototype holder

The DONA detector system consists of three parts:

a. the neutron sensitive device consisting of a series of metal disks arranged in a holder,

b. a high performance gamma-ray measurement station, and

c. the data evaluation station.

As the neutron sensitive device does not require any electronics or data acquisition system on the measurement site, this arrangement constitutes a great advantage since no delicate equipment has to be brought out in the field. On the contrary, the precise activation measurements can be done in a well established gamma-ray measurement laboratory.

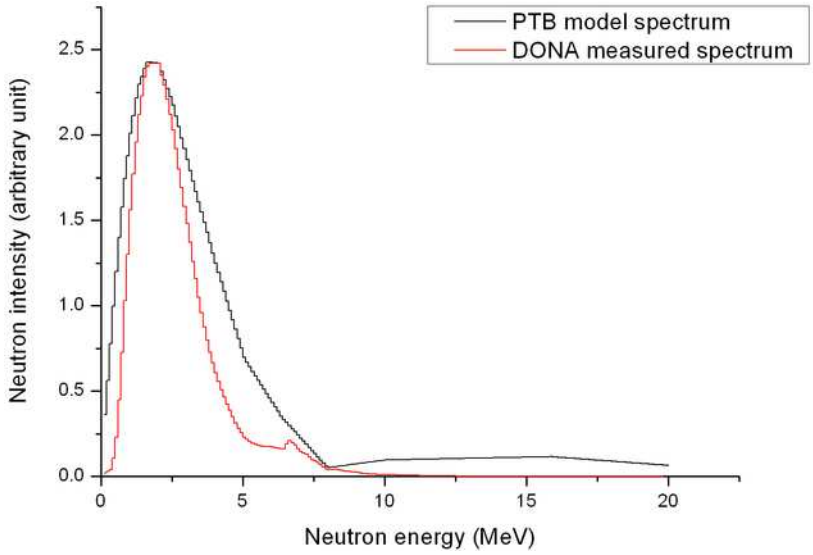

Fig. 2: Measured and typical ^{252}Cf reference neutron spectrum

A neutron spectrometry field measurement is consequently done in three steps. In the first step the detector device is positioned at the site of measurement. Either a "static measurement program" is followed, i. e. detectors are always positioned at locations where possible neutron radiation could occur, for example following an accident event, and the detectors are collected for measurements only when a neutron irradiation is suspected, or a "dynamic measurement program" is used where the detectors are positioned in a suspected neutron field only at a certain occasion and for a certain pre-defined time. Typical irradiation times are, naturally, dependent on the neutron fluence rate, but for fluence rates of 1,000 neutrons/cm^2/s about 24 h should be foreseen for low uncertainties. The choice of measurement program is, of course, dependent on the activities at the measurement sites and the character of the expected neutron fields, but a dynamic measurement program is generally easier to evaluate as the time information for the irradiation and possible fluence rate variations is normally better known.
In a second step, the detector device is transported to the γ-ray measurement laboratory where the neutron induced activity of each disk and isotope is measured. The transportation is critical as it should be done within one or two half life periods of the isotope with the shortest half life.
In the third step, the data from the gamma measurements are evaluated using a few-channel spectrum unfolding technique to obtain the measured neutron energy spectrum.
During 2007 the following results were achieved:

- A versatile detector holder has been designed and a first batch of holders has been produced and delivered.
- The detector has been tested in a certified calibrated neutron field.
- A dedicated gamma-ray measurement station has been designed and a prototype has been constructed and tested. A commercial prototype has been designed.
- A user friendly software package has been designed, constructed and tested.

- An external company has been engaged for the marketing of the system.

To validate the method including the developed prototype holder, a DONA detector was irradiation at the calibrated Californium-252 source at the Physikalisch-Technische Bundesanstalt (PTB) in Braunschweig, Germany. The short-lived radionuclides were measured in the PTB low level gamma-ray measurement laboratory while the remaining disks were transported back to IRMM for measurements in the underground ultra low-level γ-ray measurement laboratory, HADES. The validation test was successful and showed that the newly developed prototype holder was both easy to mount and had no impact on the neutron activation of the disks.

NAXSUN - Measurement of neutron activation cross section curves using moderated neutron fields

G. Lövestam[1], *E. Birgersson*[1], *J. Gasparro*[1], *W. Geerts*[1], *M. Hult*[1], *G. Marissens*[1], *S. Oberstedt*[1], *H. Tagziria*[2]

[1] European Commission, JRC-IRMM, B-2440 Geel
[2] European Commission, JRC-IPSC, I-21027 Ispra

Many fields of science require accurate neutron activation cross section data, particularly in the energy region up to about 20 MeV. Practical examples are within astrophysics, geophysical and bore-hole logging, for safety, dosimetry and environmental protection, for decommissioning of nuclear installations, at fission and fusion reactor installations, for the production of medical isotopes, and for various research activities. Several national and international data libraries of neutron activation cross section data have evolved over the years and numerous measurements have been carried out at laboratories world-wide. As the neutron activation cross section depends on neutron energy the measurements have been carried out using quasi mono-energetic neutron beams. In energy areas where measured data are scarce excitation functions are obtained either from pure calculations or by fitting measured data to nuclear models. However, the model predictions can vary considerably in the absence of good quality measured data. Indeed, many neutron activation cross section data entered in the data libraries, as well as different modellings of cross section data, show large discrepancies.

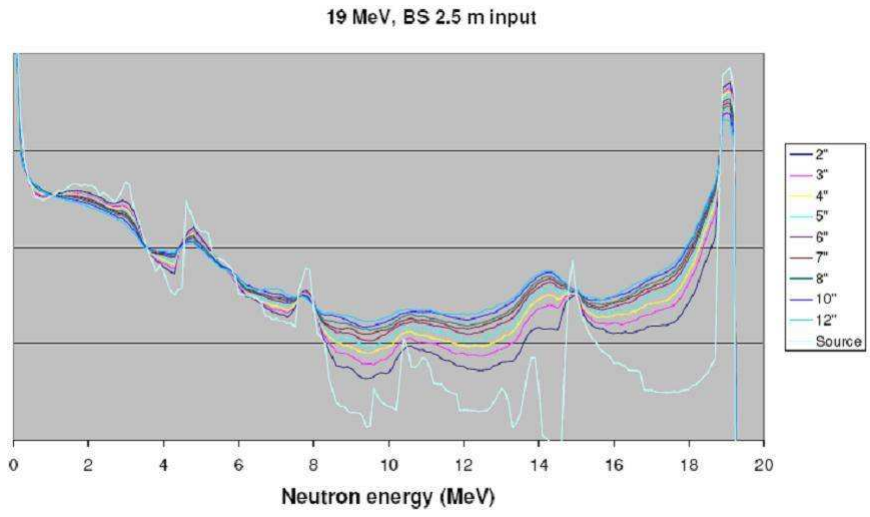

Fig. 1: Input neutron field and MCNP calculated neutron fields in the centre of the 1" and the 12" polyethylene spheres

This project concerns the measurement of neutron excitation functions using an alternative approach. Traditionally, cross sections are measured at point-wise energies to which a curve is fitted or modelled. Here, we exploit the technique of measuring the complete curve as is. This

is done by irradiating a number of identical sample disks in a series of non-mono energetic different, but well known neutron fields, followed by gamma spectrometry and spectrum unfolding to calculate the excitation function. Only one neutron energy is used and the different neutron fields are created by means of moderating the fields in polyethylene spheres with the sample material mounted in the centre. This technique has the advantage of using only one ion beam energy and a single neutron producing target. It also allows for the generating of neutron fields over the entire energy range 0.5 - 18 MeV.

The technique was tested on the well characterised excitation function for ^{115}In(n, n')^{115m}In and data evaluation is on-going.

Poly-crystalline CVD diamonds for ultra-fast fission fragment timing

S. Oberstedt[1], *C. Negoita*[1], *A. Oberstedt*[2]

[1] European Commission, JRC-IRMM, B-2440 Geel
[2] Institutionen för Naturvetenskap, Örebro Universitet, S-70182 Örebro

For the double fission-fragment time-of-flight spectrometer VERDI CVD (chemical vapour deposition) diamond detectors are chosen as fission timing detectors because of their ultra-fast timing capabilities and apparent radiation hardness proven in high-energy physics and in accelerator application [1]. Up to now, however, diamonds have not been used in low-energy fission experiments, where particle energies range from about 2 MeV/u down to well below 0.5 MeV/u.
In a first experiment we investigated the behaviour of a 100 μm thick diamond detector under irradiation with a mixed α-source and the effect of pre-irradiation (priming) with a strong ^{90}Sr/^{90}Y β-source [2].

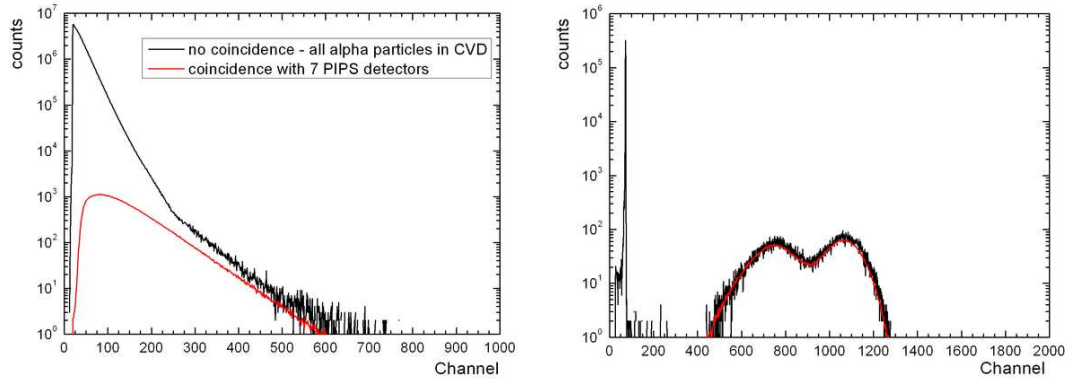

Fig. 1: Fission-fragment pulse height distribution with (red line) and without (black) coincidence condition for the CVD diamond (left) and the PIPS (right) detectors showing the effective α-particle suppression even for the low pulse-height resolving pcCVD diamond material.

In a next step a spectroscopic ^{252}Cf source with about 300 fissions/s was placed just in front of a primed pcCVD diamond detector and about 20 cm away from an array of 7 PIPS detectors. The PIPS detectors served as trigger for the unequivocal determination of a fission event. In Fig. 1 the pulse height spectra of the CVD diamond detector (left) and the PIPS detectors (right) is shown. The red lines indicate the pulse height distribution taken in coincidence between a PIPS and the CVD diamond detector. The efficient suppression of the high α-particle count rate in the diamond detector despite the well-known low pulse-height resolution is remarkable.
In Fig. 2 the diamond detector signal stability is shown as a function of the fission-fragment

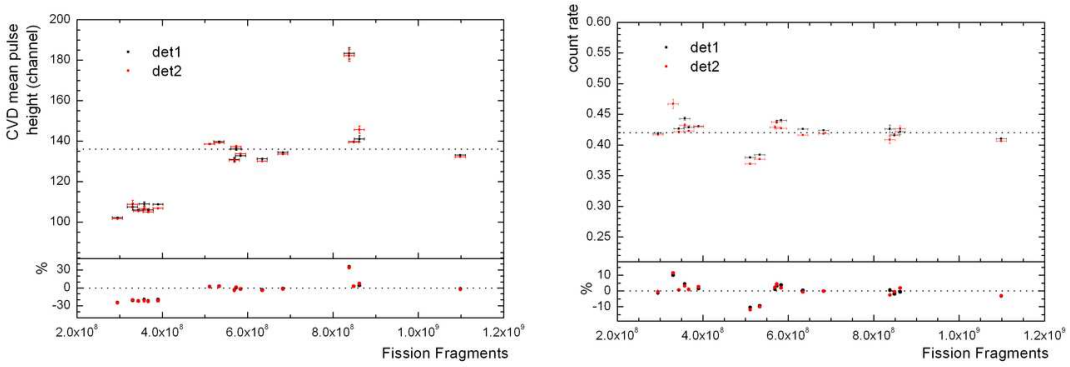

Fig. 2: Left: CVD diamond detector pulse height stability as a function of fission-fragment dose; Right: average coincident fission-fragment count-rate as a function of the fission-fragment dose.

dose. In the left part the mean pulse height is shown. After an initial increase the mean pulse height reaches a stable plateau which is kept up to an integral dose of 1.2×10^9 fission fragments, which corresponds to the dose during a typical fission experiment. The signal stability reflects in a constant fission-fragment count-rate as shown in the right part of Fig. 2.

Fission-fragment timing between a PIPS and the diamond detector, however, was found to be unsatisfactory due to limitations in the electronics set-up and/or apparent *environmental* noise, and will have to be investigated next.

[1] E. Berdermann, K. Blasche, P. Moritz, H. Stelzer, B. Voss, Diamond and Related MAterials 10 (2001) 1770

[2] S. Oberstedt, C. C. Negoita, F.-J. Hambsch, W. Geerts, EC-JRC IRMM Scientific Report, EUR 23039 EN, ISBN 978-92-7905365-8 (2007) 91

Development of an analogue signal router for cluster detectors

M. Vidali, S. Oberstedt, C. Chaves de Jesus

The fission-fragment time-of-flight spectrometer VERDI, presently under construction, will consist of two silicon detector arrays of at least 16 detectors each to provide a reasonably large geometrical detection efficiency. In order to handle this number of signal channels using our NIM-standard electronics and eight-input data acquisition an analog-signal routing (ASR) device for up to 16 detector signals after a shaping amplifier has been developed. The device is used in conjunction with a tag-word coder (TWC) to identify the detector, which was hit by a particle. The fast signal from the detector pre-amplifier is converted to a NIM signal, split and entered into the TWC module to encode the detector as well as sent to the gate input of the ASR to open the corresponding pulse height channel. The common analogue signal output is sent to a standard analogue-to-digital converter. A visual view on the two-wide NIM 16-channel anlogue-signal router as well as a block diagram resuming its functioning are given in Fig. 1.

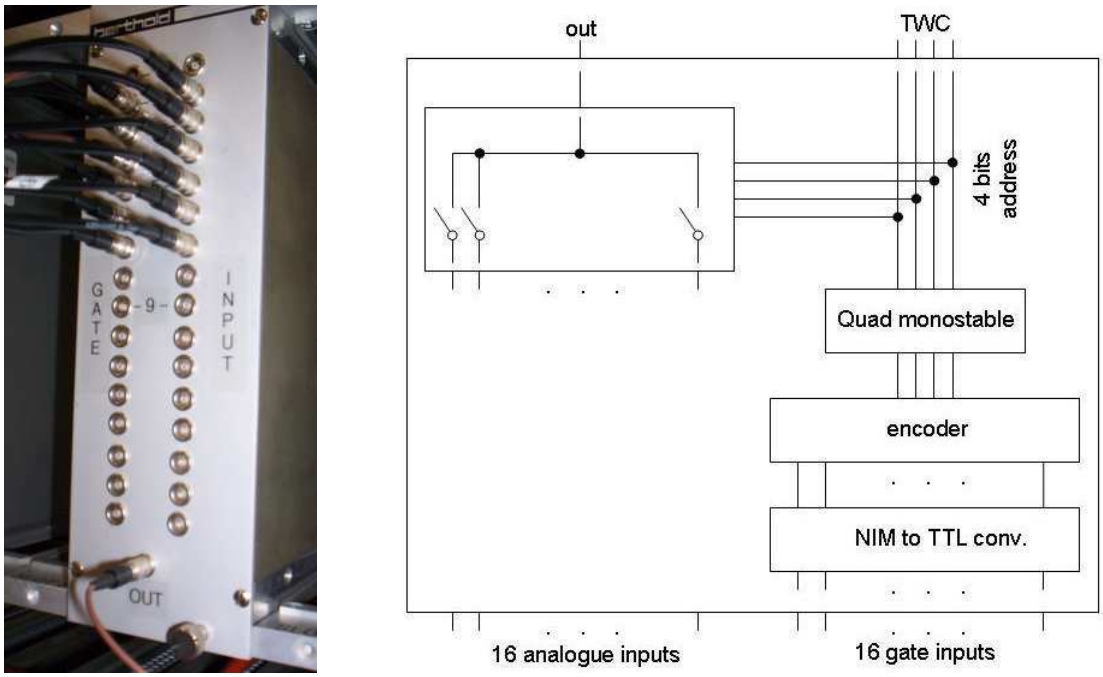

Fig. 1: Left: View on the prototype of a two-wide NIM 16-channel analogue signal router with its analogue signal inputs (right) and the NIM-logic gate inputs (left); the common out (bottom) is sent to a standard analogue-to-digital converter. Right: Logical scheme of the analogue signal router.

With an expected maximum fission-fragment count rate below 10/s per detector the simultaneous arrival of fission fragments in different detectors is low and, therefore, the analogue signal router allows to acquire data from the full VERDI spectrometer with only 8 ADC channels.

The main component of the device is a 16 channel high performance CMOS analogue multiplexer. It connects with low resistance ($\approx 50\ \Omega$) one channel at a time to the output. The channel, once triggered, remains open for a fixed amount of time (progressively adjustable between 2 and 20 μs using a panel mounted potentiometer to allow the usage of the device with different types of detectors). During this time interval all other gate signals are ignored, so if another event occurs on another channel, it does not interfere with the active one. If two gate signals occur at the same time, priority is given to the channel with the higher address.

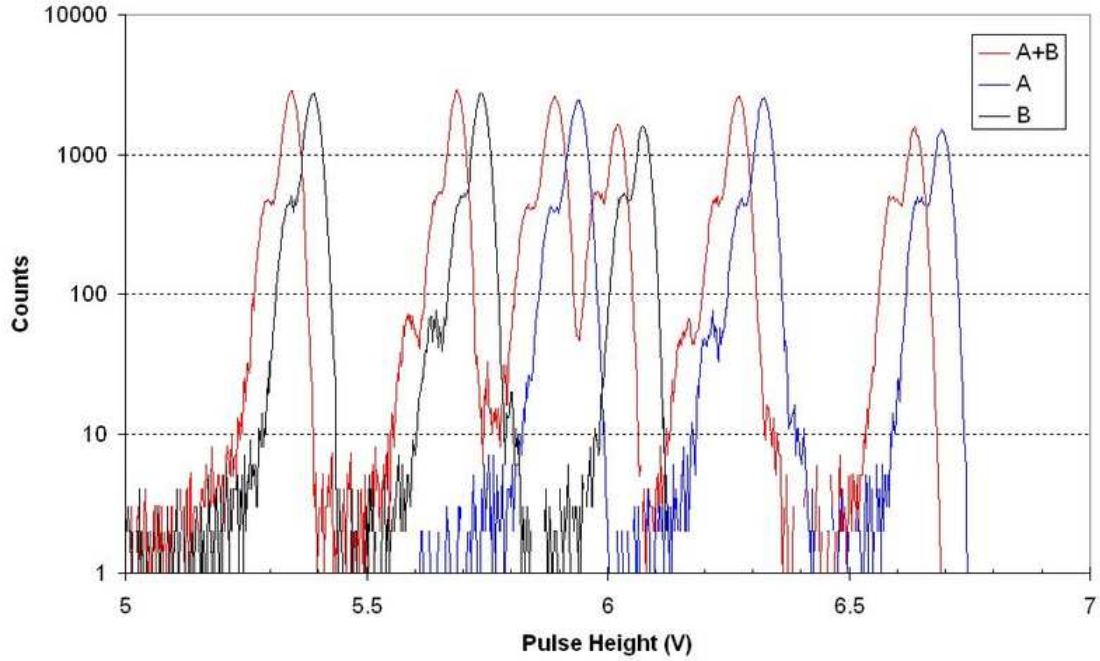

Fig. 2: Comparison between two α-particle spectra acquired by two independent ADC channels (A and B) and through the analogue signal router (A+B) by a third ADC channel.

A first prototype with reduced input channel number and capabilities has been successfully tested; the final version of the device is still under development. In Fig. 2 is shown the comparison between two α-particle spectra acquired by two independent ADC channels (A and B) and through the ASR module (A+B). Except for the shift in pulse height, due to the additional resistance introduced by the signal router, the signal is basically not affected and pulse height resolution preserved.

Investigation of pulse-pileup from proton recoils in an ionisation chamber

E. Birgersson[1], *S. Oberstedt*[1], *A. Oberstedt*[2], *F.-J. Hambsch*[1]

[1] European Commission, JRC-IRMM, B-2440 Geel
[2] Örebro University, SE-70182 Örebro

The kinetic energy of fission fragments can be measured with a Frisch grid ionisation chamber. The fission fragments ionise the gas and as the electrons move they will induce a charge on the anode of the chamber. All electrons, which are created in the region between the cathode and the grid, will induce the same charge, since the anode is shielded by the grid. If the chamber is positioned in a neutron field, elastic scattering of the neutrons with the counting gas will occur. The recoiled particles will also ionise the gas, which lead to a pulse pile-up of the fission fragment signal if they occur in coincidence. This becomes especially important if P-10 (90 % Ar + 10 % CH_4) is used as a counting gas, since it has a large hydrogen content. Neutron elastic scattering can give protons energies up until the incident neutron energy. The effect is similar to coincidence with an α-event, which was studied in Ref. [1], where it was found that as long as pile-up count rate is constant it does not constitute a major problem. The energy and the count rate of proton recoil depend on the neutron energy and neutron flux. The effect of pile-up immediately becomes an issue, since many fission studies are performed at different neutron energies and neutron fluxes. Increase of the total kinetic energy (TKE) of the fission fragments for a typical chamber can be as high as 0.7 MeV when neutron flux is 10^7 n/cm^{2}s and neutron energy is 1.8 MeV. Obviously the effect has to be corrected for and is further explained in Ref. [2].

In this investigation the pile up from proton recoils in a double sided Frisch grid ionisation chamber was performed. In parallel, fission fragment distributions from the reaction ^{238}U(n, f) were measured, which made absolute energy calibration possible. The grid-cathode distance in both chamber sides was 3 cm, the anode-grid was 0.7 cm, and the radius of the grid was 4.5 cm. The chamber was put as close as possible to the neutron source. The pile-up will also add to the signals from a pulse generator, which was used to monitor possible drift in the amplification of the set-up.

The pulse signal spectrum was successfully calculated for several neutron energies and fluxes and shows excellent agreement to measured data. To perform the calculation the following was used as inputs:

- Neutron flux and neutron energy in different parts of the chamber [3]
- cross section for the neutron-proton recoil [4]
- Discription of the chamber geometry
- P-10 gas composition and pressure
- energy loss of protons in P10-gas as a function of track length [5]
- shaping time of spectroscopic amplifier

- Position and width of the undisturbed pulse signal

The calculation was performed in two parts, which were both Monte Carlo simulations. When the recoil proton ionise the counting gas, the measured signal is only proportional to the energy if the ionisation track is in the region between the cathode and the grid. If energy is deposited outside of the sensitive volume, it is not detected. If ionisation occurs in the region between the anode and grid the full signal is not detected. This was not taken into account in the simulation, where the sensitive volume was defined as the region between the cathode and the anode. The first part of the calculation was the determination of the deposited energy spectrum in the sensitive volume. In the second part, the coincident count rate was calculated as well as the amount of energy which actually adds in the pile-up. The energy was sampled from the energy spectrum which was calculated in the first part. The pulse shape with the pile-up is described almost perfectly over 5 orders of magnitude for the chamber side closest to the neutron beam (source side) and the other side (non-source side) as can be seen in Fig.1. The description is also accurate for various neutron energies and neutron fluxes. The pile up with α-particles, from the decay of the ^{238}U-target, which have higher energies then the protons and cosmic events are clearly seen.
Here follows a more complete description of the calculations. The deposited energy spectrum in the sensitive volume of the ionization chamber from the recoiled protons was estimated in a Monte Carlo simulation. Each chamber side was divided in 30 annular disks. In each disk the average neutron energy and flux was estimated using the computer code EnergySet [3], using the known proton current and energy as well as the neutron producing reaction. The individual neutron fluxes in each annular disk were then folded with the cross section for proton recoil, which also is energy dependent. This also gave the total count rate of the proton recoils in each chamber side as a function of incident proton current, energy and neutron producing target. This count rate C_r is needed when the coincident count rate is determined in the next part of the calculation. The angular distribution for n-p elastic scattering is approximately constant in the centre-of-mass (CM) frame according to Ref. [4] and was assumed to be constant here. By assuming that the neutron and proton have equal masses conversion from CM angle, θ_{CM}, to laboratory angle, θ can be performed by

$$\tan\theta = \sin\theta_{CM}/(1+\cos\theta_{CM}). \tag{1}$$

The kinetic energy of a scattered proton Ep is then given by

$$E_p = E_n \cos^2\theta, \tag{2}$$

where θ_{CM} is the angle of the proton relative to the incident neutron in the laboratory frame and E_n is the kinetic energy of the neutron.
The deposited energy in the ionization chamber as a function of the track length was estimated using SRIM2003 [5] for $E_p = 1.8$ MeV. The result from this simulation (see Fig. 1) was then scaled to estimate the amount of deposited energy in the sensitive volume from each recoiled proton.
The result of the Monte Carlo simulation is the spectra of the deposited energy in each chamber half shown in Fig. 1. The protons created in the chamber half close the neutron source might go through the thin Uranium layer in the middle of the common cathode in the chamber. This means that some protons deposit energy in both chamber halves, which was

correctly taken into account in the simulation. Energy loss in the thin uranium sample can be neglected. The found deposited energy spectra using a LiF target with incident proton energy 3.5 MeV creating neutrons with energy 1.8 MeV in forward direction is shown (upper right) in Fig. 1. The low energy peaks in the spectra occur because the large amount of recoiled protons from the side of the chamber, where the angle of the incident neutron relative to the incident proton beam is large. These recoiled protons can only deposit a small amount of energy before leaving the sensitive volume since they are close to the edge of it. At the same time, this part of the chamber is quite large, although the neutron flux is lower than in forward direction. The structure is artificial and arises because the chamber only divided in 30 annular disks.

In the second part of the calculation the coincidence spectrum between the pulse signal and the recoiled protons was calculated. The initial position and width of the pulse signal were adjusted to best represent the experimental data. The deposited energy from the recoil protons were sampled from the previously calculated distributions. The amount of the deposited energy from the recoil protons, which are added to the pulse signal when they come in coincidence, were assumed to have equal probability up until the maximum deposited proton energy. The shaping time on the spectroscopic amplifiers were set to 3 μs, which determines the coincidence time window, $\Delta\mathrm{T} = 12$ μs. The probability of r coincidences for a given count rate C_r is given by the Poisson distribution

$$P(r) = \frac{(C_r \Delta T)^r \exp(-C_r \Delta T)}{r!} \quad , \tag{3}$$

which also was used in the simulation. The count rate in each chamber side C_r was estimated in previous section. To experimentally verify that the shaping time 3 μs gives a coincidence time window of $\Delta\mathrm{T} = 12$ μs, two independent pulse signals, which were added before being fed to a spectroscopic preamplifier, were used. The amount of energy added when the two pulse signals came in coincidence follow a square probability distribution all the way up to the maximum value also needed to be verified.

Pulse signal 1 was set to 0.2 V at 10 Hz and appears at channel 2380. Pulse signal 2 was set to 0.01 V at 3000 Hz. The spectrum is shown (bottom right) in Fig. 1. The sum of the two pulse signals (0.21 V) should be at channel 2500 which is indeed the maximum value the coincidence spectrum reaches and it appears to have a square distribution to this value. By extrapolating the pile up counts (6.5 cts/channel) to also include events under the original pulse, gives a coincident count rate of 0.37 Hz. This gives a coincidence time window of 12 μs. Both assumptions are thus confirmed.

[1] L. Demattè, F.-J. Hambsch, H. Bax, Nucl. Instr. Meth. A480 (2002) 706.

[2] E. Birgersson, PhD thesis, Örebro (2007), ISBN 978-91-7668-548-8

[3] G. Lövestam, Computer code EnergySet, Internal report No. Ge/NP/2/2002/06/20 (2002).

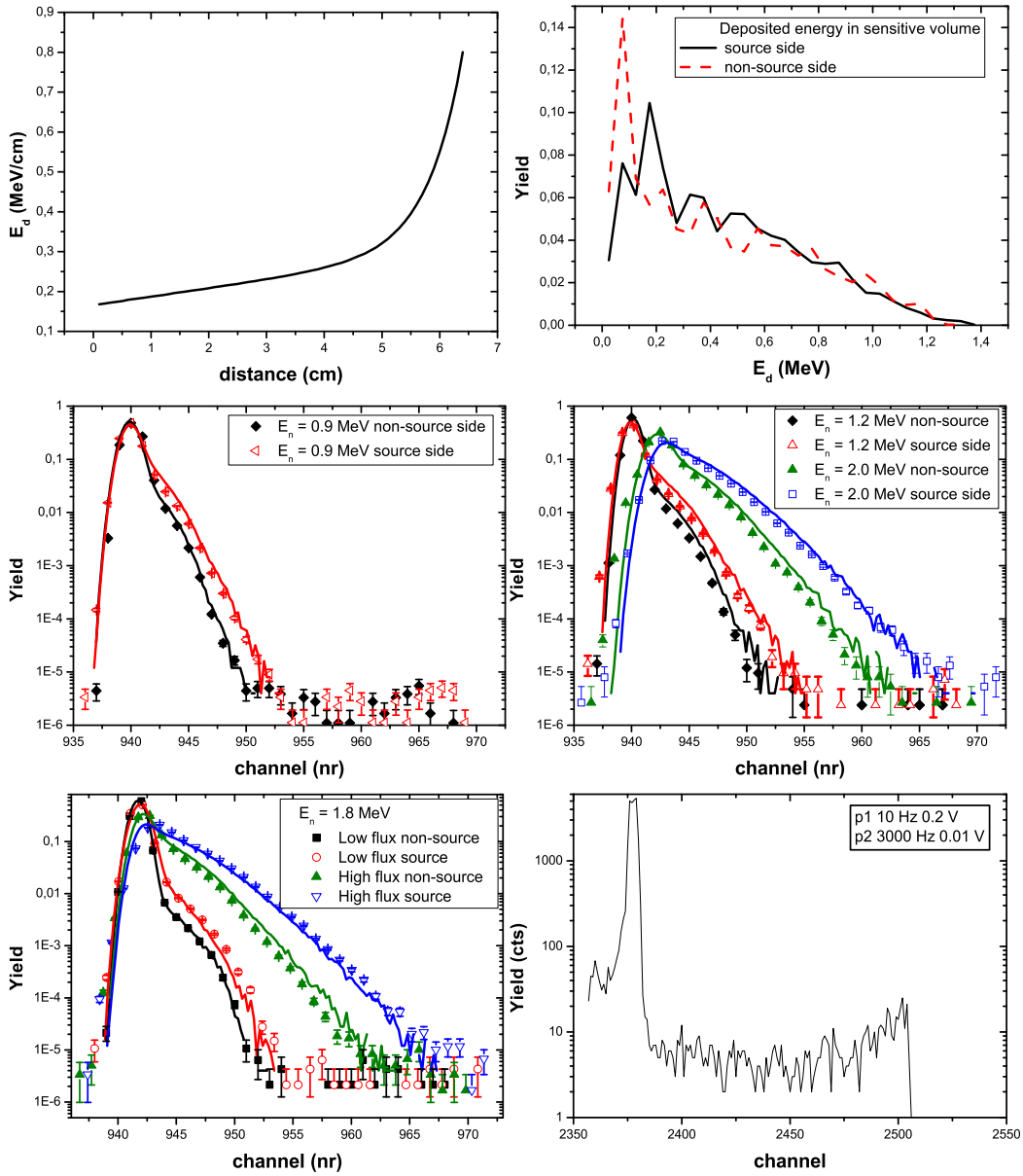

Fig. 1: Deposited energy from a proton as a function of track length (upper left), spectrum from the energy deposited by the proton recoils in the sensitive volume of each chamber side for $E_n = 1.8$ MeV (upper right), measured and calculated pulse signal and proton recoil coincidence spectra for $E_n = 0.9$ MeV (middle left), for $E_n = 1.2$ and 2.0 MeV (middle right), and for $E_n = 1.8$ MeV at two neutron fluxes (bottom left), spectrum for a pulse signal obtained with a shaping time 3 μs, a second pulse signal at high count rate comes in coincidence confirms two assumptions in this work (bottom right).

[4] A. Konig, R. Forrest, M. Kellett, H. Henriksson, and Y. Rugama, editors, The JEFF-3.1 Nuclear Data Library, JEFF report 21, NEA (2006).

[5] Computer code SRIM2003.26, available from J. F. Ziegler, IBM Research, Yorktown, NY-10598, USA and J. P. Biersack, Hanhn-Meitner Institut, Berlin-39, Germany.

Simulation of neutron fluence characteristics from ion-induced neutron sources

E. Birgersson, G. Lövestam

Quality assurance for nuclear data measurements requires development of Monte Carlo simulation techniques to model complete experimental set-ups. Within the European Facilities for Nuclear Data Measurements (EFNUDAT), IRMM has been given the task to develop methods for a unified simulation of complete neutron beam facilities. To do this, a proper description of neutron production is needed. This includes the effects of charged-particle transport in the production target and the cross section for the neutron producing reactions. The neutron transport simulation is also important for an accurate description of the neutron fluence characteristics at experimental locations. It was investigated which of the currently available general-purpose transport codes that can be adapted for this purpose.

The Target code [1] is a Monte Carlo simulation which calculates the neutron flux over a given area. The program also gives the flux of scattered neutrons. The geometry description has to be given in cylindrical symmetry and only a limited number of materials are available to describe the experimental setup. When a deuterium gas target is used as neutron producing target, the scattered neutron flux is not calculated. The gas target part of the program has been included by incorporating the main features of the SINENA code [4]. Neutrons are then created by the D(d, n)^{3}He reaction. The EnergySet code [2] on the other hand is a direct calculation of the neutron flux at a certain position and executes much faster than the target code. However, the target code is more realistic than the EnergySet code, since the incident ion beam can be given a specified energy resolution and both angular and energy straggling during ion energy loss is included. One additional difference is that the Target code takes into account that neutrons emitted in several angles and thus having different energies can reach the area of the detector. This is only important if the detector is large compared to the distance to the source. Thus determining the neutron flux far away from the neutron source on a small surface, the two programs can be compared. As seen in Fig. 1 there is a good agreement for solid targets but for gas target a discrepancy is seen. This difference is only seen at low deuteron energies. A SRIM [3] simulation were performed, where the energy loss for a deuterium ion in deuterium gas were estimated. The estimated energy loss in the target code is less than both SRIM and EnergySet ,which are in agreement.
For neutron transport simulation the program MCNP [5] is often used. It is a very flexible program, any geometry and material can be used. However, an accurate description of a neutron source is rather cumbersome to give, especially when a gas target is used.
Because of the geometry restriction and the problem with the gas target in the target code [1], the EnergySet program will be modified to produce an input file describing the neutron source for MCNP. This will then facilitate the simulation of a complete neutron beam. To make the input file accurate, the energy loss calculation in EnergySet needs to be modified to also include energy straggling.

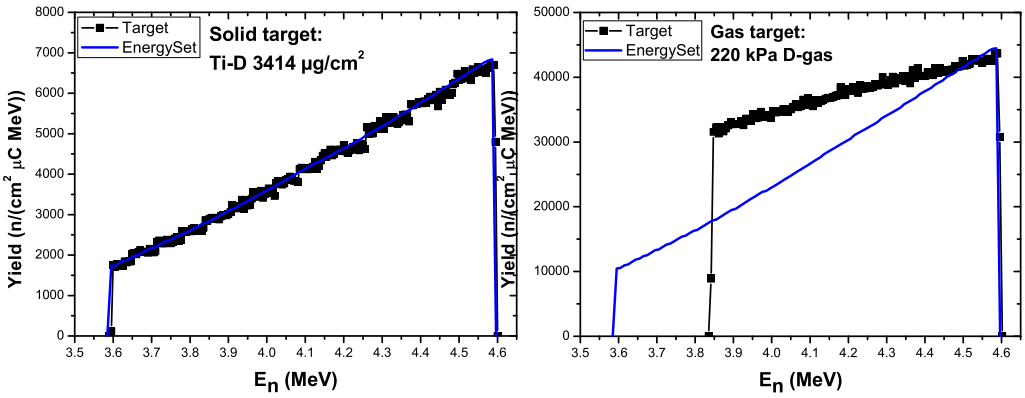

Fig. 1: Neutron spectra calculated with Target [1] and EnergySet [2] 50 cm from the source in forward direction from the D(d, n)^{3}He reaction at $E_D = 1.4$ MeV for solid target (left) and gas target (right).

[1] D. Schlegel, TARGET USERs MANUAL, PTB-6.42-05-2 (2005)

[2] G. Lövestam, Computer code EnergySet, Internal report No. Ge/NP/2/2002/06/20 (2002).

[3] Computer code SRIM2003.26, available from J. F. Xiegler, IBM Research, Yorktown, NY-10598, USA and J. P. Biersack, Hanhn-Meitner Institut, Berlin-39, Germany.

[4] B.R.L. Siebert, H.J. Brede and H. Lesiecki, "SINENA - A Monte Carlo Program for Transferring Proton-Recoil Telescope Neutron Fluence Measurements to Detectors", PTB Report PTB-ND-23, Braunschweig, (1982)

[5] X-5 Monte Carlo Team, "MCNP-A General Monte Carlo N-Particle Transport Code, Version 5 (2003)

Accelerators:
Instrumentation and development

The Geel electron linear accelerator facility GELINA

W. Mondelaers, K. Cairns, C. Diaz Vizoso, C. Ganassin, W. Mota, G. Pettinicchi, H. Spruyt, R. Van Bijlen, S. Vermeiren

The Geel Electron Linear Accelerator facility GELINA is a pulsed white-spectrum neutron source in combination with a time-of-flight (TOF) facility designed and built for high-resolution neutron cross section measurements. The neutron source is based on a linear electron accelerator producing electron beams with a typical beam operation mode characterised by 100 MeV average energy, 10 ns pulse length, 800 Hz repetition rate, 10 A peak and 80 μA average current. Using a unique post-acceleration pulse compression system, the electron pulse width can be reduced to approximately 1 ns (FWHM) while preserving the current, resulting in a peak current of 100 A. The accelerated electrons produce Bremsstrahlung in an uranium target which in turn, by photonuclear reactions, produces neutrons. Within a 1 ns pulse a peak neutron production of 4.3×10^{10} neutrons is achieved (average flux of 3.4×10^{13} neutrons/s). By using a hydrogen-rich moderator and collimators and shadow bars, moderated or unmoderated neutron beams are generated for the twelve neutron flight paths. Further tailoring of the spectral shape is done with movable filters. GELINA covers the neutron energy range from 1 meV to 20 MeV. The up to 400 m long flight paths, which point radially to the uranium target, lead to experimental locations at distances of 10, 30, 50, 60, 100, 200, 300 and 400 m. These experimental stations are equipped with a wide variety of sophisticated detectors, and data acquisition and analysis systems. GELINA is a multi-user facility operating on a continuous 24 h shift basis from Monday morning to Friday evening, and serving simultaneously a maximum of 10 concurrent experiments.

During 2007, GELINA was used exclusively in the framework of the institutional work programme and for the trans-national access programme NUDAME. The facility produced neutron beams for experiments during 2954 hours, which is 20 % more than the average of the annual beam time since the year 2000, despite the fact that we had an unscheduled loss of beam-time during six weeks in June and July, due to a failing neutron production target and the unavailability of an operational spare unit (for details, see below).

The accelerator was operated in two modes:

- high pulse repetition frequency mode (800 Hz repetition rate) with electron beams on target of 100 A peak current, 1 ns pulselength (80 μA average current). This operating mode covered 61 % of the available beam-time.
- low pulse repetition frequency mode (50 Hz repetition rate) with electron beams on target of 100 A peak current, 1 ns pulselength. During 39 % of the available beam-time the facility was used in this mode, allowing measurements at very low neutron energies.

The detailed operation statistics are shown in Fig. 1. GELINA was serving up to 9 experiments simultaneously (6.1 on average). The total number of data-taking hours, integrated over all flight paths, was 18123 hours.

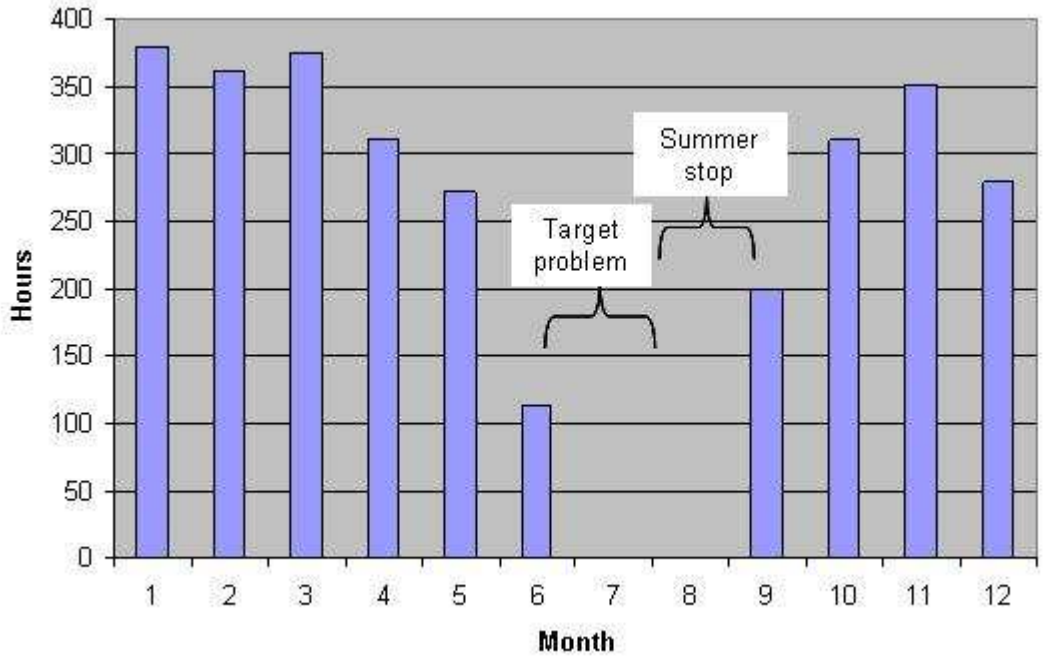

Fig. 1: Detailed operation statistics for the GELINA electron linear accelerator in 2007

The beams that were delivered were much more stable and reproducible that in the past, illustrating the impact of the modernisation work performed during the previous years. Especially the reconstruction of the three klystron modulators had a big impact on the machine reliability and stability.

Neutron production target During June and July we were confronted with a six-week unscheduled GELINA stop due to a problem with the neutron production target. The rotating uranium target is cooled with liquid mercury. An extensive interlock system (measurements of temperatures, mercury flow-rate and target rotational frequency) must guarantee fail-safe operation. The rotating target and its cooling system are located on a lift system that can be lowered down into the basement beneath the target hall so that the target can be stored in a closed underground storage vault. If a target fails we are facing extremely high radiation levels when repair actions are needed. Therefore a defect target must be stored for three to four years to let it 'cool down' before repair actions can be started. The only viable solution is redundancy of target systems; however price is here a limiting factor. We had ordered a new target system in 2004. Despite the fact that the delivery time was 12 month, the new rotating uranium target could only be supplied in November 2007, due to technical problems at the construction site in France. In May 2006 we were confronted with a defect coil of the mercury flow-rate rotameter in our target. In June 2007 we had a similar (but not the same) problem in the spare target. Because the new spare target was not yet available, we were forced to repair the target that was cooling down since 2006. We designed and constructed a special radiation shielding and a remote coil-winding system that allowed a successful repair with a very limited of exposure to our technicians. In order to create adequate redundancy for the future, we decided to buy an additional uranium target, within the 2007 budget. This implied an important reshuffling of the 2007 expenses.

Klystron pulse modulators Modulator 1 was renewed during the first quarter of 2006. Modulators 2 and 3 were already reconstructed in 2005. The technicians of the GELINA crew rebuilt the mechanical configuration of the modulators. They also redesigned and reconstructed part of the charging and discharging units and the cabling. Also the newly developed control and interlock (MCI) system and the modernised interlock hardware was installed. All home-built equipment performed very well.

The three high-power high-voltage thyristor-controlled DC power supplies were installed in 2005 (modulator 2 and 3) and in 2006 (modulator 1). They have the same power rating (150 kW), but the power supply of modulator 1 is operating typically at 22 kV, while in modulators 2 and 3 the nominal power supply voltage is 12 kV. The power supplies of modulator 2 and 3 have accumulated up to now more than 9500 high-voltage hours each and perform very well. In contrast, the power supply for modulator 1, which has similar characteristics, created serious problems since its start-up phase. Some failing components have been replaced by the constructor, but instability problems remained. The voltage regulation system ran sporadically out of control, leading to a switch off of the modulator. Noise signals in the MHz range are generated during thyratron firing. The thyratron is triggered at a stable 800 Hz pulse repetition frequency, while the six thyristors are, by the nature of the SCR-controlled power supply, fired at a multiple of the mains frequency, slowly changing in time. As a result the phase shift between thyristor firing and noise signals is also slowly changing with time, leading to occasional 'misfiring' of one of the thyristors. Replacement of a 30 years old connection between the common modulator earth and the general earth of the GELINA facility, together with some other modifications, reduced substantially the noise signals and eliminated this problem.

Since the HVDC problems were solved, the modulators operate at a rate of almost 100
Preventive replacement of compression magnet sealing rings The relativistic compression magnet is a magnet of a very special design. It transports an electron beam with an energy spread $\Delta/E = 50$ % over a maximum distance of 7.5 m. The role of this magnet is to compress the beam pulse with duration of 10 ns by a factor of 10 while preserving the charge in the pulse. The large vacuum chamber of the compression magnet is sealed with two specially-shaped elastomeric O-rings (length $\approx$ 8.1 m). Use of metallic sealing rings is not possible due to the special shape of the magnet chamber. Each two to three years the vacuum sealing rings of the relativistic compression magnet must be replaced due to radiation damage. Replacement of these seals implies opening of the magnet (weight 50 tons) and cleaning of the magnet chamber flange assemblies. Due to the high level of radioactivity in the magnet and its heavy weight, replacement of these seals is a delicate, highly demanding and time-consuming work. So, it has been decided for the future not to wait until the seals start to leak, but to plan preventive replacements of the magnet O-rings each two years at the end of the summer stops, when the radiation exposure of the technicians is lowest. This preventive action has been performed for the first time in August 2007.

Because of the great request for annual beam time and the increasing number of experimental users from outside (in the framework of the EURATOM Transnational Access to Infrastructures projects NUDAME and EUFRAT, see elsewhere), the improvement of the GELINA availability and reliability remains a permanent effort. Therefore the GELINA modernisation project is an

ongoing task, with the following schedule for the following years:

- new injector fast pulse amplifier system and peripheral equipment: Summer stop 2008
- four new water chillers for accelerator sections cooling: Summer stop 2008
- new electrical power distribution system: Summer stop 2009
- new waveguide system for klystron 1: Summer stop 2010

The IRMM Van de Graaff accelerator

G. Lövestam, C. Chaves de Jesus, T. Gamboni, W. Geerts, R. Jaime Tornin

The IRMM 7 MV Van de Graaff accelerator is operated in either DC or in fast or slow beam pulsing mode. In the fast beam pulsing mode, ion beam pulses down to about 2 ns fwhm can be produced with a pulse frequency of 2.5, 1.25 or 0.625 MHz. The slow pulsing system facilitates a minimum pulsing width of 10 μs at an adjustable frequency up to 5 kHz. In DC mode, a constant beam current up to 50 μA of protons can be maintained for long periods (week). During 2007, both the fast and the slow beam pulsing systems were tuned for enhanced performance.

Neutron production Neutrons are produced using either of the following nuclear reactions:

reaction	neutron energies (MeV)	mono-energetic neutrons (MeV)
^{7}Li(p, n)^{7}Be	0 - 5.3	0.3 - 1.9
T(p, n)^{3}He	0 - 6.2	0.3 - 6.2
D(d, n)^{3}He	1.8 - 10.1	4.0 - 7.5
T(d, n)^{4}He	12.9 - 24.1	15.7 - 20.0

In the table the full available neutron energy regions are given together with the energy regions for the mono-energetic neutrons. However, also for the latter neutron energies parasitic components may be present in the neutron spectra due to target contamination and target aging. The lower energy region for the T(d, n)^{4}He-reaction (12.9 15.8 MeV) is only available at neutron emission angles other than 0^{o}.
Other critical parameters of the produced neutron beams are the neutron yield and the full width half maximum (fwhm) of the full energy neutron peak, see table below. In the table the FWHM given in % of the total spectrum up to the full energy peak high energy limit.

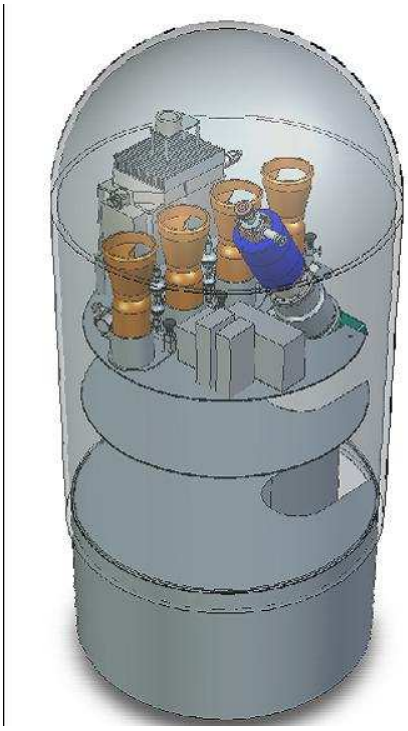

Fig. 1: Top plate of the Van de Graaff high voltage terminal with the ECR ion source. The four cylinders in the centre of the top platform are the gas bottles. The actual ion source is located down right on the platform while the cubic container up left is the microwave generator

Reaction	Target	weight (mg/cm^2)	E_{ion} (MeV)	E_n (MeV)	neutron yield (10^6/s/sr/μC)	σ_{E_n}/E_n %
^{7}Li(p, n)^{7}Be	LiF	0.5	2.1	0.3	1	21 %
	LiF	5.0	3.6	1.9	3	2 %
T(p, n)^{3}He	TiT	2.0 (T/Ti=1.4)	1.3	0.3	10	79 %
	TiT	2.0 (T/Ti=1.4)	7.0	6.2	2	0.3 %
D(d, n)^{3}He	D_2	(4 cm, 200 kPa)	1.4	4.0	10	18 %
	D_2	(4 cm, 200 kPa)	4.4	7.5	30	3 %
	TiD	2.0 (D/Ti=1.4)	1.1	4.0	5	15 %
	TiD	2.0 (D/Ti=1.4)	4.4	7.5	20	3 %
T(d, n)^{4}He	TiT	2.0 (T/Ti=1.4)	0.9	15.7	10	8 %
	TiT	2.0 (T/Ti=1.4)	3.5	20.0	4	2 %

ECR ion source The project of replacing the present and original radio frequency (RF) ion source with an ECR ion source was initiated already in 2006. During 2007 the drawings were finalised and all components were acquired by the external production company, Pantechnik in Bayeux in France, see Fig. 1. The source is expected to deliver higher beam currents

under more stable beam conditions, but also require less maintenance periods. Today about 8 maintenance periods of one week each is required for full operation. With the ECR source only one week of maintenance is planned per year. The ECR also facilitates the generation and acceleration of higher charged ions. Expected delivery is in July 2008.

Accelerator operation In 2007 the accelerator was operated for 4981 hours with a maintenance stop in August, see Fig. 2. Less than 20 % of the time was used for accelerator and beam optics tuning and tests while the rest was available for experiments. The large number of annual hours, which is a machine record, is a result of operating the machine also unattended, 24 h/day, also during week-ends. The low number of beam hours in April is due to extensive testing and fine tuning of the nanosecond beam pulsing system.

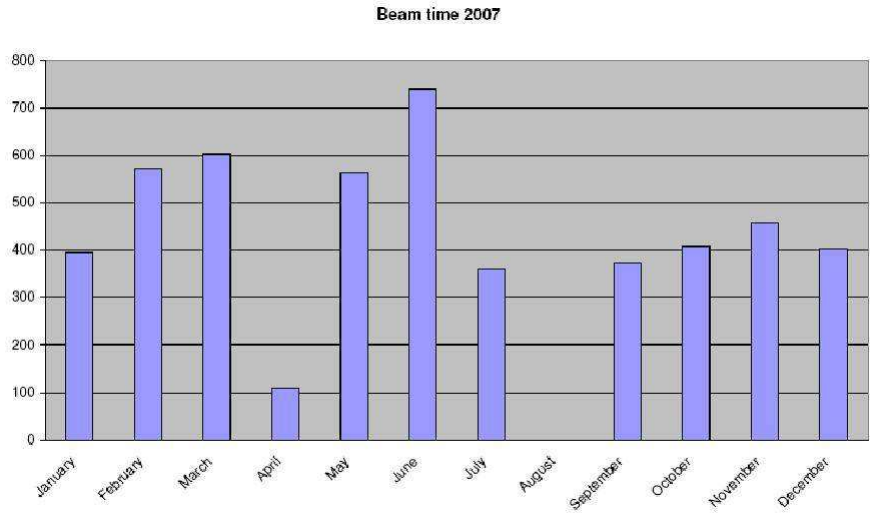

Fig. 2: Operation statistics for 2007 for the IRMM VdG accelerator

Annex

List of publications

High resolution measurement of the ^{234}U(n, f) cross section in the neutron energy range from 0.5 eV up to 100 keV
J. Heyse, C. Wagemans, L. De Smet, O. Serot, J. Wagemans, J. Van Gils
Nuclear Science and Engineering 156 (2007) 211-218

The ^{10}B(n, α_0)/^{10}B(n, α_l) Branching Ratio
F.-J. Hambsch, I. Ruskov
Nuclear Science and Engineering 156 (2007) 103-114

Light Fission-Fragment Mass Distribution from the Reaction ^{251}Cf(n$_{th}$, f)
E. Birgersson, S. Oberstedt, A. Oberstedt, F.-J. Hambsch, D. Rochman, I. Tsekhanovich, S. Raman
Nuclear Physics A791 (2007) 1-23

Energy Degrader Technique for Light-Charged Particle Spectroscopy at LOHENGRIN
S. Oberstedt, A. Oberstedt
Nuclear Instruments and Methods in Physics Research A570 (2007) 51-54

Neutron Emission in Fission
N. V. Kornilov, F.-J. Hambsch, A. S. Vorobyev
Nuclear Physics A 789 (2007) 55-72

High Resolution Measurement of Neutron Inelastic Scattering and (n, 2n) Cross-Sections for ^{52}Cr
L. C. Mihailescu, C. Borcea, A. J. Koning, A. Plompen
Nuclear Physics A 786 (2007) 1-23

Measurement of the Neutron Capture Cross Section of the s-only Isotope ^{204}Pb from 1 eV to 440 keV
C. Domingo Pardo, U. Abbondanno, P. Rullhusen, A. Plompen, and the n_TOF Collaboration
Physical Review C75, 015806 (2007)

The ^{139}La(n, γ) Cross Section : Key for the Onset of the s-process
R. Terlizzi, U. Abbondanno, P. Rullhusen, A. Plompen, and the n_TOF Collaboration
Physical Review C75, 035807 (2007)

Experimental Determination of the ^{36}Cl(n, p)^{36}S and ^{36}Cl(n, α)^{33}P Reaction Cross Sections and the the Consequences on the Origin of ^{36}S
L. De Smet, C. Wagemans, G. Goeminne, J. Heyse, J. Van Gils
Physical Review C75 (2007) 034617

The Use of C_6D_6 Detectors for Neutron Induced Capture Cross-Section Measurements in the Resonance Region

A. Borella, G. Aerts, F. Gunsing, M. Moxon, P. Schillebeeckx, R. Wynants
Physics Research A577 (2007) 626-640

Neutron Resonance Capture Analysis and Applications
H. Postma, R. . Perego, P. Schillebeeckx, P. Siegler, A. Borella
Journal of Radioanalytical and Nuclear Chemistry Vol. 271 (2007) 89-94

International Key Comparison of Neutron Fluence Measurements in Monoenergetic Neutron Fields - CCRI(III)-K10
Z. Wang, C. Rong, G. Lövestam, A. Plompen, R. Puglisi, D. M. Gilliam, C. M. Eisenhauer, J. S. Nico, M. S. Dewey, K. Kudo, A. Uritani, N. Takeda, D. J. Thomas, N. J. Roberts, A. Bennett, P. Kolkowski, N. N. Moisseev, I. A. Kharitonov, S. Guldbakke, H. Klein, R. Nolte, D. Schlegel
Metrologia 44 (2007) 06005

Measurement of Neutron Excitation Functions Using Wide Energy Neutron Beams
G. Lövestam, M. Hult, A. Fessler, T. Gamboni, J. Gasparro, W. Geerts, R. Jaime, P. Lindahl, S. Oberstedt, H. Tagziria
Nuclear Instruments and Methods in Physics Research, Section A580 (2007) 1400-1409

Data Acquisition with a Fast Digitizer for Large Volume HPGe Detectors
L. Mihailescu, C. Borcea, A. Plompen
Nuclear Instruments and Methods in Physics Research, Section A578 (2007) 298-305

Discovery of the Shape Isomer in ^{235}U
A. Oberstedt, S. Oberstedt, M. Gawrys, N. Kornilov
Physical Review Letters 99 (2007) 042502

Neutron Reactions and Nuclear Cosmo-chronology
M. Mosconi, M.Heil, F. Käppeler, A. Plompen, P. Rullhusen
Progress in Particle and Nuclear Physics 59 (2007) 165-173

Non-destructive Analysis of Materials by Neutron Resonance Transmission
G. Noguere, F. Cserpak, C. Ingelbrecht, A. J. M. Plompen, C. R. Quetel, P. Schillebeeckx
Nuclear Instruments and Methods in Physics Research A575 (2007) 476488

Neutron Resonance Capture Applied to some Prehistoric Bronze Axes
H. Postma, J. J. Buttler, P. Schillebeeckx, W. E. Van Eijk
Il Nuovo Cimento C30 (2007) 105-112

Ancient Charm: A research Project for Neutron-Based Investigation of Cultural-Heritage Objects
G. Gorini, P. Schillebeeckx, P. Siegler, and the Ancient Charm Collaboration

Il Nuovo Cimento C30 (2007) 47-58

High-Resolution Neutron Transmission and Capture Measurements of the Nucleus ^{206}Pb
A. Borella, F. Gunsing, M. Moxon, P. Schillebeeckx, P. Siegler
Physical Review C76, 014605 (2007)

Status and Outlook of the Neutron Time-of-Flight Facility n_TOF at CERN
F. Gunsing, A. Plompen, P. Rullhusen, and the n_TOF collaboration
Nuclear Instruments and Methods in Physics Research Section B261 (2007) 925-929

Radiative Neutron Capture Cross Section of ^{206}Pb and its Astrophysical Implications
C. Domingo Pardo, A. Plompen, P. Rullhusen, and the n_TOF collaboration
Physical Reviw C76, 045805 (2007)

List of conferences

Gamma Production Cross Sections for Inelastic Scattering and (n, 2n) Reactions
A. Plompen
Perspectives on Nuclear Data for the Next Decade. 26-28 September 2005, CEA/Bryres-le-Chtel, Ed. E. Bauge, Publisher: OECD-NEA (2007) 151-156

Energy Degrader Technique for Ternary Fission Studies at LOHENGRIN
A. Oberstedt, S. Oberstedt, D. Rochman
Spring Meeting of the German Physical Society (DPG), Hadrons & Nuclei. 12-16 March 2007, Giessen (DE), HK 16.9

Search for the Shape Isomer in ^{235}U
S. Oberstedt, A. Oberstedt, M. Gawrys
Spring Meeting of the German Physical Society (DPG), Hadrons & Nuclei. 12-16 March 2007, Giessen (DE), HK 46.4

Neutron-Induced Reaction Studies at the Accelerator-Based Neutron Sources of the Institute for Reference Materials and Measurements
A. Plompen
AccApp07, The Eighth International Topical Meeting on Nuclear Applications and Utilization of Accelerators, Pocatello, Idaho, July 30to August 2, 2007, Organiser: D. Beller, U. of Nevada for the American Nuclear Society

Towards a New Neutron Target for the GELINA Facility
A. Plompen, D. Ene, S. Kopecky, W. Mondelaers
AccApp07, The Eighth International Topical Meeting on Nuclear Applications and Utilization of Accelerators, Pocatello, Idaho, July 30to August 2, 2007, Organiser: D. Beller, U. of Nevada

for the American Nuclear Society

EUROTRANS/NUDATRA Low and Intermediate Energy Nuclear Data Measurements
A. Plompen
AccApp07, The Eighth International Topical Meeting on Nuclear Applications and Utilization of Accelerators, Pocatello, Idaho, July 30to August 2, 2007, Organiser: D. Beller, U. of Nevada for the American Nuclear Society

Measurement of Neutron Capture Cross-Sections at n_TOF
G. Tagliente, A. Plompen, P. Rullhusen
VI Latin American Symposium on Nuclear Physics and Applications, 3-7/10/2005, Iguazu-Argentina, AIP Conference Proceedings 884, ND 2004, 265-271, American Institute of Physics

Measurement of The Neutron Induced Fission Cross Section on Transuranic (TRU) Elements at The n_TOF Facility at CERN
P. F. Mastinu, A. Plompen, P. Rullhusen, and the n_TOF collaboration
Eleventh Latin American Symposium On Nuclear Physics And Applications Cusco (Peru), 1116 June 2007. ISBN: 978-0-7354-0461-8, AIP conference 947 (2007) 43-48

The n_TOF Facility at CERN
D. Cano-Ott, A. Plompen, P. Rullhusen, and the n_TOF collaboration
The Eighth International Topical Meeting on Nuclear Applications and Utilization of Accelerators, Pocatello, Idaho, D. Beller, U. of Nevada for the American Nuclear Society, http://www.ans.org/store/vi-700330, (2007) 821-826

Neutron Data Measurements at IRMM
A. Plompen
3^{rd} Workshop on Neutron Measurements, Evaluations and Applications (NEMEA-3) 25-28 October 2006, Borovets, Bulgaria, Organiser: Arjan Plompen, EUR22794 EN ISBN 978-92-79-06158-5

Neutron-Induced Activation Cross Sections of Different Isotopes of Zr, W and Ta from the Threshold to 20 MeV
V. Semkova, R. Jaime Tornin, A. Moens, A. Plompen
3^{rd} Workshop on Neutron Measurements, Evaluations and Applications (NEMEA-3) 25-28 October 2006, Borovets, Bulgaria, Organiser: Arjan Plompen, EUR22794 EN ISBN 978-92-79-06158-5

NEPTUNE The New Isomer Spectrometer at IRMM
S. Oberstedt, A. Oberstedt, A. Plompen, V. Semkova, G. Lövestam
3^{rd} Workshop on Neutron Measurements, Evaluations and Applications (NEMEA-3) 25-28 October 2006, Borovets, Bulgaria, Organiser: Arjan Plompen, EUR22794 EN ISBN 978-92-79-06158-5

Cadmium Transmission Measurements at GELINA

I. Ivanov, P. Siegler, S. Kopecky, A. Trkov, M. Moxon
3^{rd} Workshop on Neutron Measurements, Evaluations and Applications (NEMEA-3) 25-28 October 2006, Borovets, Bulgaria, Organiser: Arjan Plompen, EUR22794 EN ISBN 978-92-79-06158-5

Neutron Capture Cross-Section Measurements on ^{103}Rh and ^{133}Cs for Improved Nuclear Criticality Safety
L. C. Mihailescu, A. Borella, R. Capote Noy, K. H. Guber, I. Ivanov, S. Kopecky, L. C. Leal, P. Schillebeeckx, P. Siegler, I. Sirakov, R. Wynants
3^{rd} Workshop on Neutron Measurements, Evaluations and Applications (NEMEA-3) 25-28 October 2006, Borovets, Bulgaria, Organiser: Arjan Plompen, EUR22794 EN ISBN 978-92-79-06158-5

Upgrade of the Neutron Inelastic Scattering Measurements Setup at GELINA
A. Negret, C. Borcea, A. Plompen
3^{rd} Workshop on Neutron Measurements, Evaluations and Applications (NEMEA-3) 25-28 October 2006, Borovets, Bulgaria, Organiser: Arjan Plompen, EUR22794 EN ISBN 978-92-79-06158-5

EUR Reports and Special publications

Neutron Physics Unit Scientific Report 2005
S. Oberstedt and P. Rullhusen
Report EUR 23039 EN, ISBN 978-92-79-05365-8, Catalogue N^o LA-NA-23039-EN-C (2007)
published in electronic format only

Proc. enlargement workshop on NEutron Masurements, Evaluation and Applications-3, NEMEA-3, 25-28 October 2004, Borovets
A. Plompen
Report EUR 22794 EN, ISBN 978-92-79-06158-5, Catalogue N^o LA-NA-22794-EN-C (2007)

Author Index

European Commission

EUR 23440 EN – Joint Research Centre – Institute for Reference Materials and Measurements
Title: Neutron Physics Unit SCIENTIFIC REPORT 2007
Editor(s): S. Oberstedt, P. Rullhusen
Luxembourg: Office for Official Publications of the European Communities
2008 – 130 pp. – 29.7 x 20.9 cm
EUR – Scientific and Technical Research series – ISSN 1018-5593
ISBN 978-92-79-09532-0
DOI 10.2787/65683

Abstract
This report is a compilation of status reports on all ongoing neutron physics research and development activities at the European Commission JRC-IMMM

The mission of the JRC is to provide customer-driven scientific and technical support for the conception, development, implementation and monitoring of EU policies. As a service of the European Commission, the JRC functions as a reference centre of science and technology for the Union. Close to the policy-making process, it serves the common interest of the Member States, while being independent of special interests, whether private or national.

JRC
EUROPEAN COMMISSION

LA-NA-23440-EN-C

Publications Office
Publications.eu.int

ISBN 978-92-79-09532-0